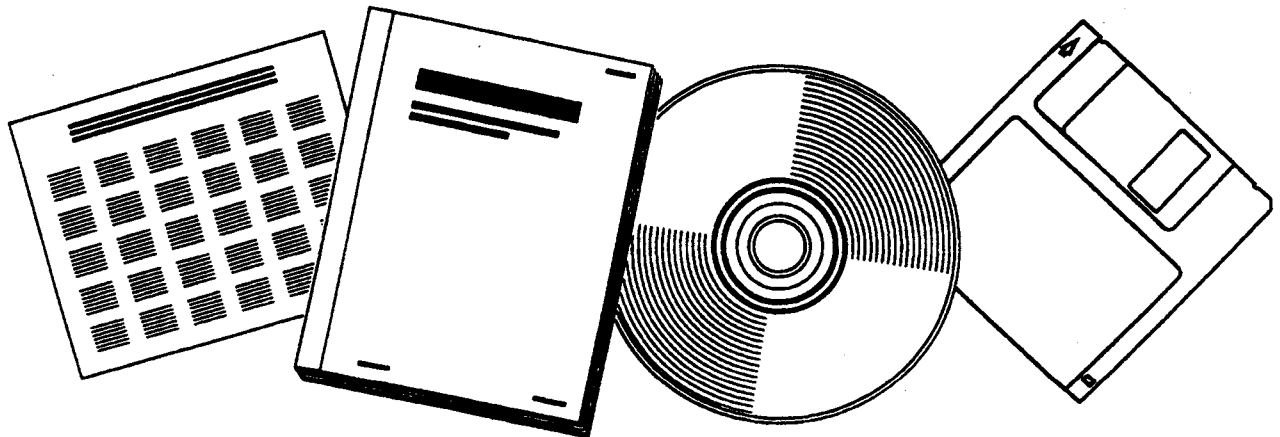**NTIS**

AIRCRAFT CRASH SURVIVAL DESIGN GUIDE - VOLUME II - AIRCRAFT DESIGN CRASH IMPACT CONDITIONS AND HUMAN TOLERANCE

SIMULA INC.
PHOENIX, AZ

DEC 89

AD-A218 435 ④

USAAVSCOM TR 89-D-22B

AIRCRAFT

CRASH

SURVIVAL

DESIGN

GUIDE

US ARMY
AVIATION
SYSTEMS COMMAND

DTIC
SELECTE
FEB 22 1990
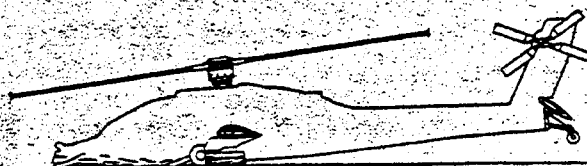D

VOLUME II – AIRCRAFT DESIGN CRASH
IMPACT CONDITIONS AND
HUMAN TOLERANCE

SIMULA INC.
10016 SOUTH 51st STREET
PHOENIX, ARIZONA 85044

DECEMBER 1989

FINAL REPORT

Prepared for

AVIATION APPLIED TECHNOLOGY DIRECTORATE
US ARMY AVIATION RESEARCH AND TECHNOLOGY ACTIVITY (AVSCOM)
FORT EUSTIS, VA 23604-5577

90 02 21 112

AVIATION APPLIED TECHNOLOGY DIRECTORATE POSITION STATEMENT

This revised edition of the Aircraft Crash Survival Design Guide (ACSDG) was prepared to assist those design engineers responsible for the incorporation of crashworthiness into the design of helicopters, light fixed-wing aircraft, and tilt rotor aircraft. Also, this guide may be used in the evaluation of the level of crashworthiness design available in the various types of aircraft.

This report documents the components and principles of crashworthiness and suggests specific design criteria. In general, a systems approach is presented for providing a reasonable level of aircrew and aircraft protection in a crash, which is considered the preferred approach. The original Crash Survival Design Guide was published in 1967 as USAAVLABS TR 67-22 and subsequent revisions published as USAAVLABS TR 70-22, USAAMRDL TR 71-22, and USARTL-TR-79-22A thru E. This edition consists of a consolidation of up-to-date design criteria, concepts, and analytical techniques developed through research programs sponsored by this Directorate and others over the past 27 years.

This document has been coordinated with other Government agencies and helicopter airframe manufacturers active in aircraft crashworthiness research and development, and is considered to offer sound design criteria and approaches to design for crashworthiness.

The technical monitors for this program were Messrs. LeRoy Burrows, Harold Holland, and Kent Smith of the Safety and Survivability Technical Area, Aeronautical Systems Division, Aviation Applied Technology Directorate.

<u>NOTE</u>: All previous editions of the Aircraft Crash Survival Design Guide are obsolete and should be destroyed.

REPORT DOCUMENTATION PAGE

Public reporting burden for this collection of information is estimated to average 1 hour per response, including the time for reviewing instructions, searching existing data sources, gathering and maintaining the data needed, and completing and reviewing the collection of information. Send comments regarding this burden estimate or any other aspect of this collection of information, including suggestions for reducing this burden, to Washington Headquarters Services, Directorate for Information Operations and Reports, 1215 Jefferson Davis Highway, Suite 1204, Arlington, VA 22202-4302, and to the Office of Management and Budget, Paperwork Reduction Project (0704-0188), Washington, DC 20503.

1. AGENCY USE ONLY (Leave blank)	2. REPORT DATE December 1989	3. REPORT TYPE AND DATES COVERED Final FROM 9/86 TO 8/89

4. TITLE AND SUBTITLE
Aircraft Crash Survival Design Guide
Volume II - Aircraft Design Crash Impact Conditions and Human Tolerance

5. FUNDING NUMBERS
DAAJ02-86-C-0028

6. AUTHOR(S)
J. W. Coltman, C. Van Ingen, N.B. Johnson, R.E. Zimmermann

7. PERFORMING ORGANIZATION NAME(S) AND ADDRESS(ES)
Simula Inc.
Phoenix, Arizona 85044-5299

8. PERFORMING ORGANIZATION REPORT NUMBER

9. SPONSORING/MONITORING AGENCY NAME(S) AND ADDRESS(ES)
Aviation Applied Technology Directorate
U.S. Army Aviation Research & Technology Activity (AVSCOM)
Fort Eustis, VA 23604-5577

10. SPONSORING/MONITORING AGENCY REPORT NUMBER
USAAVSCOM TR 89-D-22B

11. SUPPLEMENTARY NOTES
Volume II of five-volume report

12a. DISTRIBUTION/AVAILABILITY STATEMENT
Approved for public release; distribution unlimited

12b. DISTRIBUTION CODE

13. ABSTRACT (Maximum 200 words)
This five-volume publication has been compiled to assist design engineers in understanding the design considerations associated with the development of crash-resistant U.S. Army aircraft. A collection of available information and data pertinent to aircraft crash resistance is presented, along with suggested design conditions and criteria. The five volumes of the Aircraft Crash Survival Design Guide cover the following topics: Volume I - Design Criteria and Checklists; Volume II - Aircraft Design Crash Impact Conditions and Human Tolerance; Volume III - Aircraft Structural Crash Resistance; Volume IV - Aircraft Seats, Restraints, Litters and Cockpit/Cabin Delethalization; and Volume V - Aircraft Postcrash Survival. This volume (Volume II) contains information on the aircraft crash environment, human tolerance to impact, occupant motion during a crash, human anthropometry, and crash test dummies, all of which serves as background for the design information presented in the other volumes.

14. SUBJECT TERMS
Aircraft Design Guide, Crash Environment, Crashes, Crash Resistance, Crashworthiness, Human Body, Accidents, Biodynamics, Design Data, Crashworthy, Crash Landing, Human Tolerance, Impact, Anthropometry

15. NUMBER OF PAGES
120

16. PRICE CODE

17. SECURITY CLASSIFICATION OF REPORT UNCLASSIFIED	18. SECURITY CLASSIFICATION OF THIS PAGE UNCLASSIFIED	19. SECURITY CLASSIFICATION OF ABSTRACT UNCLASSIFIED	20. LIMITATION OF ABSTRACT

PREFACE

This report was prepared for the Safety and Survivability Technical Area of
the Aviation Applied Technology Directorate, U. S. Army Aviation Research and
Technology Activity (AVSCOM), Fort Eustis, Virginia, by Simula Inc. under
Contract DAAJ02-86-C-0028, initiated in September 1986. This guide is a revision of USARTL Technical Report 79-22, Aircraft Crash Survival Design Guide,
published in October 1980.

A major portion of the data contained herein was taken from U. S. Army-
sponsored research in aircraft crashworthiness conducted from 1960 to 1987.
Acknowledgment is extended to the U. S. Air Force, Federal Aviation Administration, NASA, and U. S. Navy for their research in crash survival. Appreciation is extended to the following organizations for providing accident
case histories leading to the establishment of the impact conditions in aircraft accidents:

- U. S. Army Safety Center, Fort Rucker, Alabama.

- Civil Aeronautics Board, Washington, D. C.

- U. S. Naval Safety Center, Norfolk, Virginia.

- U. S. Air Force Inspection and Safety Center, Norton Air Force Base,
  California.

Additional credit is due the many authors, individual companies, and organizations listed in the bibliographies for their contributions to the field.
The contributions of the following authors to previous editions of the
Aircraft Crash Survival Design Guide are most noteworthy:

D. F. Carroll, R. L. Cook, S. P. Desjardins, J. K. Drummond, J. H. Haley,
Jr., A. D. Harper, H. G. C. Henneberger, N. B. Johnson, G. Kourouklis, D.
H. Laananen, W. H. Reed, S. H. Robertson, L. M. Shaw, G. T. Singley, III,
A. E. Tanner, J. W. Turnbow, and L. W. T. Weinberg.

LTC. D. F. Shanahan, M.C., of the United States Army furnished assistance by
providing the occupant exposure data discussed in Section 4.0.

This volume has been prepared by J. W. Coltman, C. Van Ingen, N. B. Johnson,
and R. E. Zimmermann. Data from the investigations of recent Army aircraft
accidents were provided by the U. S. Army Safety Center. R.F. Chandler of
the FAA Civil Institute assisted in locating information on human tolerance,
anthropometry, and crash test dummies.
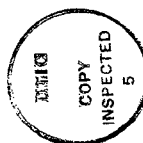
<table>
<tr><td colspan="2">Accesion For</td></tr>
<tr><td>NTIS CRA&I</td><td>☑</td></tr>
<tr><td>DTIC TAB</td><td>☐</td></tr>
<tr><td>Unannounced</td><td>☐</td></tr>
<tr><td colspan="2">Justification</td></tr>
<tr><td colspan="2">By</td></tr>
<tr><td colspan="2">Distribution /</td></tr>
<tr><td colspan="2">Availability Codes</td></tr>
<tr><td>Dist</td><td>Avail and / or
Special</td></tr>
<tr><td colspan="2">A-1</td></tr>
</table>

DTIC COPY INSPECTED 5

iii

TABLE OF CONTENTS

Preceding page blank   v

TABLE OF CONTENTS (CONTD)

TABLE OF CONTENTS (CONTD)

LIST OF ILLUSTRATIONS (CONTD)

LIST OF TABLES

LIST OF TABLES (CONTD)

INTRODUCTION

For many years, emphasis in aircraft accident investigation was placed on finding the cause of the accident. Very little effort was expended in the crash survival aspects of aviation safety. However, it became apparent through detailed studies of accident investigation reports that large improvements in crash survival could be made if consideration were given in the initial aircraft design to the following general survivability factors:

1. Crash Resistance of Aircraft Structure - The ability of the aircraft structure to maintain living space for occupants throughout a crash.

2. Tiedown Strength - The strength of the linkage preventing occupant, cargo, or equipment from becoming missiles during a crash sequence.

3. Occupant Acceleration During Crash Impact - The intensity and duration of accelerations experienced by occupants (with tiedown assumed intact) during a crash.

4. Occupant Crash Impact Hazards - Barriers, projections, and loose equipment in the immediate vicinity of the occupant that may cause contact injuries.

5. Postcrash Hazards - The threat to occupant survival posed by fire, drowning, exposure, etc., following the impact sequence.

Early in 1960, the U.S. Army Transportation Research Command* initiated a long-range program to study all aspects of aircraft safety and survivability. Through a series of contracts with the Aviation Safety Engineering and Research Division (AvSER) of the Flight Safety Foundation, the problems associated with occupant survival in aircraft crashes were studied to determine specific relationships between crash forces, structural failures, crash fires, and injuries. A series of reports covering this effort was prepared and distributed by the U. S. Army, beginning in 1959.

In October 1965, a special project initiated by the U. S. Army consolidated the design criteria presented in these reports into one technical document suitable for use as a designer's guide by aircraft design engineers and other interested personnel. The document was to be a summary of the current state of the art in crash survival design, using not only data generated under Army contracts but also information collected from other agencies and organizations. The Crash Survival Design Guide, first published in 1967, realized this goal.

Since its initial publication, the Design Guide has been revised several times to incorporate the results of continuing research in crashworthiness technology. The second revision, published in 1971, was the basis for the

---

*Now the Aviation Applied Technology Directorate, Aviation Research and Technology Activity of the U. S. Army Aviation Systems Command (AVSCOM).

criteria contained in the Army's military standard MIL-STD-1290, "Light Fixed- and Rotary-Wing Aircraft Crash Resistance" (Reference 1). The third revision, published in 1980, entitled Aircraft Crash Survival Design Guide, expanded the document to five volumes, which have been updated by the current edition to include information and changes developed from 1980 to 1987. This current revision, the fourth, contains the most comprehensive treatment of all aspects of aircraft crash survival now documented. It can be used as a general text to establish a basic understanding of the crash environment and the techniques that can be employed to improve chances for survival. It also contains design criteria and checklists on many aspects of crash survival and thus can be used as a source of design requirements.

The current edition of the Aircraft Crash Survival Design Guide is published in five volumes. Volume titles and general subjects included in each volume are as follows:

Volume I - Design Criteria and Checklists

   Pertinent criteria extracted from Volumes 2 through 5, presented in the same order in which they appear in those volumes.

Volume II - Aircraft Design Crash Impact Conditions and Human Tolerance

   Crash impact conditions, human tolerance to impact, military anthropometric data, occupant environment, test dummies, accident information retrieval.

Volume III - Aircraft Structural Crash Resistance

   Crash load estimation, structural response, fuselage and landing gear requirements, rotor requirements, ancillary equipment, cargo restraints, structural modeling.

Volume IV - Aircraft Seats, Restraints, Litters, and Cockpit/Cabin
            Delethalization

   Operational and crash environment, energy attenuation, seat design, litter requirements, restraint system design, occupant/restraint system/seat modeling.

Volume V - Aircraft Postcrash Survival

   Postcrash fire, ditching, emergency escape, crash locator beacons.

This volume (Volume II) contains information on aircraft design impact conditions and the response of the human body to impact. Following a general discussion of aircraft crash resistance in Chapter 1, a number of words commonly referred to in discussing crash impact conditions are defined in Chapter 2. Chapter 3 describes the aircraft design crash impact conditions. Chapter 4 presents occupant exposure data and includes accident statistics, terrain impact, injury frequency and injury mechanisms. Chapter 5 discusses the tolerance of the human body and various body parts to impact loading. Chapter 6 presents data on occupant motion during a crash. Chapter 7 provides data on human anthropometry that may be useful directly, as in cockpit design, or indirectly, as in preparing input for computer simulation

models such as those discussed in Volume IV. Chapter 8 describes the crash test dummies used in evaluating protective systems such as seats and restraints.

The units of measurement shown in the Design Guide vary depending upon the units used in the referenced sources of information, but are mostly USA units. In some cases the corresponding metric units are shown in parentheses following the USA units. For the convenience of the reader a conversion table of some commonly used units follows.

USA Unit	Abbr. or Symbol	Metric Equivalent	Abbr. or Symbol
Weight			
Ounce	oz.	28.35 grams	g
Pound	lb or #	0.454 kilogram	kg
Capacity (U.S. liquid)			
Fluidounce	fl oz	29.57 milliliters	ml
Pint	pt	0.473 liter	l
Quart	qt	0.946 liter	l
Gallon	gal	3.785 liters	l
Length			
Inch	in.	2.54 centimeters	cm
Foot	ft	30.48 centimeters	cm
Yard	yd	0.9144 meter	m
Mile	mi	1.609 kilometers	km
Area			
Square Inch	sq in. or in.^{2}	6.452 square centimeters	sq cm or cm^2
Square Foot	sq ft or ft^2	0.093 square meter	sq m or m^2
Volume			
Cubic Inch	cu in. or in.^{3}	16.39 cubic centimeters	cu cm or cm^3
Cubic Foot	cu ft or ft^3	0.028 cubic meter	cu m or m^3
Force			
Pound	lb	4.448 newtons	N
		4.448 x 10^5 dynes	

1.0 BACKGROUND DISCUSSION

This volume deals with the variables involved in Army aircraft design impact conditions and the effects of resulting impact forces on the human body. An understanding of the impact conditions and of the ability of the human body to survive them is necessary for the effective design of more crash-resistant aircraft. The following background discussion presents general considerations that are of importance in understanding and applying the included information.

The overall objective of designing for crash resistance is to eliminate unnecessary injuries and fatalities in relatively mild impacts. Results from analyses and research have shown that the relatively small cost in dollars and weight of including crash-resistant features is an extremely wise investment. Consequently, new generation aircraft are being procured to rather stringent crash-resistant requirements.

To maximize aircraft crash resistance or, in the sense being discussed, to provide as much occupant protection as possible, all aspects of the complete system must be considered. In other words, every available subsystem must be employed to the fullest extreme in order to maximize the protection afforded to vehicle occupants. When an aircraft impacts the ground, deformation of the ground absorbs some energy. This is an uncontrolled variable since the quality of the impacted surface usually cannot be selected by the pilot. If the aircraft lands in the proper attitude and on an appropriate surface, the landing gear can be used to absorb a significant amount of the impact energy. After stroking of the gear, crushing of the fuselage provides the next level of energy absorption. Of course, one of the functions of the fuselage is to provide a protective shell around the occupant while energy-absorbing stroke is occurring outside the shell. The functions of the seat and restraint system are to restrain the occupant within the protective shell during the crash sequence and to provide additional energy-absorbing stroke to further reduce the loads. The structure and components immediately surrounding the occupant also must be considered. Structures such as cyclic controls, glare shields, instrument panels, and sidewalls, must be delethalized in some manner if they lie within the strike envelope of the occupant.

The original edition of the Design Guide dealt primarily with modifications that could be made to existing aircraft to increase their crash resistance; now, two approaches to improving aircraft crash resistance are open. The first approach is to influence the design of new aircraft, and the second is to improve the crash resistance of existing aircraft. Obviously, much higher levels of crash resistance can be achieved in the design and development of new aircraft if crash resistance is considered from the beginning. This is being accomplished at the present time through the use of procurement packages that include pertinent specifications that require certain levels of crash resistance of various subsystems as well as for the entire aircraft. However, some of the available potential is still being lost due to the historical approach used in designing aircraft. The basic aircraft is designed leaving space and providing attachment provisions for subsystems. Later the subsystems are designed and then are limited by the previously established, somewhat arbitrary, boundary conditions. The boundary conditions may unnecessarily limit the performance of the subsystems. The better approach is that

in which all systems and subsystems are, at least preliminarily, designed at the same time. This approach enables subsystem considerations to affect the larger systems and will produce a more nearly optimum vehicle.

The same principles for improving crash resistance can be applied to the retrofit of existing aircraft; however, the "cast-in-concrete" status of existing production structure is a more costly and difficult obstacle to overcome. When crash resistance features must be included through retrofit, the level that can be achieved is usually reduced. However, even in retrofit situations, the overall objective can be met; i.e., occupant protection can be maximized to eliminate unnecessary injuries.

As mentioned above, the entire system should be considered in any analysis resulting in apportionment of the crash energy to be absorbed by the various components. However, any valid systems approach will consider probable alternate crash impact conditions wherein all subsystems cannot perform their desired functions; for example, an impact situation in which the landing gear cannot absorb its share of the impact crash energy because of the angle of impact, loss of gear, or terrain properties. To achieve the overall goal, therefore, minimum levels of crash protection have been required of the various individual subsystems, such as the seat.

In earlier editions of the Design Guide, requirements were given for providing occupant protection in crashes up to and including the severity of the 95th-percentile survivable crash. With the deployment of aircraft designed for crash safety, the link to the 95th-percentile survivable crash pulse has been dropped, and the recommended design environment is simply presented as the design impact pulses. The severity of a survivable crash pulse may be much greater for the new aircraft than for aircraft having no crash-resistant requirements placed upon them during their development. The extent of the crash protection provided to the occupant cannot indefinitely continue to be linked to the survivability of the crash, as improved crash resistance increases the severity of the survivable crash producing a never-ending increase in the level of crash resistance at the expense of aircraft performance. The crash resistance levels recommended herein are felt to be a near optimum mix of requirements including consideration of life cycle cost, weight, and performance.

Also in earlier editions of the Design Guide, information was provided on design of fixed-wing aircraft. Considering the volume of new information on crash-resistant design and in an effort to ensure that the size of this document remains within reasonable limits, only the primary aircraft in the Army inventory are considered. Therefore, information given herein is intended to apply primarily to rotary-wing aircraft.

2. DEFINITIONS

2.1 GENERAL TERMS

The following text defines words commonly used in discussions of aircraft design crash impact conditions:

- **The Term "G"**

  The ratio of a particular acceleration (a) (a negative acceleration may be referred to as a deceleration) to the acceleration (g) due to gravitational attraction at sea level (32.2 ft/sec^2); G = a/g. With respect to the crash impact conditions, unless otherwise specified, all acceleration values (G) are those at a point approximately at the center of the fuselage floor. In accordance with common practice, this report will refer to accelerations measured in G. To illustrate, it is customarily understood that 5 G represents an acceleration of 5 x 32.2, or 161 ft/sec^2. As a result, crash forces can be thought of in terms of multiples of the weight of objects being accelerated. Therefore, also in keeping with common practice, the term G is used in this document to define accelerations or forces.

- **Survivable Accident**

  An accident in which the forces transmitted to the occupant through his seat and restraint system do not exceed the limits of human tolerance to abrupt accelerations and in which the structure in the occupant's immediate environment remains substantially intact to the extent that a livable volume is provided for the occupants throughout the crash sequence.

- **Survival Envelope**

  The range of impact conditions--including magnitude and direction of pulses and the duration of forces occurring in an aircraft accident--wherein the occupiable area of the aircraft remains substantially intact, both during and following the impact, and the forces transmitted to the occupants do not exceed the limits of human tolerance when current state-of-the-art restraint systems are used.

  It should be noted that, where the occupiable volume is altered appreciably through _elastic_ deformation during the impact phase, survivable conditions may not have existed in an accident that, from postcrash inspection, outwardly appeared to be survivable.

- **Strike Envelope**

  The extent of space surrounding a restrained occupant defined by the flailing of extended body parts during a crash impact of the aircraft. Parts of the body may strike objects located within this envelope.

2.2 AIRCRAFT PARAMETERS

● **Aircraft Coordinates**

Positive directions for velocity, acceleration, and force components and for pitch, roll, and yaw are illustrated in Figure 1.
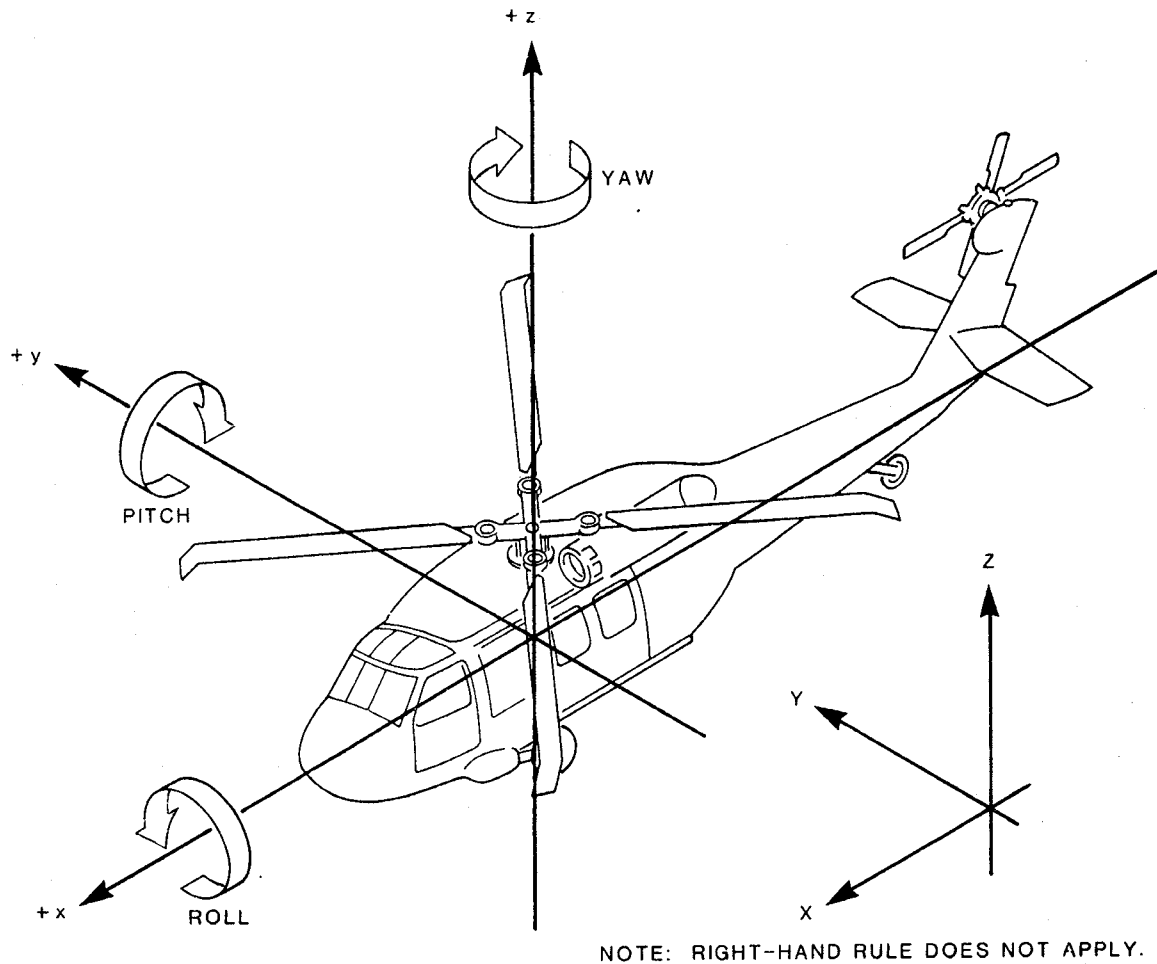
FIGURE 1. AIRCRAFT COORDINATE AND ATTITUDE DIRECTIONS.

● **Velocity Change in Major Impact (ΔV)**

The decrease in velocity of the airframe during the <u>major impact</u>, expressed in feet per second. The <u>major impact</u> is the one in which highest forces are incurred, not necessarily the initial impact. For the acceleration pulse shown in Figure 2, the major impact should be considered ended at time t_2. Elastic recovery in the structure will tend to reverse the direction of aircraft velocity before t_2.

7
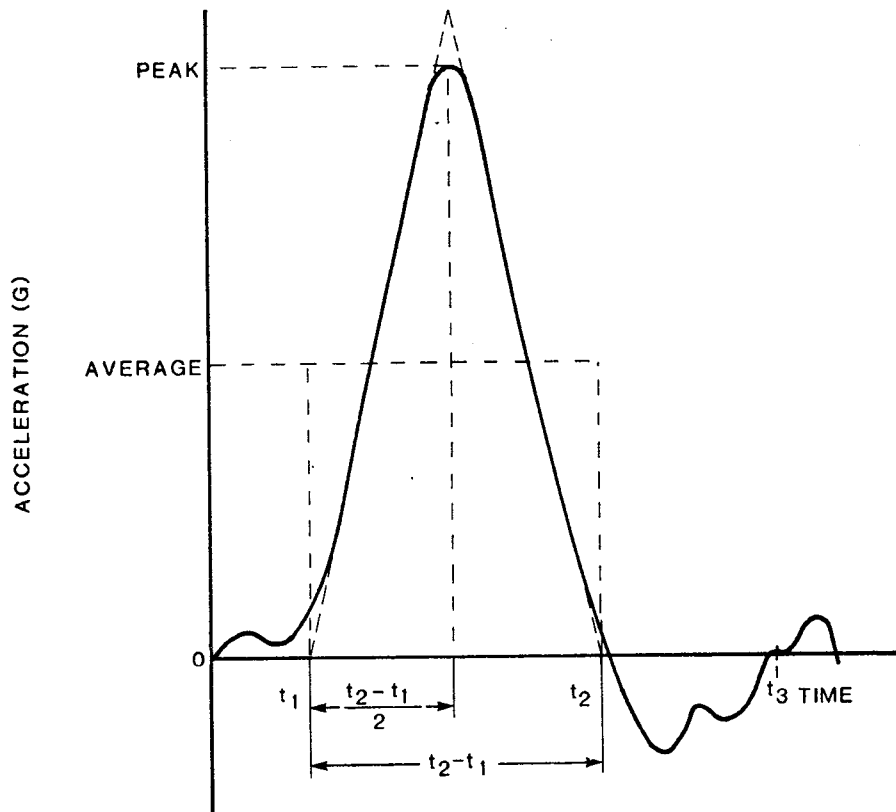
FIGURE 2. TYPICAL AIRCRAFT FLOOR DECELERATION PULSE.

Should the velocity actually reverse, its direction must be considered in computing the velocity change. For example, an aircraft impacting downward with a vertical velocity component of 30 ft/sec and rebounding with an upward component of 5 ft/sec should be considered to experience a velocity change

$$\Delta V = 30 - (-5) = 35 \text{ ft/sec}$$

during the major impact. After the aircraft rebounds upward, gravity will accelerate it downward again, as illustrated by the negative acceleration between t_2 and t_3 in Figure 2.

● Longitudinal Velocity Change

The decrease in velocity during the major impact measured along the longitudinal (roll) axis of the aircraft. The velocity may or may not reach zero during the major impact. For example, an aircraft impacting the ground at a forward velocity of 100 ft/sec and slowing to 35 ft/sec would experience a longitudinal velocity change of 65 ft/sec during this impact.

8

- <u>Vertical Velocity Change</u>

  The decrease in velocity during the major impact measured along the vertical (yaw) axis of the aircraft. The vertical velocity generally reaches zero during the major impact. (Where vertical rebound is present in a crash impact, the rebounding (negative) velocity is additive in calculating the total vertical velocity change.)

- <u>Abrupt Accelerations</u>

  Accelerations of short duration primarily associated with crash impacts, ejection seat shocks, capsule impacts, etc. One second is generally accepted as the dividing point between abrupt and prolonged accelerations. In abrupt accelerations the effects on the human body are limited to mechanical overloading (skeletal and soft tissue stresses), there being insufficient time for functional disturbances due to fluid shifts.

- <u>Rate of Onset</u>

  Rate of application of G's, expressed in G's per second (rate of change of acceleration).

  $$\text{Rate of Onset} = \frac{\Delta G}{\Delta t} \quad \text{(G's per second)}$$

- <u>Flight Path Angle</u>

  The angle between the aircraft flight path and the horizontal at the moment of impact (see Figure 3).

- <u>Terrain Angle</u>

  The angle between the impact surface and the horizontal, measured in a vertical plane (see Figure 3).

- <u>Impact Angle</u>

  The angle between the flight path and the terrain, measured in a vertical plane. The impact angle is the algebraic sum of the flight path angle plus the terrain angle (see Figure 3).

- <u>Attitude at Impact</u>

  The aircraft attitude in degrees at the moment of initial impact. The attitude at impact is stated in degrees of pitch, yaw, and roll (see Figure 1).

UPHILL FLIGHT

DOWNHILL FLIGHT
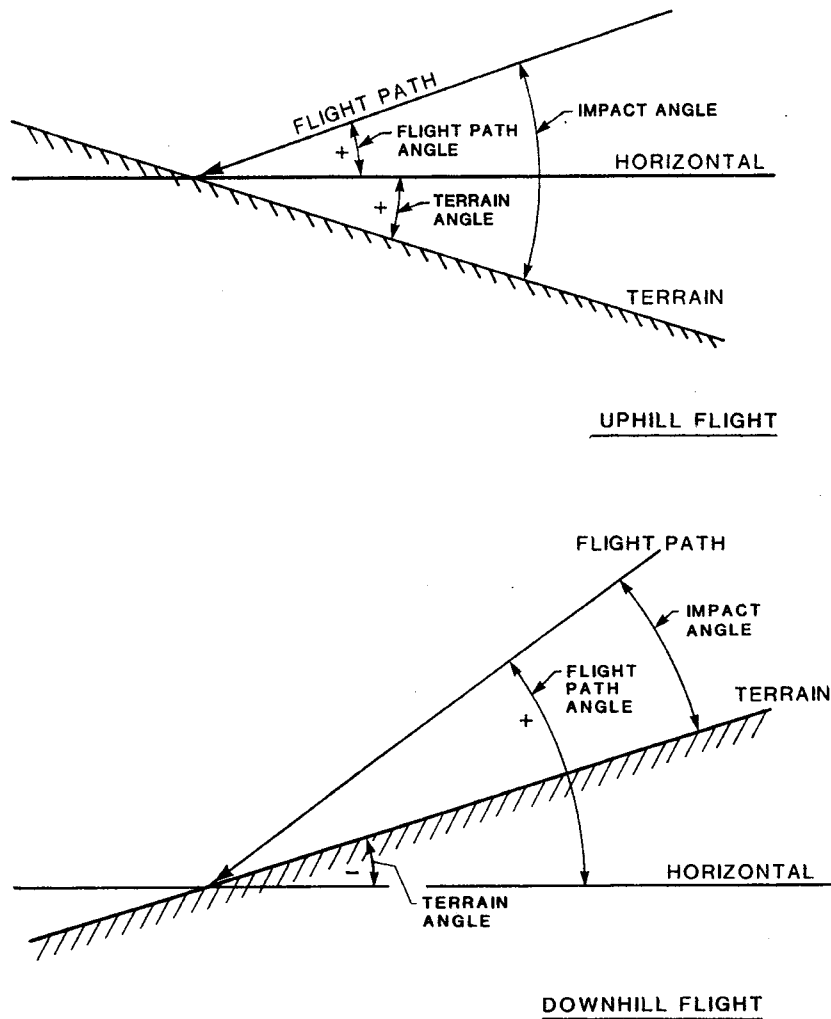
FIGURE 3. SCHEMATIC OF FLIGHT PATH, TERRAIN, AND IMPACT ANGLES.

2.3 HUMAN BODY PARAMETERS

● **Human Body Coordinates**

In order to minimize the confusion sometimes created by the terminology used to describe the directions of forces applied to the body, a group of NATO scientists compiled the accelerative terminology table of equivalents shown in Figure 4 (Reference 2).

Terminology used throughout this guide is compatible with the NATO terms as illustrated.

Headward
$(+G_z)$

Back to chest
(sternumward)
$(+G_x)$

Lateral right
$(+G_y)$

Lateral left
$(-G_y)$

Chest
to back
(spineward)
$(-G_x)$

Tailward
$(-G_z)$

Direction of
accelerative force

Vertical

Headward – Eyeballs-down
Tailward – Eyeballs-up

Transverse

Lateral right – Eyeballs-left
Lateral left   – Eyeballs-right
Back to chest – Eyeballs-in
Chest to back – Eyeballs-out

Note:

The accelerative force on the body acts in the same direction as the arrows.

FIGURE 4. TERMINOLOGY FOR DIRECTIONS OF FORCES ON THE BODY.

● Human Tolerance to Crash Impact Conditions

Obviously, the tolerance of the human body to crash impact conditions is a function of many variables, including the unique characteristics of each person as well as the loading variables. The loads applied to the body include decelerative loads imposed by seats and restraint systems as well as localized forces due to impact with surrounding structure. Tolerable levels of the decelerative loads depend on the direction of the load, the orientation of the body, and the means of applying the load. For example, the critical nature of the loads parallel to the occupant spine manifests itself in any of a number of spinal fractures. Forces perpendicular to the occupant spine can produce spinal fracture through flexure that results from jackknife bending over a lap-belt-only restraint. The lap belt might inflict injuries to the internal organs if it is not retained on the pelvic girdle but is allowed to exert its force above the iliac crests in the soft stomach region. Excessive rotational or translational acceleration of the head can produce concussion. Further, skull fracture can result from localized impact with surrounding structure. Therefore, tolerance is a function of the method of occupant restraint as well as the variable of specific occupant makeup.

For the purpose of this document, human tolerance is defined as a selected array of parameters that describe a condition of decelerative loading for which it is believed there is a reasonable probability for survival without major injury. As used in this volume, designing for the limits of human tolerance refers to providing design features that will maintain these conditions at or below their tolerable levels to enable the occupant to survive the given crash impact conditions.

- ## Submarining

A rotation of the hips under and about the lap belt as a result of a forward inertial load exerted by deceleration of the thighs and lower legs accompanied by lap belt slippage up and over the iliac crests. Lap belt slippage up and over the iliac crests can be a direct result of the upward loading of the shoulder harness straps at the center of the lap belt.

- ## Dynamic Overshoot

The amplification of decelerative force on cargo or personnel above the floor input decelerative force (ratio of output to input). This amplification is a result of the dynamic reponse of the system.

- ## Rebound

Rapid return toward the original position upon release or rapid reduction of the deforming load, usually associated with elastic deformation.

- ## Anthropomorphic Dummy

A device designed and fabricated to represent not only the appearance of humans but also the mass distribution, joint locations, motions, geometrical similarities such as flesh thickness and load/deflection properties, and relevant skeletal configurations such as iliac crests, ischial tuberosities, rib cages, etc. Attempts are also made to simulate human response of major structural assemblages such as thorax, spinal column, neck, etc. The dummy is strapped into seats or litters and used to simulate a human occupant in dynamic tests.

3. AIRCRAFT DESIGN CRASH IMPACT CONDITIONS

3.1 INTRODUCTION

Design crash impact conditions for Army aircraft are specified by MIL-STD-1290, "Light Fixed- and Rotary-Wing Aircraft Crash Resistance" (Reference 1). This standard contains complete information on impact velocities, angles, and attitudes to be used by aircraft designers to assure that structures will satisfy crash-resistance requirements. These criteria for new aircraft development were initially substantiated through the use of actual crash and engineering test data.

3.2 HISTORICAL DEVELOPMENT OF CRITERIA

The major source of data for initial development of impact conditions was actual crash data for U.S. Army aircraft. Data were accumulated through a study of U.S. Army accidents for the periods 1 July 1960 through 30 June 1965 and 1 January 1971 through 31 December 1976. Data from before 1977 considered pertinent were also obtained from FAA (then Civil Aeronautics Board), U.S. Navy, and U.S. Air Force accident reports.

Rotary-wing and light fixed-wing aircraft of mission gross weight no greater than 12,500 lb were included. The accident cases selected were limited to those in which one or more of the following factors applied: (1) Substantial structural damage, (2) postcrash fire, (3) personnel injuries, and (4) at least one person survived the crash. Mid-air collisions and other accidents resulting in catastrophic uncontrolled free falls from altitudes of 100 ft or more were not considered. Such accidents almost invariably result in random, unpredictable crash kinematics and nonsurvivable impact forces, and are of little value in establishing realistic crash survival envelopes that would be useful to the aircraft designer. Analysis of impact forces in many of the accidents involving fire was impossible due to extensive burn damage to the aircraft.

Altogether, 563 rotary-wing accidents and 92 fixed wing accidents were reviewed in the preparation of earlier editions of the Design Guide. Impact attitude data from an additional 108 attack and 10 cargo helicopters (mission gross weight greater than 12,500 lb) collected during 1971-1976 were also utilized in the preparation of later editions.

Analysis of the data from Army accident records showed a similarity in impact conditions between rotary- and light fixed-wing STOL aircraft (O-1, U-6, U-1). Except for the lateral direction, the similarities between rotary-wing and light STOL aircraft impact conditions were sufficient to allow treating them as being the same.

The major velocity change was estimated for each of the cases used. This was done for all three coordinate axes. Design impact conditions were then selected such that 95 percent of the cases used were within the selected values. These impact conditions were thought to include all crash conditions for which it would be economically and technically feasible to provide crash protection. The initial criteria were assumed to be applicable, since survivors had experienced crashes of equivalent severity.

Subsequent examination of the crash data supported the criteria in general. However, all data from such studies were not directly comparable, because later data involved newer, more crash-resistant aircraft and survival in more severe crashes could be expected. Economic and operational constraints did eventually necessitate that the criteria be relaxed in several areas. Specifically, longitudinal velocity changes and attitude angles were reduced as a result of trade-offs of crash-resistance factors with operational factors. However, lateral and vertical velocity change criteria remain unchanged from the original recommendations (1-G lift was added to the vertical impact criteria).

3.3 IMPACT CONDITIONS

MIL-STD-1290 specifies seven impact conditions which must be considered in the design of the aircraft. These criteria were developed as an optimized design criteria based on crash statistics (described in the previous section), human tolerance, system cost, weight, and performance. The criteria are shown in Table 1.

TABLE 1. CRASH IMPACT DESIGN CONDITIONS, WITH LANDING GEAR EXTENDED, MIL-STD-1290

Condition No.	Impact Direction (Aircraft Axes)	Object Impact	Velocity Change ΔV (ft/sec)
1	Longitudinal (cockpit)	Rigid	20
2	Longitudinal (cabin)	vertical barriers	40
3	Vertical*	Rigid	42
4	Lateral, Type I**	horizontal	25
5	Lateral, Type II***	surface	30
6	Combined high angle*	Rigid	
	Vertical	horizontal	42
	Longitudinal	surface	27
7	Combined low angle	Plowed	
	Vertical	Soil	14
	Longitudinal		100

*For the case of retracted landing gear the seat and airframe combination shall have a vertical crash impact design velocity change capability of at least 26 ft/sec.
 **Type I - Light fixed-wing aircraft.
***Type II - Rotary-wing, including tilt-prop/rotor aircraft.

3.3.1 Longitudinal (ΔV_x) Impact

In MIL-STD-1290 the designer is required to demonstrate analytically that the basic airframe is capable of impacting longitudinally into a rigid vertical barrier at a contact velocity of 20 ft/sec without crushing the pilot and copilot stations to an extent which would either preclude pilot and copilot evacuation of the aircraft or preclude a livable volume for the aircraft occupants. For this impact, the engine(s), transmission, and rotor system are required to remain intact and in place in the aircraft. The basic airframe's capability to impact longitudinally into a rigid barrier or wall at a contact velocity of 40 ft/sec without reducing the length of the passenger/troop compartment by more than 15 percent should be demonstrated analytically. Any consequent inward buckling of walls, floor, and/or roof is not to be hazardous to the occupants and/or restrict their evacuation.

3.3.2 Vertical (ΔV_z) Impacts

MIL-STD-1290 requires the designer to analytically demonstrate the capability of the aircraft system, with rotor/wing lift equal to design gross weight (DGW) and with landing gear extended, to withstand vertical impacts of 42 ft/sec on a rigid horizontal surface without (1) reducing the height of the cockpit and passenger/troop compartments by more than 15 percent and (2) allowing the occupants to experience injurious accelerative loading. For vertical impacts higher than 42 ft/sec, the crew and troop compartments should preclude catastrophic collapse of overhead structure and maintain a survivable volume for occupants. It is desired that in a 50 ft/sec impact the height of occupiable areas not be reduced by more than 50 percent and that surrounding structures not fracture. For the case of retracted landing gear the designer is required to analytically demonstrate the capability of the aircraft to withstand impacts of at least 26 ft/sec on a rigid horizontal surface without (1) reduction in height of the cockpit and passenger/troop compartments of more than 15 percent or (2) causing the occupants to experience injurious accelerative loading. The above capabilities, with gear up or down, are required for all aircraft orientation (attitudes) upon impact in $+15^0$ to -5^0 pitch and $\pm 10^0$ roll as defined in Figure 5A (taken from MIL-STD-1290).

3.3.3 Lateral (ΔV_z) Impacts

Lateral accelerations are found to be present particularly in accidents where a rotary-wing aircraft autorotated into trees or where rotor blades struck trees or other obstacles during normal operation (Reference 3). Impact with trees often causes the fuselage to rotate and finally impact the ground on its side. Two out of three helicopters that hit the ground with a yaw are subjected to enough lateral forces to cause them to roll over (Reference 4). Roll over impacts are discussed in Section 3.2.5.

The designer should demonstrate the capability of the aircraft to withstand lateral impacts of 30 ft/sec without reducing the width of occupied areas by more than 15 percent. To design for this impact, the engine(s), transmission, and rotor system need not be considered intact or retained on the aircraft.

15
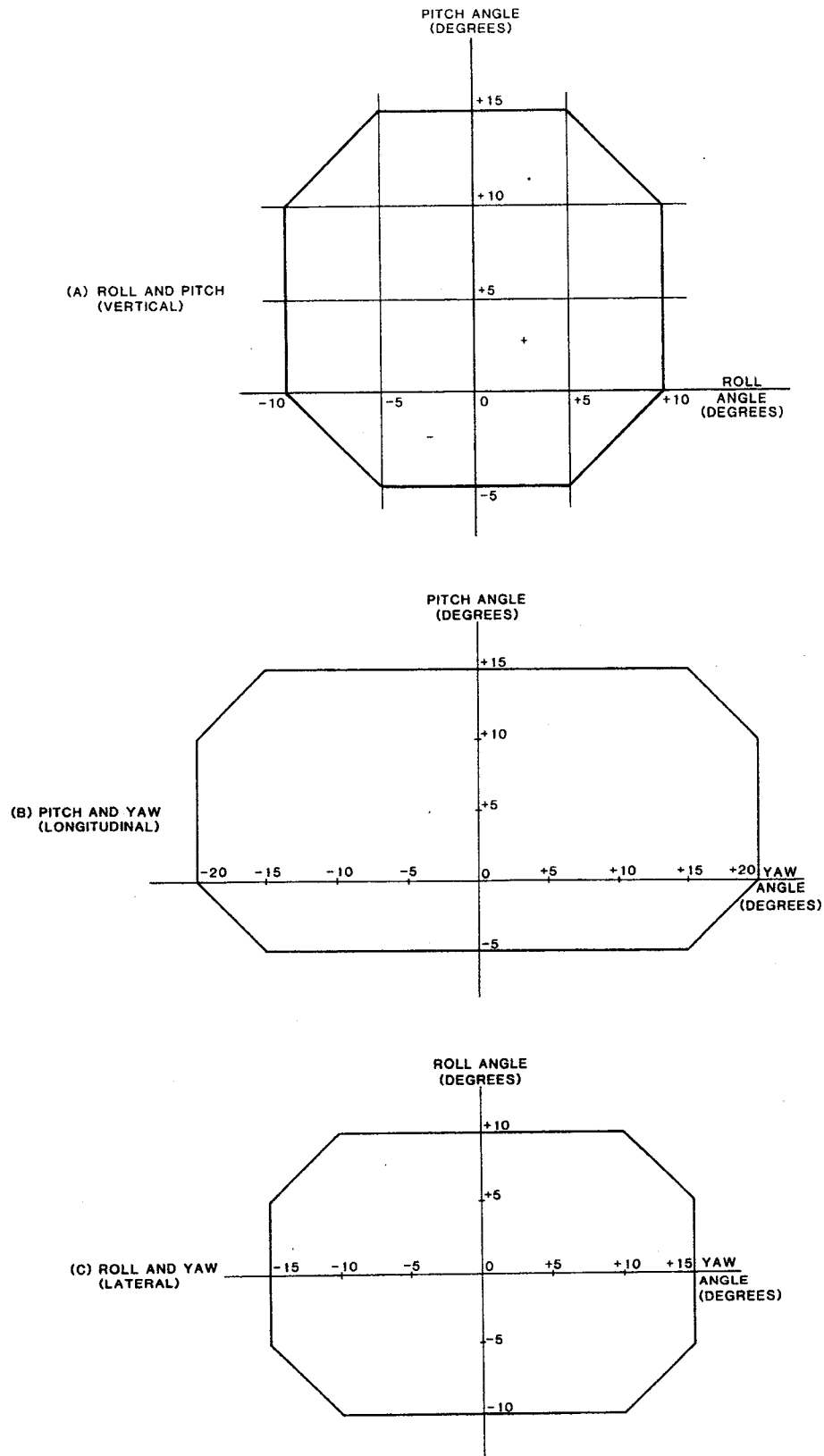
FIGURE 5. AIRCRAFT IMPACT ATTITUDES ENVELOPES.

16

3.3.4 Combined Impacts

The designer should analytically demonstrate the capability of the aircraft, with 1G DGW rotor/wing lift and with landing gear extended, to withstand the following combined impacts without a reduction of the cockpit or cabin compartments that would seriously injure the occupants: (1) a combined impact on a rigid horizontal surface with vertical and longitudinal velocity changes of 42 and 27 ft/sec respectively, and (2) a combined impact on plowed soil for the conditions described in Figure 6.


```
                    IMPACT CONDITIONS

         1. SOIL OF CALIFORNIA BEARING RATIO = 2.5
         2. AIRCRAFT PITCH (β) = 5° NOSE DOWN
         3. AIRCRAFT ROLL (δ) = ±10°
         4. AIRCRAFT YAW (γ) = ±20°
         5. FLIGHT PATH ANGLE (α) = −8° DOWN
         6. GROUND IMPACT SPEED = 100 FT/SEC
         7. IMPACT SINK SPEED = 14 FT/SEC
```
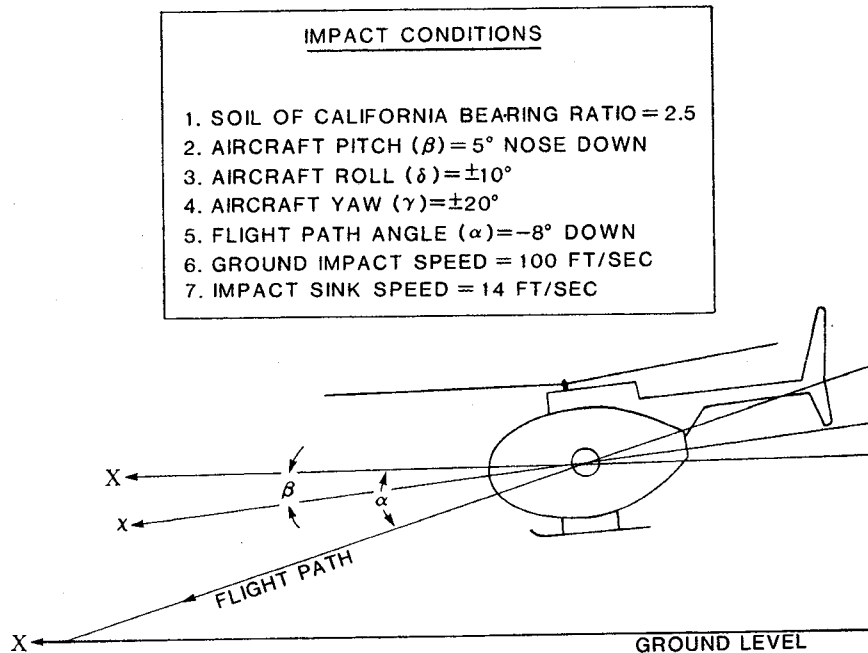
FIGURE 6.   LOW ANGLE IMPACT DESIGN CONDITIONS.

3.3.5 Rollover Impacts

The aircraft should be designed to resist an earth impact loading as occurs when the aircraft strikes the ground and rolls to either a 90° (sideward) or 180° (inverted) attitude. If the forward fuselage roof or side can impact the ground, assume it is buried to a depth of 2.0 in. in soil and the load is uniformly distributed over the forward 25% of the occupiable fuselage length. The fuselage should sustain a 4 G (i.e., 4x aircraft DGW) load applied over the area(s) described for either inverted or sideward attitudes without permitting deformation sufficient to cause injury to seated, restrained occupants. For both cases, the 4 G distributed load shall be analyzed for any angle of load application ranging from perpendicular to the fuselage skin (i.e., compressive loading) to parallel to the fuselage skin (i.e., shear loading). When designing for this condition, assume that emergency exit doors and windows cannot carry any loading.

17

Where the aircraft configuration precludes the occurrence of the above, an alternate design criterion should be applied. The aircraft should be assumed to be resting inverted on the ground in the most likely attitude which is critical for the safety of the occupants. Loads should then be individually applied locally and consist of the following multiplication factors times the DGW:

1. Perpendicular to the ground: 4

2. Parallel to the ground, along the longitudinal axis: 4

3. Parallel to the ground, along the lateral axis: 2

MIL-STD-1290 does specify a complete range of pitch and roll angles to be considered by the designer. As stated above, for vertical impacts Figure 5A shows that pitch may range from $+15^\circ$ to -5° and roll from $+10^\circ$ to -10°. However, when pitch and roll are combined, the extremes are limited, as shown by the figure; for example, the designer need not consider $+15^\circ$ pitch combined with $+10^\circ$ roll. The criteria were modified in this way because of the lesser probability of these combined conditions and because of severe fuselage weight penalties associated with combined extremes of pitch and roll.

MIL-STD-1290 does not prescribe off-axis attitudes for longitudinal and lateral impacts. However, to assure survivability in such impacts with pitch, yaw, or roll, it is recommended that envelopes of impact attitude also be considered in the design phase for longitudinal and lateral impacts. Recommended envelopes are shown in Figures 5B and 5C, respectively.

4. OCCUPANT EXPOSURE DATA

4.1 INTRODUCTION

The conditions to which an aircraft occupant is exposed during a crash play a major role in occupant survivability. This chapter summarizes a study on injury in U.S. Army helicopter crashes (Reference 5) during a six-year period, 1980-1985. The type and number of aircraft are listed in Section 4.2. Typical impacted terrain is discussed in Section 4.3, and frequency and mechanisms of injury are addressed in Sections 4.4 and 4.5, respectively.

4.2 ACCIDENT STATISTICS

A study reporting the injury patterns and mechanisms in U.S. Army helicopter crashes was conducted over a six-year period, 1 October 1979 to 30 September 1985 (Reference 5). All U.S. Army Class A and B mishaps involving AH-1 (Cobra), OH-58 (Kiowa), UH-1 (Iroquois), and UH-60 (Black Hawk) helicopters were analyzed for this study. Class A mishaps are defined as mishaps that result in a total cost of property damage, occupational illness, or injury that is $500,000 or greater or an aircraft is destroyed, or permanent total disability or a fatality occurs. Class B mishaps are defined as mishaps in which the total cost of property damage and personnel injuries is greater than $100,000 but less than $500,000, or permanent partial disbility or hospitalization of five or more personnel in a single occurrence occurs (Reference 6). Mishaps of lesser degree were not included in the study since they usually do not involve significant ground impact or injury. The data was obtained from computer data tapes supplied by the U.S. Army Safety Center.

4.2.1 Number of Aircraft

Included in the study were 303 aircraft involved in 298 separate mishaps during the six-year analysis period. More than one aircraft was involved in five of the mishaps. Table 2 lists the total number of aircraft, by type, used in this study. In comparison, each aircraft varies in size, capacity, performance, and mission requirements, as seen in Table 3. It should also be recognized that the Black Hawk is the only one of the study aircraft for which crash resistance was a major design objective.

TABLE 2. U.S. ARMY AIRCRAFT IN ACCIDENT
STUDY FOR FY 1980 - FY 1985

Type	Class A	Class B	Number
AH-1	37	17	54
OH-58	69	16	85
UH-1	99	35	134
UH-60	23	7	30
Total	228	75	303

19

TABLE 3. AIRCRAFT COMPARISON DATA

Designation	Name	Mission	Seating Capacity	Gross Weight (lb)	Maximum Speed (kt)
AH-1S	Cobra	Attack	2	10,000	190
OH-58C	Kiowa	Observation	4	3,200	120
UH-1H	Huey	Utility	13	9,500	124
UH-60A	Black Hawk	Utility	16	20,250	193

4.2.2 Number of Accidents

During the six-year study period, there were 223 Class A mishaps and 75 Class B mishaps. This represents 84 percent of all Army Class A and B helicopter mishaps occurring over the six-year period.

4.2.3 Accident Rates

The Class A, B, and combined accident rates for the four study aircraft during the six-year period are summarized in Table 4. The relative risk of having a Class A or B mishap for the UH-60 and AH-1 series aircraft was approximately three times that of the UH-1, whereas the OH-58 has a mishap rate only slightly higher than that of the UH-1.

TABLE 4. MISHAP RATES BY AIRCRAFT TYPE FOR FY 1980 - FY 1985 (MISHAPS PER 100,000 FLYING HOURS)

Type Aircraft	Class A	Class B	Total	Relative Risk
AH-1	5.6	2.6	8.2	2.7
OH-58	4.0	0.9	4.9	1.6
UH-1	2.2	0.8	3.0	1.0
UH-60	6.9	2.5	9.4	3.1

4.3 IMPACTED TERRAIN

The probability of impacting a given type of terrain may influence an air-
craft design in several ways. For example, the types of landing gear and the
escape systems installed may be based on the terrain most likely to be encoun-
tered in operation. An analysis of terrain characteristics was made using
the data from the previously mentioned study of the 298 reported mishaps.
Table 5 lists the distribution of the general terrain characteristics into
which the aircraft impacted. Of the 303 aircraft involved, 13 accident
reports listed two types of the terrain, 216 listed one, and 74 had no com-
ments. This resulted in a total of 242 responses. Table 6 lists the types
of surface impacted by the 303 aircraft; 13 reports had two types, 228 re-
ports listed one type, and 62 had no comments, resulting in a total of 254
responses.

TABLE 5. DISTRIBUTION OF THE GENERAL TERRAIN
IMPACTED BY ARMY AIRCRAFT DURING THE
PERIOD FY 1980 - FY 1985

Terrain	Number of Aircraft	Percent
Flat	84	34.7
Water	14	5.8
Rolling	78	32.2
Desert	18	7.4
Mountains	48	19.8
Total	242	99.9

TABLE 6. DISTRIBUTION OF THE SURFACE IMPACTED
BY ARMY AIRCRAFT DURING THE PERIOD
FY 1980 - FY 1985

Surface	Number of Aircraft	Percent
Prepared Surface	33	13.0
Sod	160	63.0
Soggy	38	15.0
Ice	3	1.2
Snow	16	6.3
Water	4	1.6
Total	254	100.1

21

These data show that 87 percent of impacted surfaces were unprepared. Thus, energy-absorbing landing gear cannot be expected to function with full efficiency in many accidents. Therefore, as much energy absorption as possible should be achieved by the seats, as they are not terrain sensitive. The lower fuselage structure should also be designed to minimize the effects of plowing or earth scooping during a longitudinal impact (Volume III). For a primarily vertical impact, loose soil would prove beneficial through additional energy being absorbed by soil compaction. On the other hand, in a primarily horizontal (longitudinal and/or lateral) impact, loose soil may increase deceleration due to earth scooping.

4.4 IMPACT INJURY FREQUENCY

The Army classifies all mishaps according to survivability: survivable, partially survivable, or nonsurvivable (Reference 7). A survivable mishap is one in which the forces at impact were considered to be within the limits of human tolerance. The occupied volume in a survivable mishap must also be sufficiently maintained throughout the crash sequence to permit occupant survival in all potentially occupied areas. A nonsurvivable mishap is one in which either of these two conditions is not met in all potentially occupied positions. Partially survivable mishaps have some survivable and some nonsurvivable positions. These judgments are made by the investigation board based solely on the condition of the aircraft after impact without consideration of actual occupancy or injury sustained by the occupants. This classification method was used to categorize the data discussed in the following sections.

4.4.1 Number of Occupants and Injuries

During the six-year study period, FY 1980 through 1985, there were 1,060 occupants aboard the mishap aircraft. The injured occupants numbered 611, of which 136 were fatally injured. Table 7 lists the number and kind of injuries. Distinction between disabling and nondisabling injury was made based on the criteria established in DA PAM 385-95 (Reference 7).

TABLE 7. NUMBER OF OCCUPANTS AND INJURIES
            FY 1980 - FY 1985

Injury	Number Of Occupants
Fatalities	136
Disabling Injury	372
Nondisabling Injury	103
No Injury	449
Total Number of Aircraft Occupants	1060

4.4.2 Injury by Body Region

When considering crash-resistance improvements to an airframe, it is important to know what regions of the body are at risk for injury, particularly in survivable crashes. Table 8 shows the distribution by body region of all 2,090 injuries reported over the 1980-1985 study period for all mishaps and for survivable mishaps. This injury total represents all reported injuries (an occupant may have had more than one injury). Note that the severity of each injury has been encoded in the Army Safety Center data base only since 1983. As a result, the majority of injuries considered were not classified according to severity. In Table 8, therefore, "All Injury" includes all reported injuries and all unclassified injuries, and "major/fatal" injuries represents all fatal and major injuries reported since 1983.

The most frequent form of fatal injury identified in survivable helicopter crashes was head injury (62.5 percent). This occurred despite mandatory use of flight helmets by helicopter crewmembers. The second most common location of fatal injury was the thorax (18.8 percent).

TABLE 8. DISTRIBUTION OF INJURY BY BODY REGION (PERCENT)

Body Region	All Mishaps			Survivable Mishaps		
	All Injury (N=2090)	Major/ Fatal (N=545)	Fatal (N=214)	All Injury (N=1484)	Major/ Fatal (N=260)	Fatal (N=32)
General	3.8	4.6	6.1	1.8	1.9	6.3
Head	23.8	27.0	41.1	22.9	26.2	62.5
Neck	3.7	0.9	0.5	4.9	1.5	0
Cervical Spine	2.3	2.8	3.7	1.6	3.9	12.5
Thorax	19.1	28.6	42.5	14.3	18.5	18.8
Abdomen	6.7	6.2	4.7	5.3	5.0	0
Vertebrae (thoracic and lumbar)	6.5	9.2	1.4	6.5	12.3	0
Upper Extremities	12.3	7.3	0	15.5	9.6	0
Lower Extremities	21.7	13.8	0	27.4	21.2	0

Note: There were 8 injuries for which a body region was not assigned.

Although extremity injuries generally do not result in fatalities, they constituted an excessively high percentage of the total injuries. Extremity injuries are of considerable concern in the military because they hinder egress from a damaged, and possibly burning, aircraft.

Abdominal injury was relatively rare in Army helicopter crashes constituting only 5.3 percent of injuries in survivable mishaps. The majority of abdominal injuries were superficial, consisting of contusions, abrasions, and lacerations. No fatal abdominal injuries were reported.

4.4.3 Injury by Aircraft

Table 9 summarizes the degree of occupant injury for crashes involving the AH-1, OH-58, UH-1, and UH-60 during the six-year study period. For all mishaps, the UH-60 had a higher percentage of fatalities relative to the other aircraft because of higher impact velocities. For survivable crashes, the table shows that the degree of injury is similar to that of the other aircraft.

TABLE 9. DEGREE OF INJURY FOR OCCUPANTS OF CLASS A AND B MISHAPS

All Mishaps

	Fatal	Disabling	Nondisabling	No Injury	Total
AH-1	23(19.8)	31(26.5)	14(11.8)	49(41.9)	117
OH-58	24(10.8)	88(39.8)	20 (9.1)	89(40.3)	221
UH-1	55 (9.3)	214(36.2)	60(10.1)	263(44.4)	592
UH-60	34(26.2)	39(30.0)	9 (6.9)	48(36.9)	130
	136(12.8)	372(35.1)	103(9.7)	449(42.4)	1,060

Survivable Mishaps

	Fatal	Disabling	Nondisabling	No Injury	Total
AH-1	7(7.1)	31(31.3)	14(14.1)	47(47.5)	99
OH-58	12(6.1)	86(43.4)	20(10.1)	80(40.4)	198
UH-1	17(3.2)	208(38.5)	59(10.9)	256(47.4)	540
UH-60	7(8.1)	31(36.1)	9(10.5)	39(45.4)	86
	43(4.7)	356(38.6)	102(11.1)	422(45.7)	923

( ) Indicates row percent.

Table 10 shows that the vertical velocity change in the survivable crashes was much greater for the UH-60 than for the other three aircraft. The mean velocity change was twice that experienced by the other aircraft, and the velocity change experienced in the most severe 5 percent of the survivable accidents exceeded the design criteria of 42 ft/sec identified in Section 3.

TABLE 10. VERTICAL VELOCITY CHANGE IN SURVIVABLE CRASHES (FEET PER SECOND)

Aircraft	Mean	95th-Percentile
AH-1	13.5	39.3
OH-58	12.5	29.5
UH-1	11.5	33.5
UH-60	28.9	47.2

This clearly demonstrates the benefits of a crash-resistant aircraft design. The same degree of injury is being experienced, but in more severe crashes. The higher impact velocities for the UH-60 are probably due to different performance characteristics and a higher percentage of severe crashes associated with a new aircraft as well as the fact that greater crash resistance places more severe crashes in the survivable category.

When the distribution of injury by body region was compared among the four study aircraft using chi-square analysis, it was determined that the AH-1, OH-58, and UH-1 had similar distributions which differed from the distribution seen in the UH-60. Table 11 compares the injury distribution by body region of the UH-60 versus the other three aircraft combined for all survivable mishaps, and Figure 7 graphically illustrates this comparison. When survivable mishaps were considered, there was a significantly greater proportion of thoracic injury in the UH-60 for both the all-injury category and the major/fatal category.

A reciprocally lower incidence of spinal and lower extremity injuries in the UH-60 is shown. The reduced number of spinal injuries is attributed to the crash-resistant crewseats used in the UH-60, which are designed to reduce the G loads on the occupant's spine. Similarly, the reduced incidence of lower extremity injuries may be related to the crash-resistant seating structure.

25

TABLE 11.   DISTRIBUTION OF INJURY BY BODY REGION (PERCENT) –
COMPARISON BETWEEN UH-60 AND OTHER HELICOPTERS

| | Survivable Mishaps | | | |
| | All Injuries N = 1484 | | Major/Fatal Injuries N = 260 | |
Body Region	UH-60	Other	UH-60	Other
General	3.5	1.5	1.4	2.2
Head	26.9	22.3	23.0	27.4
Neck	2.9	5.1	0	2.2
Cervical Spine	0.6	1.7	1.4	4.8
Thorax	25.2	12.8	35.1	11.8
Abdomen	5.3	5.2	8.1	3.8
Vertebrae (thoracic and lumbar)	4.7	6.8	6.8	14.5
Upper Extremities	11.7	16.0	8.1	10.2
Lower Extremities	19.3*	28.3*	16.2	23.1
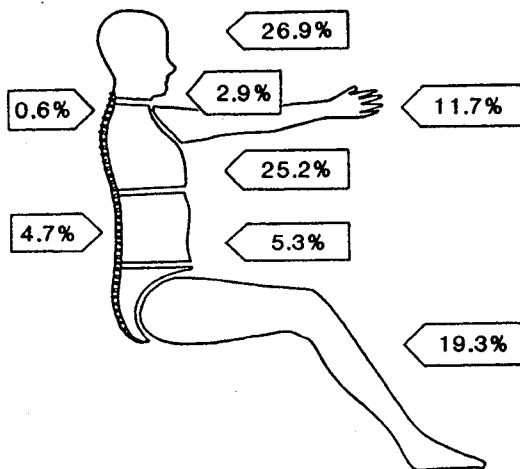
a. Frequency of all injuries,
   UH-60.
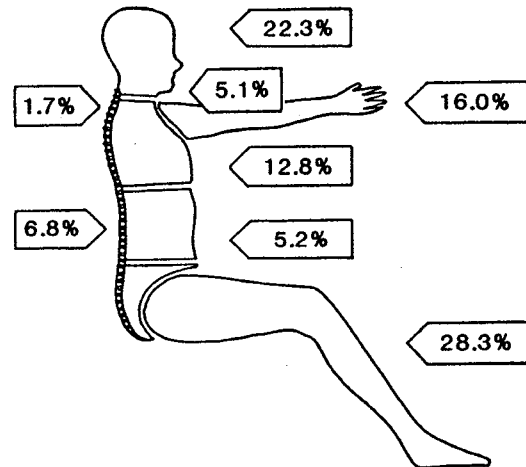
c. Frequency of all injuries,
   UH-1, AH-1, OH-58.
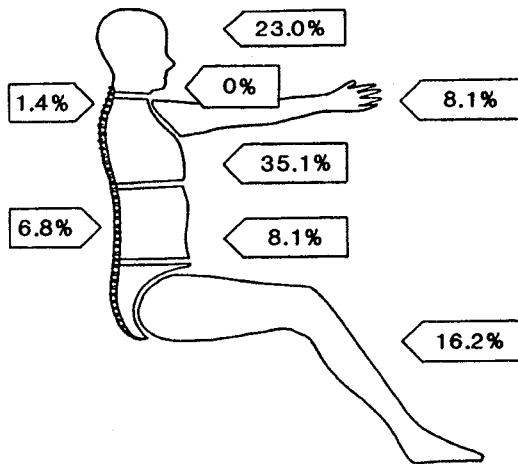
b. Frequency of major and fatal
   injuries, UH-60.
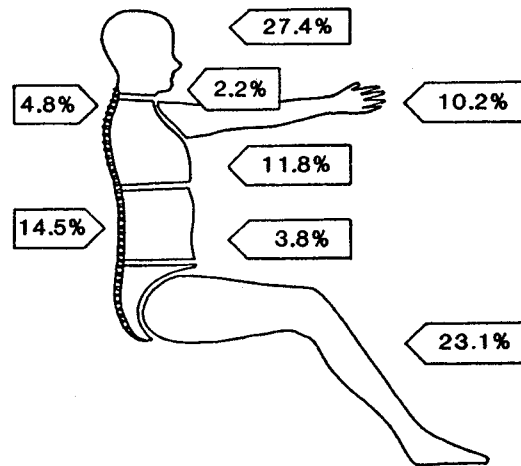
d. Frequency of major and fatal
   injuries, UH-1, AH-1, OH-58.

FIGURE 7. DISTRIBUTION OF INJURIES TO BODY PARTS IN SURVIVABLE
           U.S. ARMY AIRCRAFT ACCIDENTS, 1980-1986.

27

4.5 MECHANISMS OF INJURY

Mechanisms of injury have been required to be reported for each injury occurring in Army aviation mishaps since 1983. Table 12 summarizes the reported mechanisms for these injuries.

TABLE 12. MECHANISMS OF INJURY IDENTIFIED IN SURVIVABLE CLASS A AND B MISHAPS

Struck/By/Against	345	(60.1)	Caught In Or Under		33	(5.7)
Int. Obj./Structure	128		Aircraft	15		
Seat/Seat Armor	35		Instrument Panel	4		
Cyclic	17		Restraint System	7		
External Object/			Other	7		
Intruding Object	31					
Console	10		Experienced/Exposed To		117	(20.4)
Instrument Panel	9		Excess Decel. Forces	71		
Ceiling	4		Mult. Mechanisms	24		
Door	9		Fire	4		
Windshield	8		Other	18		
Litter	4					
Collective	6		Thrown From Aircraft		21	(3.7)
Floor	6					
Restraint	26		Unknown		58	(10.1)
Unknown	37					
Other	8					
Helmet	7		Total		574	(100.0)

( ) Indicates percent.

5. HUMAN TOLERANCE TO IMPACT

5.1 INTRODUCTION

The objective of this chapter is to provide the designer of aircraft systems with a summary of available information on tolerance of the human body to forces of the type experienced in crash situations. Knowledge of human tolerance is vital to understanding and effectively applying the principles of crash resistance design that are defined elsewhere in this guide.

A great deal of research has been conducted in the field of biodynamics, and general guidelines and approximate end points have been determined. However, there still remain many areas of uncertainty and disagreement, and much more research is needed to provide accurate, proven figures. An obvious difficulty is that the usual test method of stressing a specimen beyond the point of failure in order to establish tolerance limits is not possible when one is dealing with injurious and fatal ranges of forces acting on the human body. Experiments using human volunteers have necessarily been conducted, for the most part, at subcritical levels. The few instances that have inadvertently approached the critical range of forces have provided valuable, but often unverifiable, data. Test animals such as chimpanzees, monkeys, bears, pigs, and mice have been used in attempts to establish a better definition of the injurious and fatal ranges of forces. Human cadavers also have been utilized as test specimens. While these approaches have provided valuable data in many areas of investigation, a means of reliably extrapolating these results to the tolerance of a live human is not yet available.

As discussed in Volume IV, mathematical models of the human body have been used successfully in studying the overall kinematic response of the body to crash forces and in evaluating the crash resistance of vehicle interiors. Mathematical models directly related to injury prediction are discussed in this chapter. Anthropomorphic dummies, as mechanical models, have been refined to remarkable levels of physical resemblance to the human body. However, interpreting the results from mathematical and mechanical simulators remains a problem, as tolerable levels of the predicted variables are neither well defined nor widely agreed upon.

The following sections discuss the factors that affect human tolerance to impact and summarize the existing data on tolerable levels for various body parts. An in-depth review of research in human tolerance before 1970 can be found in Reference 9.

5.2 FACTORS AFFECTING HUMAN TOLERANCE

5.2.1 Body Characteristics

The tolerance of the human body to impact forces depends on a number of variables, including characteristics of the individual such as age, sex, and general state of health. Military systems can be expected to be used by personnel who are generally younger and in better physical condition than the general population for which much tolerance data has been obtained. Thus, in some cases, a degree of conservatism may be built into the application of tolerance criteria in designing Army aircraft. However, whole-body tolerance criteria have been based on experiments involving subjects seated with "correct" upright posture.

Because a helicopter pilot is unlikely to maintain such posture in flight, particularly when near the ground, tolerable levels of such variables as $+G_z$ may be significantly reduced under actual crash conditions.

5.2.2 Restraint System

The overall probability of survival in a crash depends to a large extent on the manner of restraint. It would be extremely difficult to prevent the arms and legs from contacting the cabin interior during a severe impact, but the use of upper and lower torso restraints to prevent such critical body parts as the head and chest from striking surrounding structure can significantly reduce the probability of serious or fatal injury under given crash conditions.

The method of body restraint, of all the factors affecting human tolerance, offers the designer the greatest opportunity for effective application of crashworthy design. The effectiveness of the restraint system is dependent upon the area over which the total force is distributed, the location on the body at which the restraint is applied, and the degree to which it limits residual freedom of movement (Reference 10).

The greater the contact area between the body and the restraint system, the greater the human tolerance. The restraint system should be located on the body at those points that are best able to withstand the loads exerted by the decelerative force and that are best able to distribute further the force to the remainder of the body. These points are primarily the pelvic girdle and the shoulder structure. An additional restraint around the rib cage has been shown to increase tolerance to spineward, eyeballs out $(-G_x)$ accelerations. Restraint systems located over soft tissue tend to be much less effective, often resulting in crushing of the viscera between the restraint system and body structures. Residual freedom of movement should be limited to an absolute minimum consistent with the necessary comfort and movements required by the duties of the occupant.

5.2.2.1 Lap Belt. When restrained only by a lap belt, the occupant's tolerance to abrupt acceleration is relatively low. A complete analysis of the effect of lap-belt-only restraint on human tolerance is presented in Reference 11. The author reviewed all available existing data from dynamic tests of volunteer human subjects applicable to transport aircraft crash conditions and established minimum human tolerance levels for transport aircraft seat design. Since the data were acquired in human subject testing, the tolerance levels are minimum levels and survivable tolerance levels may be substantially higher.

In forward-facing seats, a longitudinal impact will cause a rotation of the upper torso over the belt, a whipping action of the head, and often impact of the upper torso on the legs, resulting in chest, head, and neck injuries. Head injuries due to impacts with the surrounding environment are very common for occupants restrained only with lap belts. When longitudinal forces are combined with a vertical component, there is a tendency for the occupant to slip under the belt to some degree. This motion, often referred to as submarining, can shift the belt up over the abdomen. The longitudinal component of the pulse then causes the upper torso to flex over the belt, with the restraining force concentrated at some point on the spine and not on the pelvic girdle. In this configuration, tolerance is extremely low.

5.2.2.2 Shoulder Harness and Lap Belt Tiedown Strap. The addition of a shoulder harness greatly reduces injuries from head impacts and helps to maintain proper spinal alignment for strictly vertical impact forces. However, this standard configuration may be unsatisfactory for impacts with both vertical and longitudinal components. Pressure by the upper torso against the shoulder straps causes these straps to pull the lap belt up into the abdomen and against the lower margin of the rib cage. This movement of the lap belt allows the pelvis to move forward under the lap belt, causing severe flexing of the spinal column, as shown in Figure 8. In this flexed position, the vertebrae are very susceptible to anterior compression fracture and, if the lap belt slips off the top of the pelvic bone structure (over the top of the iliac crests), severe injury can occur as a result of viscera crushing. A lap belt tiedown strap prevents raising of the lap belt by the shoulder harness and may nearly double the tolerance to impact forces.
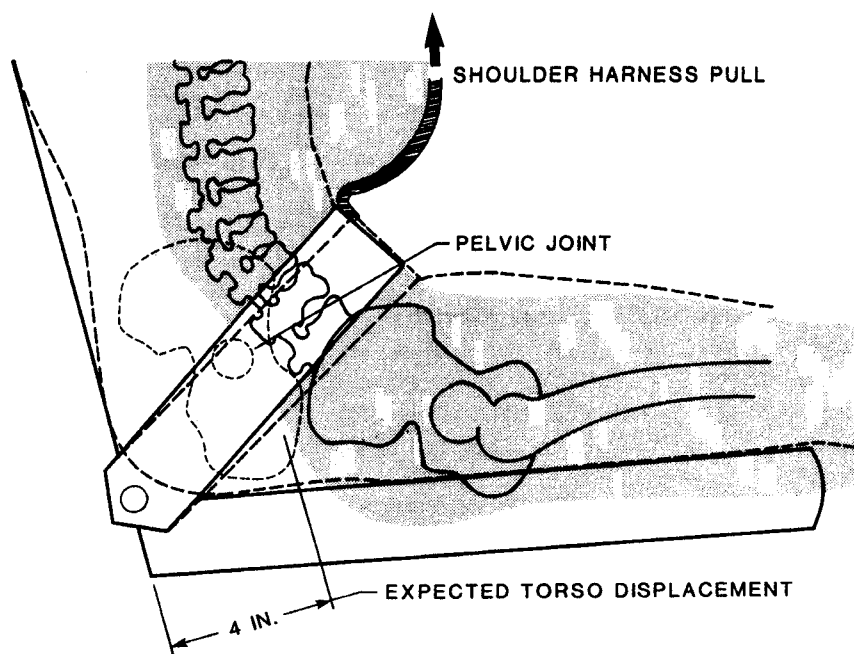
FIGURE 8. PELVIC ROTATION AND SUBMARINING CAUSED BY HIGH LONGITUDINAL FORCES COMBINED WITH MODERATE VERTICAL FORCES.

The restraint system used in new Army aircraft crewseats, as defined by MIL-S-58095 (Reference 12) consists of a lap belt, lap belt tiedown strap, and two shoulder straps connected by a single-point release buckle. This single lap belt tiedown and the two side-mounted lap belt tiedowns in use in some helicopters have given excellent performance in crashes.

The amount of slack in the restraint system can affect tolerance to a given acceleration pulse. In general, the lower the elongation properties of the link between the occupant and the seat, the greater the occupant's tolerance to an abrupt acceleration. A loose restraint system also will result in the occupant's receiving a significantly greater magnification of the accelerative

31

force applied to the seat than would occur with a snug system. The inertia of the occupant will cause him to maintain a near constant velocity, independent of the decreasing velocity of the seat, until the slack in the restraint system is taken up. As this point is reached, the velocity of the occupant is abruptly reduced to that of the seat, resulting in high G levels. This is often referred to as dynamic overshoot. Dynamic overshoot is a complex phenomenon involving the elasticity, geometry, mass distribution, and thus the natural frequency of the occupant, and the restraint and seat systems. An example is discussed in detail in Volume IV.

5.2.3 Crash Conditions

The known human tolerance levels are based on single input forces, which is not the usual case in a crash. Crashes usually involve multiple impacts, and often those impacts following the first are more severe. Human tolerance to the multiple impacts of a crash may not be as high as indicated by the known human tolerance levels to single impacts.

5.3 WHOLE-BODY ACCELERATION TOLERANCE

This section describes experimental results applicable to well-restrained (including full-torso restraint) seated occupants.

5.3.1 Spineward (-G_x) Acceleration

The magnitude and duration of the applied accelerative force have definite effects on human tolerance, as shown in Figure 9 (Reference 13). As indicated by this curve, a spineward chest-to-back accelerative force of 45 G has been tolerated voluntarily by some subjects when the pulse duration is less than 0.044 sec. Under similar conditions, when the duration is increased to 0.2 sec, the tolerable magnitude is reduced to about 25 G. Accordingly, Figure 9 shows that the tolerable limits on acceleration loading are a function of duration.

The whole-body tolerance data displayed in Figure 9 were collected for a variety of full-torso restraint and, in some cases, head restraint. With less optimum restraint, the tolerable level will be significantly reduced, and some debilitation and injury will occur.

With respect to whole-body deceleration, the rate of onset of the applied force also has a definite, although not yet well understood, effect on human tolerance. Under some impact conditions, the rate of onset appears to be a determining factor, as indicated by the diagram in Figure 10 (Reference 13). Lower rates of onset were more tolerable than higher rates under the test conditions present. Under other impact conditions, such as extremely short durations that occur in impacts from free falls, rates of onset as high as 28,000 G/sec were survivable and appeared to have little effect on human tolerance (Reference 16). It appears that in certain ranges the effects of the rate of onset are related to the natural frequencies of the body and of the various body organs (Reference 15).
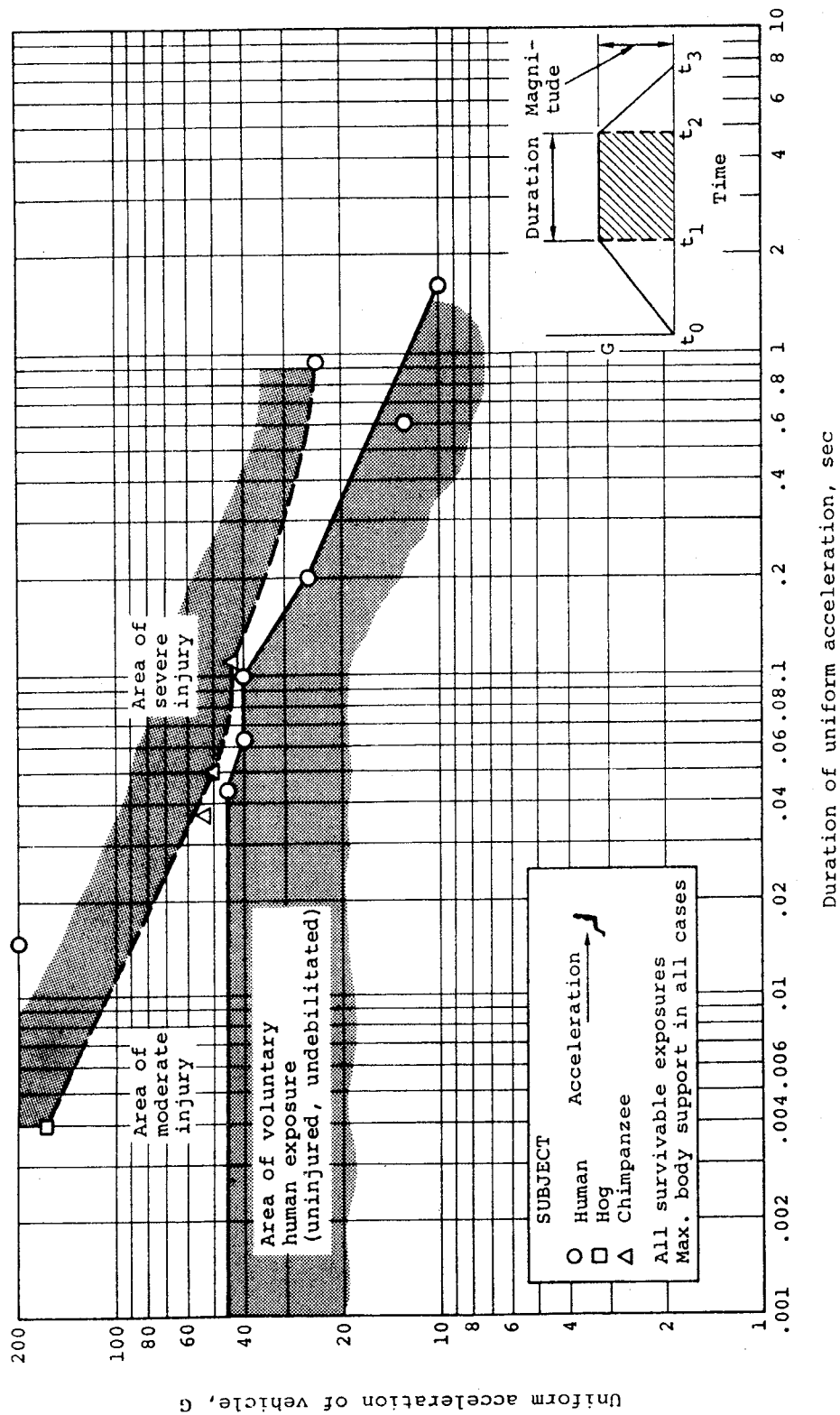
FIGURE 9. DURATION AND MAGNITUDE OF SPINEWARD ACCELERATION ENDURED BY VARIOUS SUBJECTS. (FROM REFERENCE 13)

33

SUBJECT | SUPPORT

☐ Human — Lap, shoulder, thigh, and chest straps
○ Human — Lap, shoulder, thigh, and chest straps
◇ Human — Lap, shoulder, thigh, and chest straps
▽ Chimpanzee — Military lap and shoulder straps
△ Chimpanzee — 3-in. cotton webbing, 5 horizontal, 2 vertical straps

Acceleration

Acceleration of vehicle, maximum peak G

Cardiovascular shock

Definite shock signs

No shock signs

No shock (conjunctival and retinal hemorrhage)

Shock

3400 G/sec
1370 G/sec
600 G/sec
1060 G/sec
500 G/sec

$$\text{Onset rate} = \frac{G_{max}}{t_1 - t_0}$$

Time, sec

FIGURE 10. INITIAL RATE OF CHANGE OF SPINEWARD ACCELERATION ENDURED BY VARIOUS SUBJECTS. (FROM REFERENCE 13)

5.3.2 Sternumward (+G_X) Acceleration

The human tolerance limit for sternumward, eyeballs-in (+G_X), acceleration has not yet been accurately established. Due to the high degree of restraint provided by a full-length seat back in this configuration, it can be safely assumed that tolerance is greater than for spineward acceleration. A maximum of 83 G measured on the chest with a base duration of 0.04 sec was experienced on one run in a backward-facing seat. However, the subject was extremely debilitated, went into shock following the test, and required on-the-

scene-medical treatment (Reference 16). Human tolerance to sternumward accel-eration, therefore, probably falls somewhere between this figure of 83 G for 0.04 sec and 45 G for 0.1 sec, which is the accepted end point for the $-G_x$ (eyeballs-out) case.

5.3.3 Headward ($+G_z$) Acceleration

The human body is able to withstand a much greater force when the force is applied perpendicular to the long axis of the body in a forward or backward direction (G_x) than when applied parallel to the long axis (G_z). This is shown by a comparison of the curves in Figures 9 and 11. A primary reason for the significantly lower tolerance to headward ($+G_z$) loading is the sus-ceptibility of the lumbar vertebrae, which must support most of the upper torso load, to compression fracture. Spinal alignment is necessary to carry the maximum upper torso loads.

The skeletal configuration and mass distribution of the body are such that vertical loads cannot be distributed over as large an area as can loads ap-plied forward or aft (G_x). These vertical loads, therefore, result in greater stress per unit area than do sternumward or spineward loads. Fi-nally, along the direction of the long axis, the body configuration allows for greater displacement of the viscera within the body cavity. Forces applied parallel to the long axis of the body, headward or tailward (G_z), place a greater strain on the suspension system of the viscera than do forces applied sternumward or spineward (G_x), thereby increasing the suscept-ibility of the viscera to injuries.

As in the case of the longitudinal direction (Figure 10), rate of onset also affects tolerance to vertical accelerative loads; however, insufficient data were available to establish the limits. (Figure 12 presents one set of available data.)

5.3.4 Tailward ($-G_z$) Acceleration

The human tolerance limit for tailward, eyeballs-up ($-G_z$), acceleration, is approximately 15 G for a duration of 0.1 sec. The shoulder/hardness/lap belt restraint has been used in all human testing with tailward accelerations. Most experiments also have included a lap belt tiedown strap, and the 15 G tolerance limit is based on this latter configuration.

5.3.5 Lateral (G_y) Acceleration

Very little research has been conducted on human tolerance to lateral (G_y) accelerations. Two studies, one involving restraint by a lap belt alone (Ref-erence 17) and another involving restraint by the lap belt/shoulder harness configuration (Reference 18), provide the principal available data. In both cases, a side panel provided additional restraint. With restraint by the lap belt alone, volunteers were able to withstand a pulse with an average peak of approximately 9 G for a duration of approximately 0.1 sec. At this level, the tests were discontinued due to increasing concern about lateral spinal flexion. In the experiments with restraint by lap belt and shoulder harness,
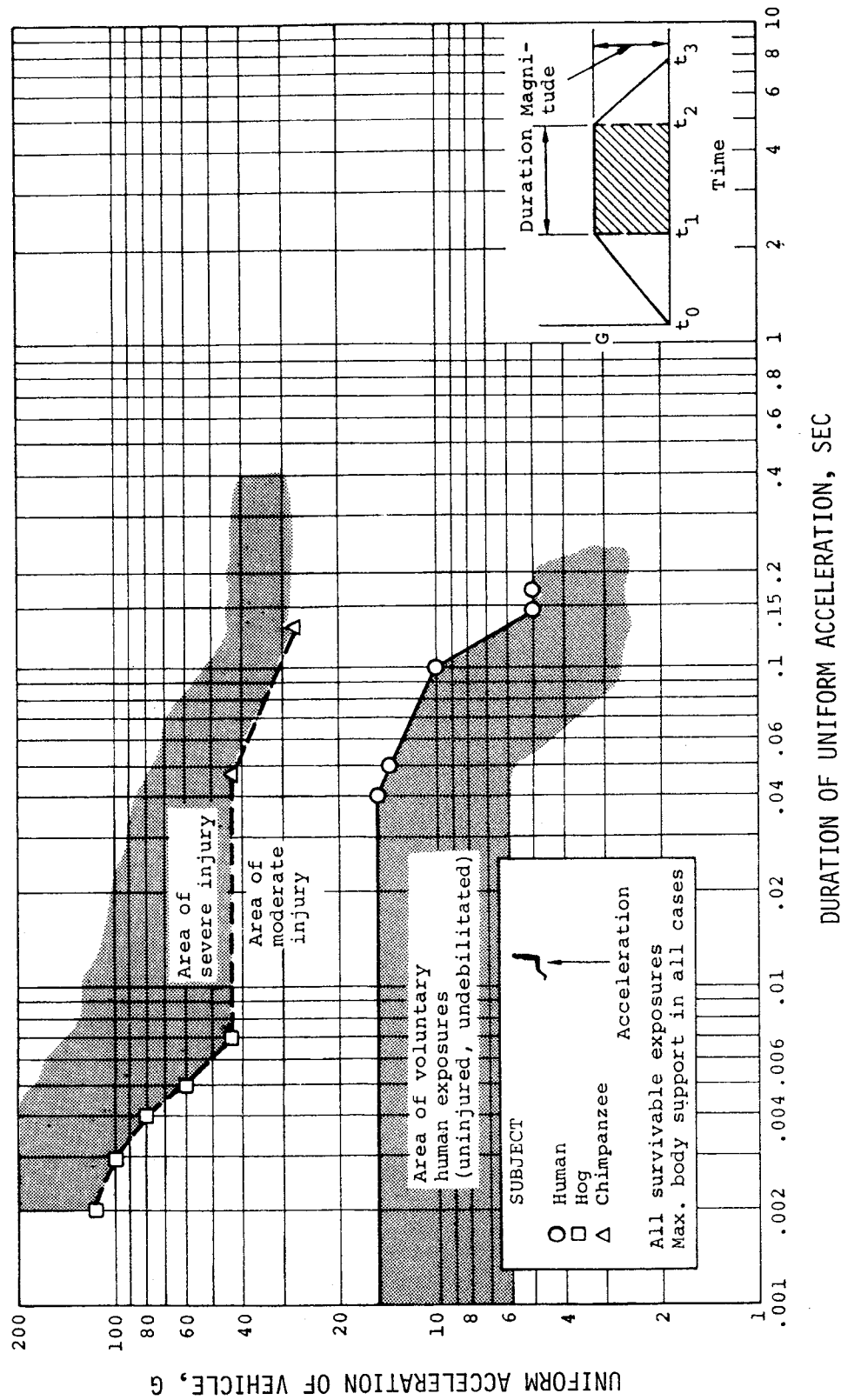
FIGURE 11. DURATION AND MAGNITUDE OF HEADWARD ACCELERATION ENDURED
BY VARIOUS SUBJECTS. (FROM REFERENCE 13)

36
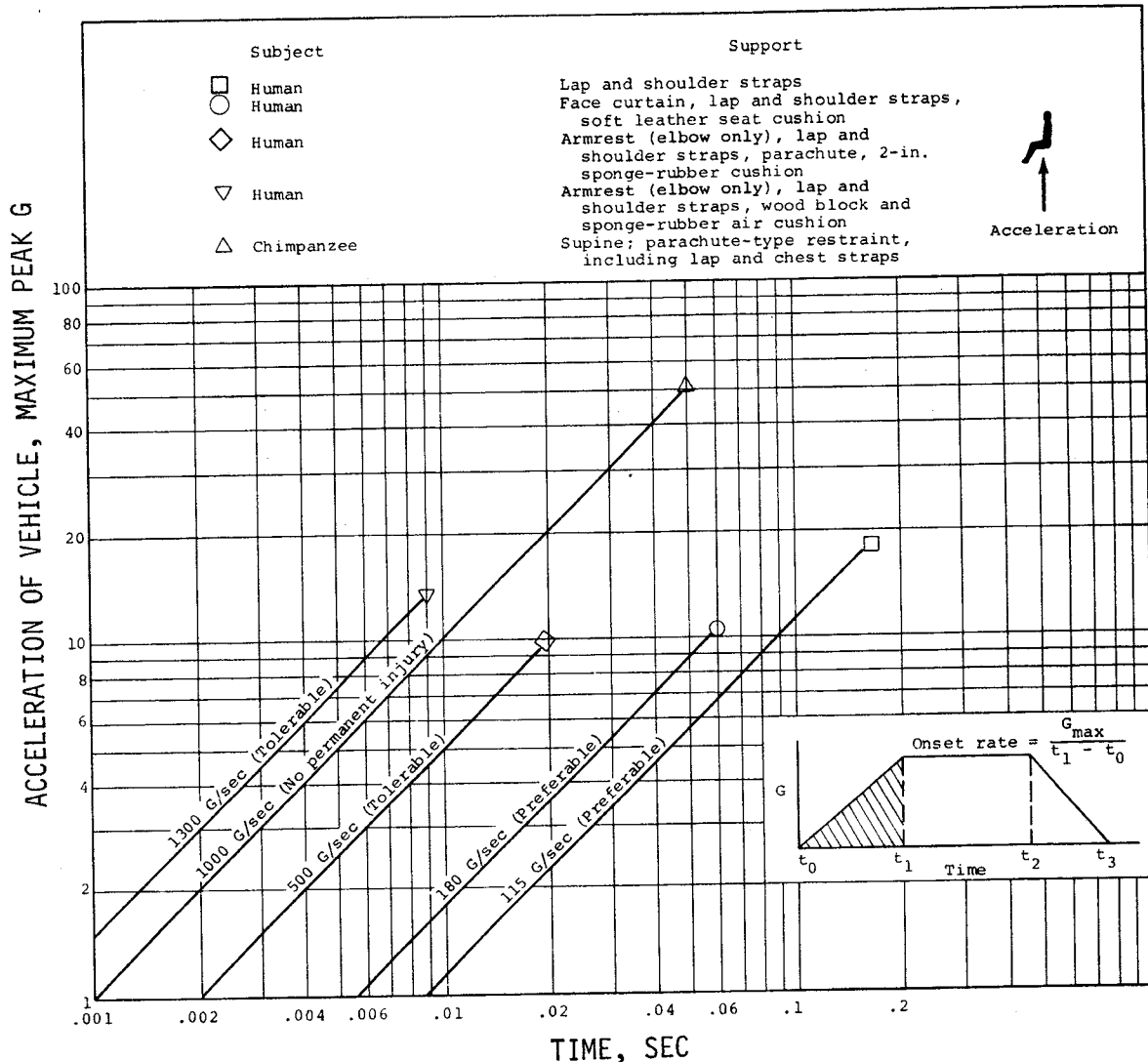
FIGURE 12. INITIAL RATE OF CHANGE OF HEADWARD ACCELERATION ENDURED BY VARIOUS SUBJECTS. (FROM REFERENCE 13)

volunteers were able to withstand a pulse with an average acceleration of approximately 11.5 G for a duration of approximately 0.1 sec with no permanent physiological changes. Tests were discontinued at this level due to possible cariovascular involvement experienced by one of the two subjects tested. No end points for human tolerance to lateral impacts were proposed in the reports of these experiments. The only reasonable conclusions from these data at this time are that a pulse of 11.5 G with a duration of 0.1 sec is readily sustained by subjects restrained by a lap belt and shoulder harness and that the human survival limit is at some point beyond this level, probably at least 20 G for 0.1 sec.

The above values are supported by a series of human volunteer experiments conducted to measure the inertial response of the head and neck to $+G_y$ whole-body acceleration (Reference 19). Acceleration inputs ranged from long-duration pulses with magnitudes of 2 to 7.5 G to short duration pulses of 5 to 11 G.

37

5.4 HEAD IMPACT TOLERANCE

As indicated by the accident data discussed in Chapter 4, over 60 percent of the Army aircraft crash fatalities in survivable mishaps result from head injuries. The injuries may result either from impact of the head on some aircraft structure or equipment, or from head acceleration without impact. In the case of mechanical impact, tolerance conditions often are based on the presence or absence of skull fracture. However, concussion can result from nonimpact motion of the head, whether in flexion or hyperextension (References 20 and 21). Concussion that may be nonfatal in itself can temporarily immobilize an individual and reduce his chances of survival by subjecting him to postcrash hazards such as fire or drowning.

Human tolerance to head impact was assessed by determining the force levels required to duplicate damage seen in SPH-4 aviator helmets retrieved from U.S. Army helicopter crashes with resulting head injury (Reference 22). Drop testing of undamaged helmets on humanoid head forms was utilized to match the damage seen from the helmets in the actual crashes. Accelerations and peak forces were measured on the head forms during the tests. This study showed that head injury occurred at peak acceleration levels far below 400 G, which is the value currently used by the U.S. Army as the pass/fail criterion in evaluating the performance of prospective aircrew helmets. The investigators also found that the peak transmitted force was a much better predictor of injury severity than was the peak acceleration. Thus, the peak transmitted force may be a more effective criterion to use in the evaluation of helmet impact attenuation performance than is peak G. The study also found that the peak transmitted force was a much better estimator of injury severity than either the severity index or the head injury criteria (HIC), which are discussed in Sections 5.4.1 and 5.4.2.

Fatal head injury has been shown to result from such severe brain damage as laceration of brain tissue or shear of the brain stem (Reference 23). Head impact studies with anesthetized monkeys and dogs have been conducted to relate the severity and duration of concussion to intracranial pressure change (Reference 24). Moderate to severe concussion effects were observed in the range of 30 to 90 lb/in.^{2} intracranial pressure change concurrent with head impact.

According to a hypothesis developed by Holburn, shear stresses induced by head rotation also can produce concussion (Reference 25). Kornhauser, in Reference 26, indicated a relationship between damaging velocity and damaging accelerations as follows:

$$\dot{\theta} = \frac{\ddot{\theta}}{\omega} \qquad (1)$$

where $\dot{\theta}$ = damaging rotational velocity, rad/sec

$\ddot{\theta}$ = damaging rotational acceleration, rad/sec

ω = natural frequency of rotation of brain, rad/sec

38

Ommaya, et al., developed scaling factors needed to predict concussion thresholds for humans from data taken on subhuman primates (Reference 27). This study showed that θ can be represented by the equation:

$$\ddot{\theta} = \frac{c}{m^{2/3}} \qquad (2)$$

where m = mass of the brain, gm

   c = an experimentally derived constant, $gm^{2/3}$ rad/sec^2

The investigators found c = 21,600 $gm^{2/3}$ rad/sec^2, and further showed that the relationship of Equation (1) produced reasonable agreement between predictions and empirical data. Limiting values thus predicted to produce a 50-percent probability of concussion in a man having a brain mass of 1,300 gm are as follows (Reference 28):

$$\ddot{\theta} = 1,800 \ rad/sec^2$$

$$\dot{\theta} = 50 \ rad/sec$$

In general, assessing the probability of injury by observation of oversimplified parameters, such as peak acceleration of the imposed acceleration time environment, usually is not constructive. The problem has been to define some form of parameter that is indicative of the degree of severity of a particular input excitation. Various indicators have been developed, based on experiments, and several of these for the head are presented and discussed in Sections 5.3.1 through 5.3.7.

5.4.1 Weighted Impulse Criterion (Severity Index)

It can be seen from human tolerance data presented previously that high forces or accelerations can be tolerated for only very short periods of time, while lower values of these quantities can be tolerated for longer periods of time. This same relationship for head injury in forehead impacts, which was established on the basis of impact tests performed at Wayne State University on animals and human cadavers, is illustrated in Figure 13 (Reference 29). In these tests, longitudinal impacts of the subject's forehead against unyielding flat surfaces were conducted, and the acceleration-time history of the specimen head was measured at a point on the skull diametrically opposite the point of impact. The curve shown in Figure 13, the Wayne State Tolerance Curve, was based on the observation of linear skull fracture.
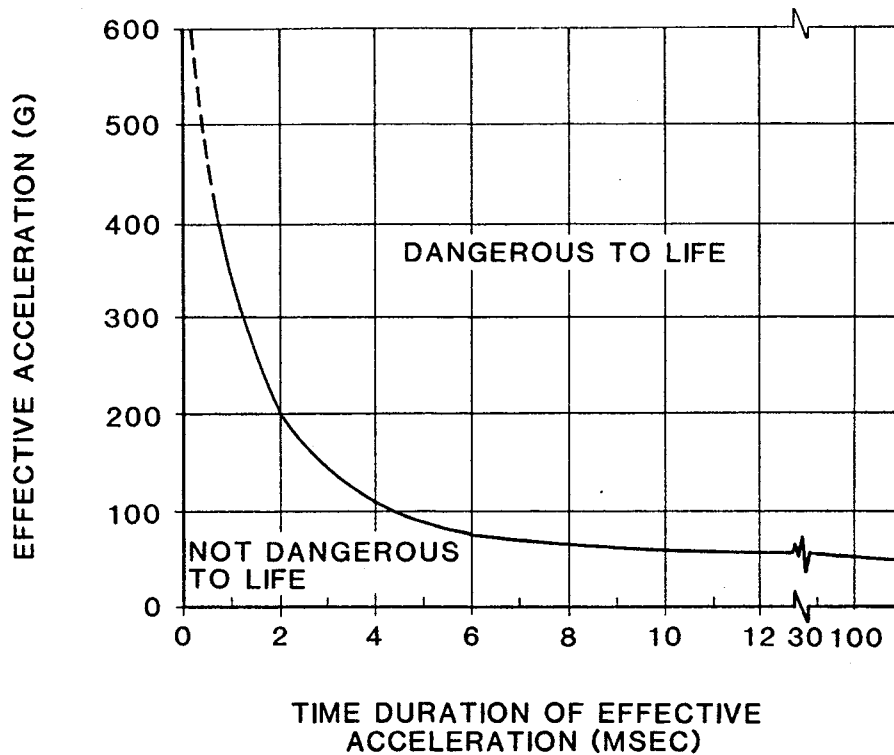
FIGURE 13. WAYNE STATE TOLERANCE CURVE FOR THE HUMAN BRAIN IN
FOREHEAD IMPACTS AGAINST PLANE, UNYIELDING SURFACES.
(FROM REFERENCE 29)

Based on such data as that collected at Wayne State, Gadd suggested a weight-
ed impulse criterion as an evaluator of injury potential (Reference 30). The
severity index is defined as

$$SI = \int_{t_o}^{t_s} a^n dt \qquad (3)$$

where   SI = severity index

a = acceleration as function of time

n = weighting factor greater than 1

t = time

40

Based on data in References 13 and 29, the exponent n has been determined to be 2.5 for head and facial impacts. A severity index of 1,000 was proposed by Gadd (Reference 30) for the danger-to-life threshold from head injury in frontal impacts. Severity index values exceeding 600 produced concussion in head impacts sustained by U.S. Army aircrewmembers in aircraft accidents (Reference 29). A lower value of n has also been suggested for regions of softer tissue, which behave viscoelastically.

The severity index can be calculated by dividing the time base of the acceleration time curve into sufficient segments to define the acceleration curve. The G value then read from the curve for the center of the increment is raised to the 2.5 power, and the result is multiplied by the time increment. The sum of all the values obtained gives the severity index. A severity index sample calculation is shown in Figure 14, which is taken from Reference 31.

5.4.2 Head Injury Criteria (HIC)

An alternative interpretation of the Wayne State University Tolerance Curve was developed by Versace. That analysis led to the Head Injury Criteria (HIC). The HIC was later included in Federal Motor Vehicle Safety Standard 208 (FMVSS 208) as a head impact tolerance specification. The HIC is calculated by

$$
HIC = \left[(t_2 - t_1) \left[\frac{1}{t_2 - t_1} \int_{t_1}^{t_2} a(t)\, dt \right]^{2.5} \right]_{max}
\qquad (4)
$$

where t_1 and t_2 are the initial and final times during which HIC attains a maximum value and a(t) is the resultant acceleration (G) measured at the head center of gravity (Reference 32).

FMVSS 208 sets a maximum value of 1000 for the HIC. It also specifies that the time interval between t_1 and t_2 shall not exceed 36 milliseconds (Reference 33). The time interval limitation effectively eliminates lower level accelerations that are not injurious and focuses on the short-duration, high-level impact peaks.

There has been some question as to the appropriateness of using the HIC to determine severe head impact tolerance because of significant skull deformation which occurs, even without fracture. These deformations prevent skull-mounted accelerometers from accurately measuring the acceleration of the c.g. of the head (Reference 34). Therefore, the HIC may not be well defined or repeatable for severe head impacts. Other critical limitations of head injury research and of the HIC also may be found in Reference 34. For example, a study by Hoskins and Thomas concluded that the critical HIC interval must be less than 15 milliseconds in duration in order to pose a concussion hazard even if the HIC value exceeds 1000 (Reference 32). However, Slobodnik found during the SPH-4 helmet study (Reference 22) that concussive head injuries occurred at HIC values below 1000.

41
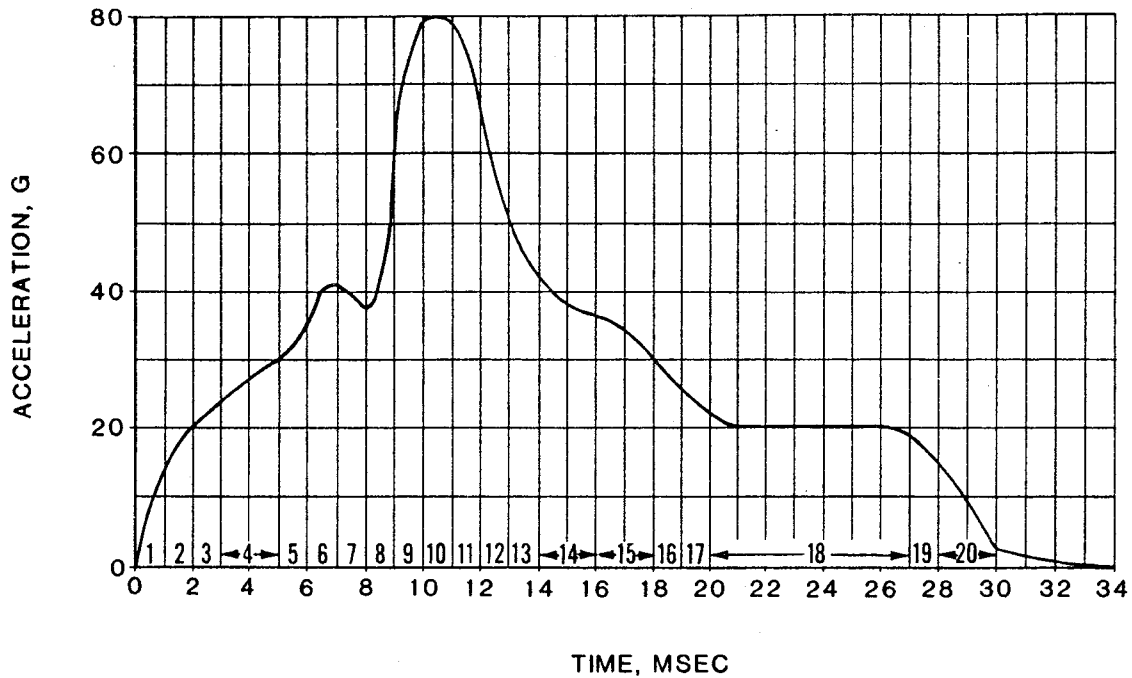
CALCULATIONS

Increment Number	Time Increment (sec)	Midpoint G Value	$G^{2.5}$	Incremental SI (Time x $G^{2.5}$)
1	0.001	7	130	0.13
2	0.001	18	1,400	1.40
3	0.001	23	2,500	2.50
4	0.002	27	3,800	7.60
5	0.001	33	6,300	6.30
6	0.001	40	10,000	10.00
7	0.001	38	8,800	8.80
8	0.001	47	15,000	15.00
9	0.001	75	48,000	48.00
10	0.001	80	57,000	57.00
11	0.001	73	46,000	46.00
12	0.001	56	23,000	23.00
13	0.001	43	12,000	12.00
14	0.002	37	8,300	16.60
15	0.002	33	6,200	12.40
16	0.001	27	3,800	3.80
17	0.001	24	2,800	2.80
18	0.007	20	1,800	12.60
19	0.001	17	1,200	1.20
20	0.002	10	330	0.66

Severity Index   287.79

FIGURE 14.   SAMPLE CALCULATION OF A SEVERITY INDEX.
(FROM REFERENCE 31)

42

Although correlations of the HIC with actual injuries might not be as success-ful as desired, it is still one of the most widely used criteria for testing in relation to head injury protection, and a HIC of 1000 is still used as the criterion for head injury tolerance. Lockett has pointed out that the HIC and Gadd Severity Index are plausible and fundamentally correct forms of cri-teria (Reference 35). The reasons for the lack of correlation might include the inadequacy of the human surrogates, whether they be cadavers or anthropo-morphic dummies, to model the living human system and the coarseness of the observed injury scales against which the HIC is often compared. It should be noted that the HIC is not related to all possible injury mechanisms. For example, it does not consider a pressure-induced localized crushing or pene-tration of the brain (Reference 36).

The HIC equation can be manipulated into a form with integer power that is convenient for computation and can be computed efficiently by special algo-rithm. One such algorithm was developed by Rodden, et al., and is presented in Reference 37.

5.4.3 J-Tolerance

Slattenschek, after noting different head deceleration curves when different types of windshield glass were used, developed a method of assessing multiple impact tolerance by a "J-tolerance" value (Reference 38). A second-order vibrational model, based on the Wayne State Tolerance Curve, is used to determine the tolerable amplitude of brain motion. The response of the simple, damped, spring-mass system shown in Figure 15 is given by

$$\ddot{x} + 2D\omega\dot{x} + \omega^2 x = -b(t) \tag{5}$$

where x = relative displacement

$\dot{x}$ = relative velocity of mass

$\ddot{x}$ = relative acceleration of mass

b = acceleration of system at point N (driving acceleration)

D = damping coefficient

ω = angular frequency
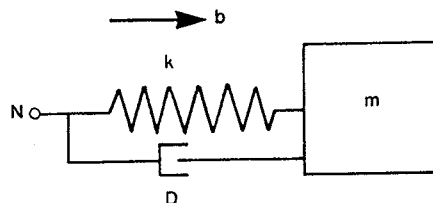
FIGURE 15.   DAMPED, SPRING-MASS SYSTEM USED IN COMPUTING
J-TOLERANCE.   (FROM REFERENCE 38)
43

Two accelerations from the Wayne State Tolerance Curve were used to determine the frequency and the tolerable amplitude of the displacement. The value of the damping factor was selected as 1 to achieve a best fit to the Wayne State data. The resulting model fit the Wayne State Curve within better than one-half percent.

For assessment of an impact, the maximum displacement is calculated for the given acceleration pulse, and the ratio of this maximum amplitude to the tolerable amplitude is evaluated. The tolerance value, J, is defined as

$$J = \frac{x_{max}}{x_{tolr}} \qquad (6)$$

Values of J less than 1 are assumed to correspond to survivable impacts.

5.4.4 Effective Displacement Index

The Effective Displacement Index (EDI), reported by Brinn and Staffeld, is derived from a mathematical spring-mass model based on the work described in Section 5.4.3 (Reference 39). The peak deflection of the model, in inches, is taken as the index of damage. Using a natural frequency of 77 Hz and a damping value of 70.7 percent, a tolerable EDI of 0.15 in. was obtained by fitting the Wayne State Tolerance Curve.

It should be noted here that, as in the case of the Gadd Severity Index, a tolerable EDI is based on anterior-posterior impact only, due to the unavailability of data for other directions.

5.4.5 Strain Energy Considerations

Melvin and Evans considered the basic types of skull fracture and investigated the effects of impactor size and shape, skull geometry, and soft tissue (Reference 40).

5.4.6 Mean Strain Criterion (MSC)

In a study conducted by Enouen to simulate pedestrian head injury, the Mean Strain Criterion (MSC) is considered as a means of evaluating head injury. This method is relatively new and at the time of this publication was still in the final stages of development (Reference 41).

MSC is a computer simulation of head impact response. The program translates an acceleration input into a mean strain produced in the brain. It then relates the strain to concussive head injury by computing the Abbreviated Injury Scale (AIS) value for head injury. Four versions of the program allow impact simulation from four different directions on the head, which significantly improves head injury correlation (Reference 41).

44

5.4.7 Comparison of Head Injury Predictors

Hodgson and Thomas investigated skull fractures in 40 cadavers that were dropped with their heads striking rigid, flat, hemispherical, and cylindrical surfaces on the front, side, and rear (Reference 42). The Severity Index and the Effective Displacement Index (EDI) were compared at fracture level for all frontal impacts, and their average values at fracture were found to agree closely with the critical values predicted by the authors of the methods. Results for the frontal flat-plate impacts are shown in Figure 16, where A_{CG} refers to calculation of the indices from resultant acceleration at the head center of gravity. A_{A-P} refers to calculation from anterior-posterior acceleration measured at the point on the skull most distant from the impact site, the condition used in the derivation of the Wayne State Tolerance Curve.

Test no.	SI		EDI-in.	
	A_{CG}	A_{A-P}	A_{CG}	A_{A-P}
2	749	400	.14	.11
3	2020	1800	.18	.12
4	1280	792	.17	.13
6	565	390	.13	.11
29	1020	724	.16	.13
30	1250	561	.19	.11
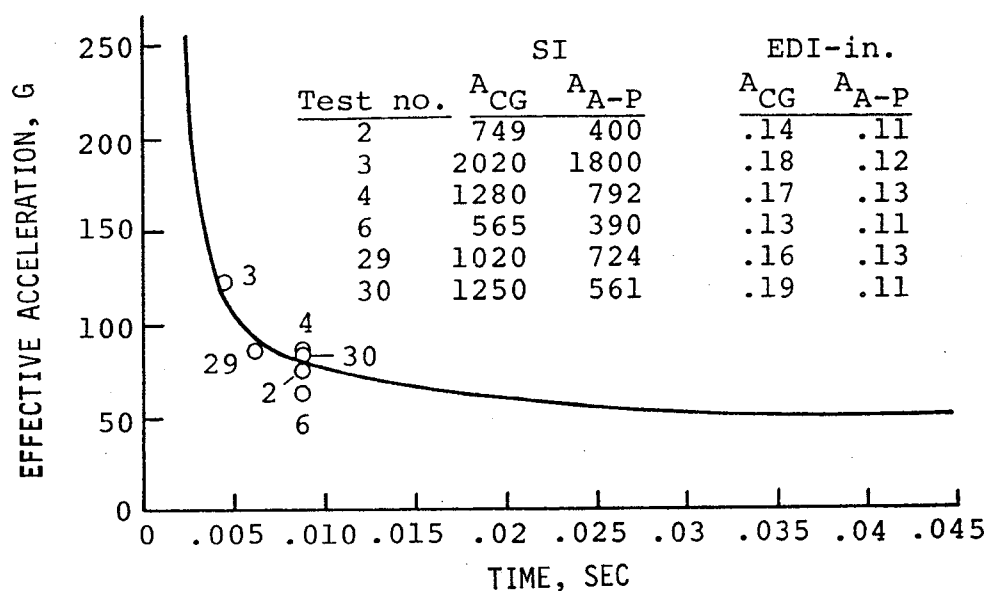
FIGURE 16. COMPARISON OF SI, EDI, AND KINEMATICS OF SIX FRONTAL IMPACTS PRODUCING LINEAR FRACTURE. (FROM REFERENCE 37)

For the drop height range that produced linear fracture in the cadaver's skull due to frontal impact against a rigid, flat plate, the SI for the Alderson 50th-percentile dummy head acceleration response was significantly higher than for the cadaver. The higher acceleration measured for the dummy head would, of course, be expected in such an impact because of the greater rigidity of its metal skull. The EDI, on the other hand, was essentially the same for both cadaver and dummy.

Fan analyzed predictions of the Gadd Severity Index and the Vienna Institute of Technology Brain Model (J-tolerance) and concluded that improvements in both techniques could be made (Reference 43). He concluded that the SI puts too much weight on the acceleration but ignores the time factors of an impulse. Fan's revised approach to SI calculation involves a successive

approximation method where variable weighting factors are applied to both acceleration and time. A revised brain model also is presented, based on the Vienna model, with additional information included on dynamic properties of the human skull-brain system. The revised brain model utilized an equivalent viscous damping of 40 percent of critical damping and, on comparison with the Wayne State Tolerance Curve, yielded tolerable values of brain deformation, velocity, and angular velocity of 1.25 in., 135.5 in./sec, and 175 rad/sec, respectively. The maximum deviation from the Wayne State Curve was reported to be within 5 percent.

5.5 FACIAL IMPACT TOLERANCE

Impact tolerance of the face is lower than that of the head, with a recommended facial injury threshold of SI equals 500 (Reference 30). Fracture forces for the major facial bones--the zygoma (cheekbone), the maxilla (upper jaw), and the mandible (lower jaw)--are listed in Reference 32. When these bones are impacted directly by a small circular impacter, the fracture forces range from 258 lb for the maxilla to 697 lb for the mandible.

The nasal bone tends to be the most fragile of all the facial bones and has a higher frequency of injury. The remaining bones of the face have a much higher level of fracture tolerance than the nasal bones. Impact studies wherein a 1-inch-diameter aluminum bar is impacted into the face at the bottom of the eye sockets showed that a force of about 675 lb was necessary to produce fracture patterns more extensive than nasal bones only (Reference 44).

Studies of the full face indicate that the facial skeleton is remarkably strong when the face contacts a padded, deformable surface. Figure 17 from Reference 45 reproduces summary data showing the tolerances of the human face and head to resisting fractures during impact against deformable, padded surfaces.
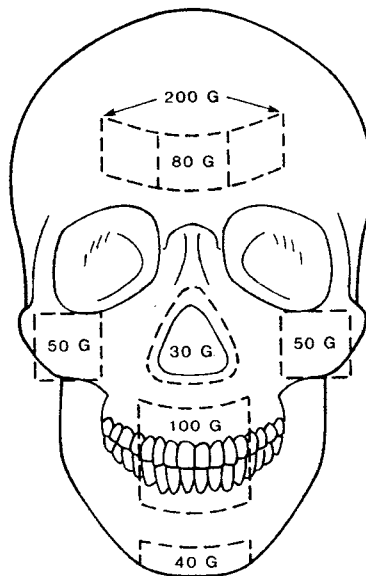
FIGURE 17. SUMMARY OF MAXIMUM TOLERABLE IMPACT
FORCES ON A PADDED DEFORMABLE SURFACE.

46

5.6 NECK IMPACT TOLERANCE

Tolerance of the human neck to rotation, as experienced in whiplash, and to localized impact loading has been investigated. Mertz and Patrick determined the moment about the occipital condyles (protruberances near the back of the skull that articulate with the cervical spine and are considered to be the center for rotation of the head with respect to the neck) at the threshold of pain for volunteer subjects. On the basis of their investigations, tolerable levels for neck flexion (forward rotation) and neck extension (backward rotation) of a 50th-percentile adult male are proposed in Reference 46. The neck appears to be at least three times stronger in resisting flexion than extension (Reference 47).

Gadd, Culver, and Nahum, using unembalmed, elderly cadavers, investigated the relationship between rotation and resisting moment in hyperextension and lateral flexion (Reference 48).

Hodgson presents a comparison of peak neck load data for inertia and direct impact loading of the heads of volunteers, cadavers, and the Hybrid III dummy (Reference 47). Hodgson, in another study, emphasizes that the consciousness of the occupant may be dependent on relative motion at the head and neck junction (Reference 49). Relative motion between head and neck should be minimized when abrupt $-G_x$ can be anticipated.

A helmet adds mass and a higher center of gravity to the head, which tends to aggravate the head/neck motion during impact. The relative motion of the head and neck during acceleration loads has been extensively researched through human and manikin sled runs for various directions and magnitudes at the Naval Biodynamics Research Laboratory (NBDL) in New Orleans (Reference 50). These tests were conducted to support the development of greater fidelity manikins for testing purposes and were all conducted below the human tolerance level. A number of these tests were done with helmets and with additional head weights added. It was found that the maximum resultant force at the occipital condyles was proportional to the product of the nominal impact acceleration and the sum of the head and added mass. The effect of the mass additions was to increase, in a consistent manner, head angular travel as well as torques and forces. References 51, 52, and 53 present head acceleration and displacement profiles for various impact loads in the $-G_x$ direction. Wismans, et al. (Reference 53) also analyzed the displacement profiles in oblique and lateral directions of the NBDL tests and found that maximum head excursions in frontal impacts are slightly larger than in oblique impacts and much larger than in lateral impacts.

Neck injuries in U.S. Navy aircrew personnel who ejected from their aircraft were examined for a 10-year period by Guill (Reference 54). The study found that ballistic haul-back inertia reels can reduce the incidence of sprain/strain type ejection-associated neck injuries.

A preliminary analysis of the head/neck response to impact loads has been initiated by the U.S. Air Force, Aerospace Medical Division, Wright-Patterson Air Force Base in an effort to improve manikin neck response to more closely simulate human neck response in high accelerations. Navy data with live volunteers was used. In comparing the human responses of $-15 \, G_x$ and $12 \, G_z$ impacts, it could be seen that the neck angular responses were similar, but the head responses were different. For the $-G_x$ impact, the head began to

47

rotate forward after the neck rotated approximately 5 degrees, but for the G_z impacts, the head did not rotate significantly until the neck rotated approximately 35 degress and the head/neck joint bottomed out. Another phenomenon shown by the test films was that there were two types of human responses to $+G_z$ impacts. In the Type 1 response, the head initially rotates slightly forward until the head/neck joint bottoms out and then the head violently rotates forward. In the Type 2 response, the head initially rotates backward as the neck is rotating forward and then, similar to the Type 1 response, the head violently rotates forward when the head/neck joint bottoms out. The determining factor as to which response will result depends upon the position of the head system center of gravity (c.g.), with a Type 2 response resulting when the c.g. is located further toward the rear of the head as compared to the Type 1 response.

To better understand the kinetics of the head/neck system, plots were made of the calculated moment, head/torso angle and head/neck angle with respect to the NBDL runs in 12 G_z and -15 G_z impacts. Figure 18 shows that, for the G_z impact, the moment at the occipital condyles increases as the head/torso angle increases and that the head moment is related to the head/neck angle, with the neck imparting a high positive moment on the head when the head/neck angle exceeds approximately 15 degrees. For the $-G_x$ impact, Figure 19 shows that the moment at the occipital condyles increases as the head/torso angle increases, but that the head/neck angle is not directly related to the moment at the occipital condyles. This is consistent with the biomechanics of the neck, since the neck structure would be expected to apply little moment on the head unless the joints bottom out.

The tolerance of the human neck to external vertical (z-direction) loads has been determined from dynamic impacts on cadavers performed with a moving mass impactor. Fracture of the cervical vertebrae occurred for peak forces over 1280 lb, peak impactor velocity over 24.6 ft/sec, and initial impact pulse energy values of 280 ft-lb (Reference 55).

5.7 CHEST IMPACT TOLERANCE

An extensive research program on impact response of the human thorax has been reported by Kroell, Schneider, and Nahum (Reference 56). A 6-in.-diameter rigid impactor of varying mass and moving at a range of speeds was used to strike unembalmed, seated cadavers. Deflection and force were measured as functions of time. Figure 19 (from Reference 56) shows the Abbreviated Injury Scale (AIS) (Reference 57) plotted against normalized chest deflection (deflection divided by chest anterior-posterior diameter). The least-squares fit shown has an associated correlation coefficient of 0.772. However, as seen in Figure 20, the restrained back data appear to follow a different trend. Scaling of the relationships between force and penetration has been reported in Reference 58.

The Effective Displacement Index (EDI), which was discussed in Section 5.3.4 in reference to head injury, also has been applied to chest injury by Brinn and Staffeld (Reference 39). They point out that there is evidence that rib cage deflection may be the governing criterion for chest injury and that the measurement of this deflection might be the basis for a chest survivability index. However, the acute distress experienced by human volunteers subjected to whole-body deceleration has been considered a justification for an independent hazard index based on acceleration. Using a natural frequency of 15 Hz and a

48
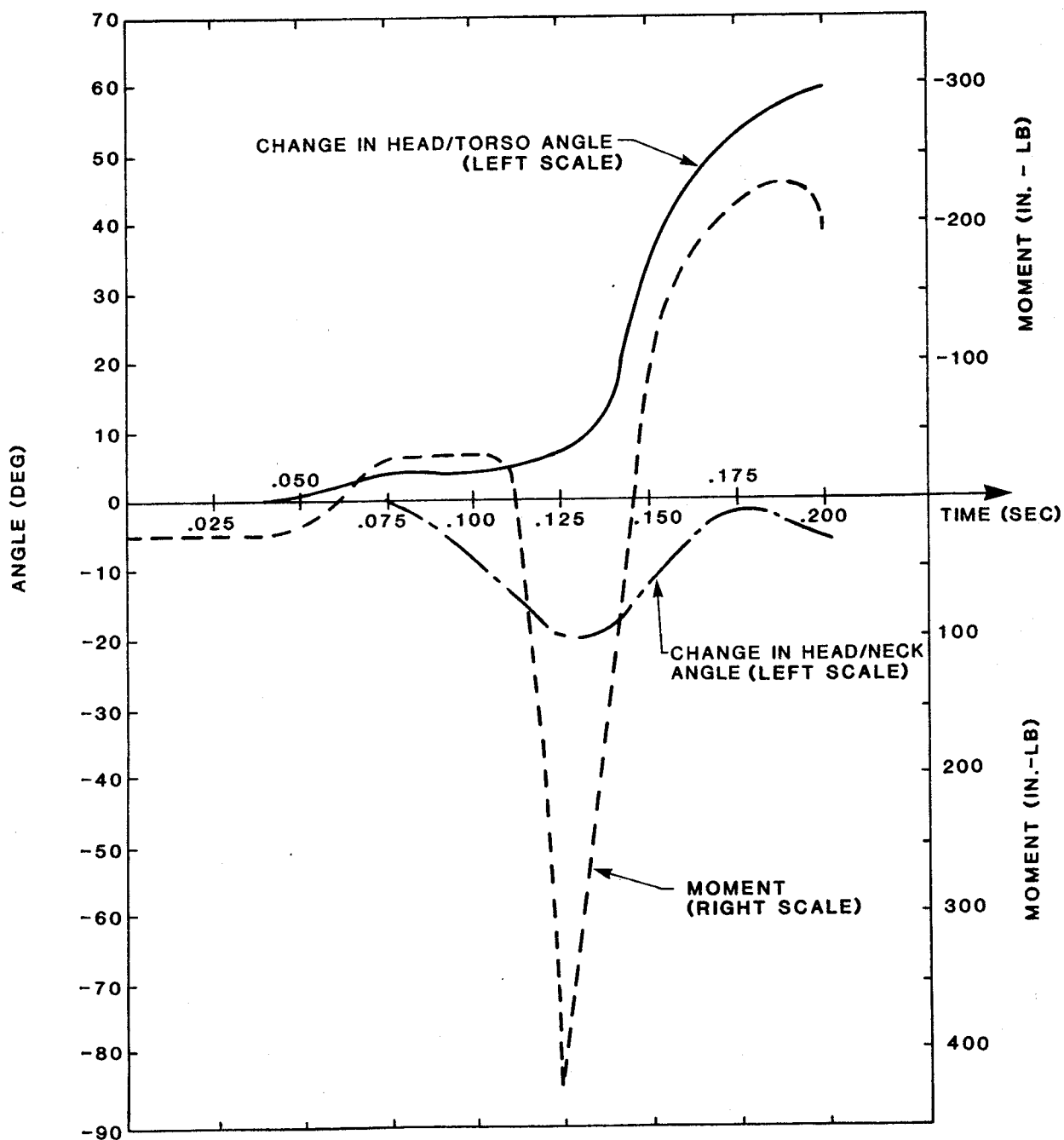
FIGURE 18. MOMENT AT THE OCCIPITAL CONDYLES AND RELATIVE CHANGE IN HEAD/TORSO ANGLE AND HEAD/NECK ANGLE DURING NBDL HUMAN RUN NO. LX 4651, 12-G_z IMPACT.
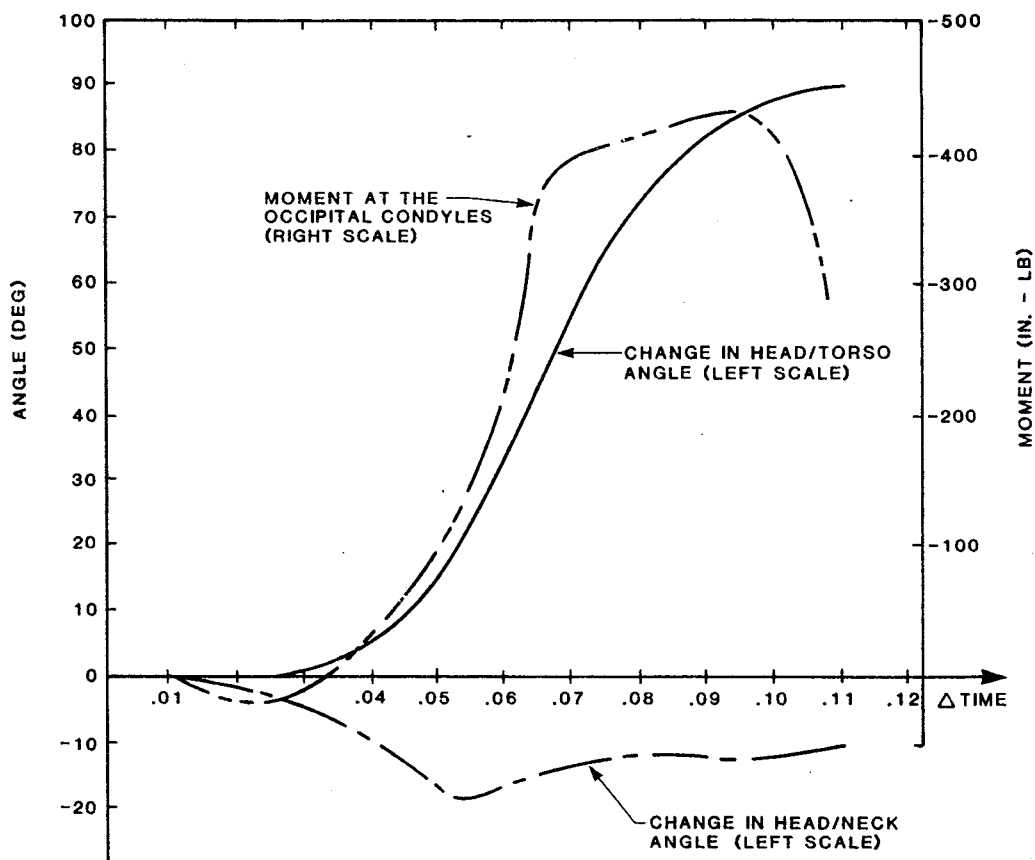
FIGURE 19. MOMENT AT THE OCCIPITAL CONDYLES AND RELATIVE CHANGE IN HEAD/TORSO ANGLE AND HEAD/NECK ANGLE DURING HUMAN RUN NO. LX 3983, -15 G_X IMPACT.

damping value of 25 percent of critical, a maximum EDI of 2.2 in. was obtained for voluntary human exposure. Based on experience with energy-absorbing steering columns, EDI of 2.8 in. was suggested as a test limit for current-design anthropomorphic dummies.

On the basis of 16 dives performed by an instrumented professional high diver onto a mattress, combined with the results of earlier studies, a long-duration acceleration tolerance level of 60 G with a pulse duration of 100 msec has been recommended for the thorax in the anterior-posterior direction (Reference 59). Federal Motor Vehicle Safety Standard (FMVSS) 208 specifies an acceptable level of 60 G for chest acceleration (Reference 33). The acceleration is the resultant measured at the center of gravity of the dummy chest.

After investigation of blunt thoracic impact to anesthetized swine, Kroell, et al. (Reference 60), concluded that both compression and velocity are significant parameters of impact exposure severity. Qualitatively, exacerbation of

50
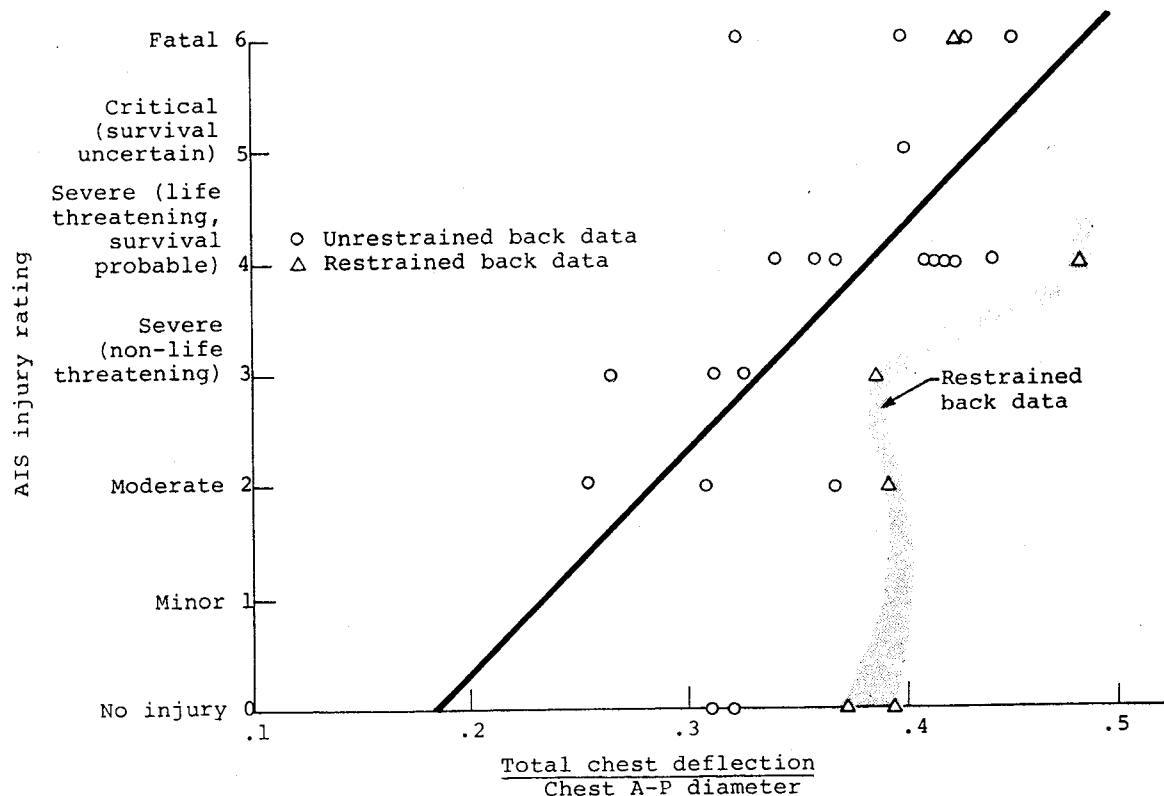
FIGURE 20. AIS INJURY RATING VERSUS NORMALIZED CHEST DEFLECTION. (FROM REFERENCE 56)

injury was seen when either variable was increased with the other held constant. Quantitatively, better logistic regression models were found relating the probability of heart rupture and of Abbreviated Injury Scale (AIS) 4 or greater injury to products of velocity and compression, including the viscous response, than to normalized compression or peak spinal acceleration alone. (See Section 5.11 for a description of the Abbreviated Injury Scale.) At striking velocities of 30 msec, gross cardiac rupture occurred at applied normalized compression levels as low as 0.15. No such injury was observed at 15 m/sec and comparable compression levels.

Lau and Viano summarized several different criteria for chest injury (Reference 61). They point out that the usefulness of the acceleration criterion is restricted to predicting the severity of skeletal injury and it is not useful in predicting soft tissue injury. Maximum chest compression is a superior indicator of chest injury severity. Research showed that human volunteers could sustain 20 percent chest compression in quasi-static loading with no injury. As compression increased above 20 percent in human cadavers at impact velocity between 5 and 7 m/sec, rib fractures occurred regularly. Maximum compression of 40 percent induced multiple rib fractures. The latest analysis of data indicates that 40 percent of maximum chest compression corresponds to a 50/50 chance of the occupant sustaining AIS 4 or greater chest injury. However, this criterion was derived with impact velocities between 5 and 7 m/sec, and it is known that even moderate impact velocity injury can occur well before maximum compression.

51

In their research, Lau and Viano found that rate sensitivity of soft tissue must be accounted for in understanding soft tissue injuries. Severity of lung injuries in rabbits was found to increase as chest compression or impact velocity was increased. Studies done on swine showed that the velocity of impact on the sternum or the myocardium was the primary determinate of risk of developing ventricular fibrillation.

Lau and Viano's studies showed a Viscous Criterion, based on the rate sensitivity of soft tissue, is the best indicator for soft tissue injury in many body regions for velocities of deformation between 3 to 30 m/sec, as shown in Figure 21. When velocity of deformation is below 3 m/sec, the influence of impact velocity on soft tissue injury gradually diminishes. At very low velocity, the compression criterion becomes the best indicator. At velocities less than 1 m/sec, injury is essentially induced by crushing of the tissue. When the velocity of deformation approaches 30 m/sec, impact velocity becomes such a predominate factor in determining injury outcome that the influence of compression becomes secondary. At these very high velocities, blast injury begins to occur first in the lung and then in other hollow organs. The authors showed that an impact producing a peak Viscous response (the product of the velocity of deformation times the instantaneous compression) of 1.3 m/sec had a 50/50 chance of inducing thoracic injury of AIS 4 or greater. An impact producing a peak Viscous response of 2 m/sec had a 50/50 chance of inducing cardiac rupture.
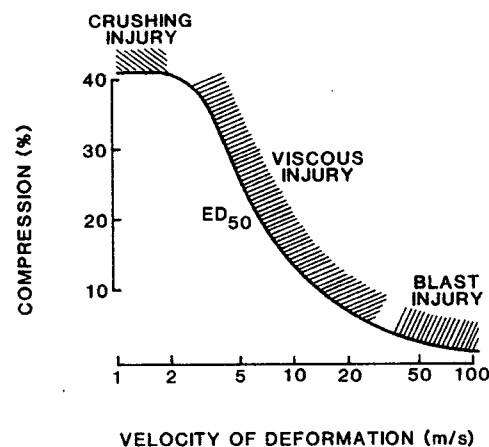
FIGURE 21. RANGE OF VALIDITY FOR THE VISCOUS CRITERION AND THE COMPRESSION CRITERION.

All of the above tolerance data have been for thoracic impacts in an anterior-posterior orientation only. A great deal of effort is currently being expended in defining human tolerance to lateral impacts in association with the Department of Transportation's efforts toward developing a test method and standard requiring side impact protection of motor vehicle occupants. The thoracic trauma index (TTI) has been proposed as the human tolerance criterion. Investigations by Morgan, et al. (Reference 62), have shown

that the TTI is an accurate and usable predictor of thoracic injury level
resulting from a lateral impact. The TTI is based on the age of the test
subject, the maximum absolute lateral accelerations of either the fourth or
eighth rib and the 12th thoracic vertebra, and the subject's mass. Data from
cadaver studies were used in calculating the TTI, and injury probability
curves were generated for determining injury probability functions. The
curves for AIS 4 or greater injury for left side and right side impacts are
shown in Figure 22. The increased risk of injury in right side impacts as
compared to left side seems to stem from increased injury severity to the
liver because of the asymmetry of the abdomen.
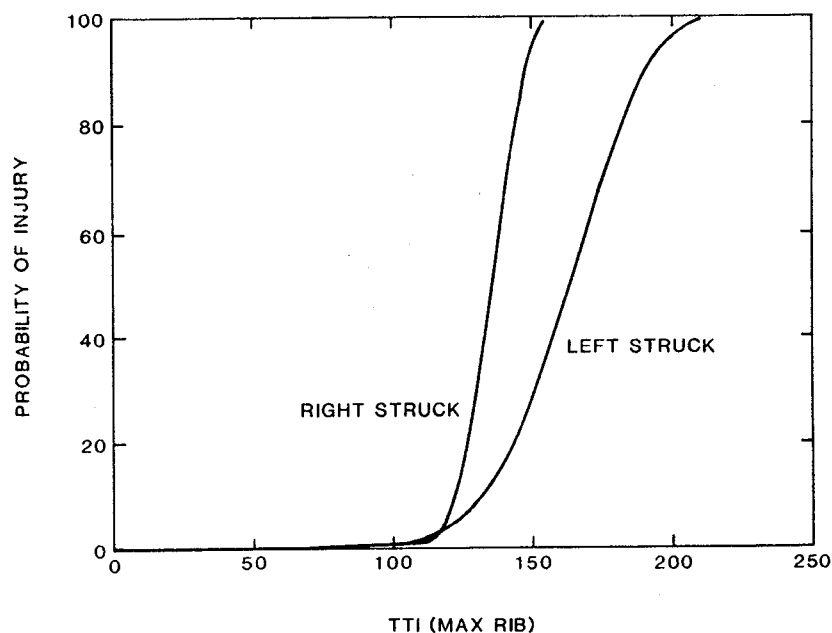
FIGURE 22. COMPARISON OF AIS $\geq$ 4 PROBABILITY FOR LEFT-
SIDE AND RIGHT-SIDE IMPACTS.

The TTI should be used with caution in aircraft applications since it, along
with the side impact dummy, was developed specifically for automobile side im-
pacts in which the occupant loading is of an intrusive and impulsive nature.
The accuracy of the TTI over nonimpulsive, longer term G loads, as most fre-
quently occurs in aircraft crashes, has not been investigated.

5.8 ABDOMINAL IMPACT TOLERANCE

Before 1980, the abdomen received very limited attention in biomechanics re-
search, and little information was available concerning abdominal tolerance
to blunt impact trauma. This was partly due to the difficulty in describing
the mechanical behavior of the highly deformable mobile organs in the abdomen

and partly due to greater concern for the prevention of injury to more critical organs of the body (Reference 63). Experiments found that the nature of the loading surface had a great influence on the reaction of the abdomen to load. They also found the organs to be strain rate sensitive, especially the liver, which was found to fail due to dynamic pressures generated in the tissue during impact. Summaries of research in abdominal impact prior to 1980 may be found in References 63 and 64.

More recent research has shown that the liver is the most commonly injured organ (Reference 65). It was found that the spleen can also be lacerated, but this smaller organ is protected by the rib cage and is more freely movable, and thus, less likely to be damaged. The kidneys, pancreas and adrenals are rarely injured.

Cavanaugh, et al., tested 12 unembalmed human cadavers for lower abdominal injury tolerance and mechanical response (Reference 66). The impacts were in an anterior to posterior direction, and the level of impact was primarily in the lower abdomen at the L3 level of the lumbar spine. See Figure 23 in Section 5.9 for an illustration of the spine anatomy. This is in a direct line with lower portions of the head of the pancreas, lower portions of the kidney and duodenum, the inferior vena cava, and the abdominal aorta. Impacts concentrated at the L3 level involve little or no rib contact. Thus, the response attained is involved with primarily the solid and hollow visceral elastic structures. These researchers found that the loading portion of the force-deflection curve of the lower abdomen of the human cadaver could be characterized by an almost linear rise from zero force to peak force and the hysteresis on unloading was approximately a vertical line, They found that a strong relationship existed between abdomen stiffness and impactor velocity, momentum, and kinetic energy. In comparing their results with those obtained on live animal surrogates, they found that the force-deflection responses of the cadavers were much less stiff than those of animal tests involving impacts into the upper and middle abdomen. They postulated that the lower abdomen is less stiff than the upper abdomen, which is less stiff than the chest. They also found that the lower abdomen shows a viscous elastic rate dependence.

A study conducted by Rouhana, et al. (Reference 67), utilized white rabbits as the test surrogates to determine the injury mitigating effects from a force-limiting or energy-absorbing material. They found that the probability of serious abdominal injury was well correlated to the product of the preimpact velocity and the maximum abdominal compression.

In studies on swine, Lau and Viano (Reference 61) found that a viscous response of 1.4 m/sec had a 50/50 chance of causing severe laceration of the liver (AIS equal to or greater than 5) in the fore/aft direction. These two numbers are not directly correlative, because the AIC is a less rigorous and more specific form of the Viscous Criterion. The AIC is the product of the preimpact or maximum velocity and the maximum compression ($V_{max}C_{max}$). In contrast, the Viscous Response (VC) is the maximum of the product of the instantaneous rate of compression and the compression, as discussed in Section 5.7.

5.9 SPINAL INJURY TOLERANCE

To understand spinal injury tolerance, it is necessary to briefly describe the anatomy of the human spine. The spine consists of a curved column of 33 vertebrae, typically, together with ligaments and intervertebral discs. At the

54

CERVICAL VERTEBRAE — ATLAS AXIS

THORACIC VERTEBRAE

LUMBAR VERTEBRAE

SACRUM

COCCYX

VERTEBRAL COLUMN IN RELATION TO BODY OUTLINE
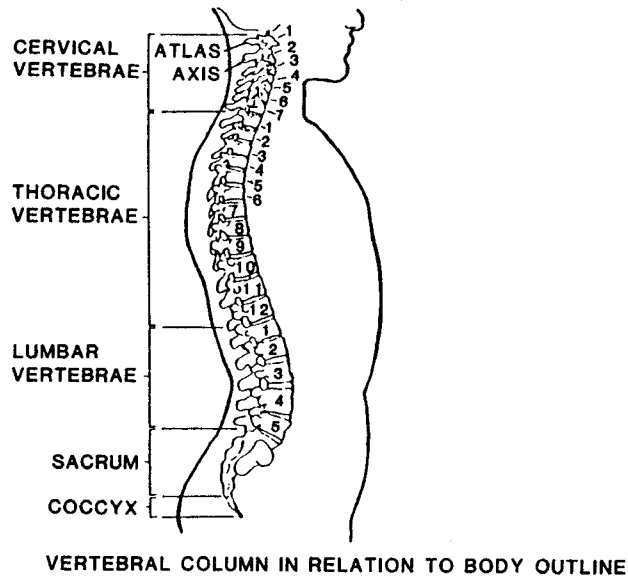
FIGURE 23. ANATOMY OF THE SPINE (VERTEBRAL COLUMN).

lower end four vertebrae are fused to form the coccyx, and immediately above this five vertebrae are fused to form the sacrum. The flexible portion of the spine is customarily divided into three sections: seven vertebrae of the cervical spine (neck), C1-C7; 12 vertebrae of the thoracic spine (articulated with ribs), T1-T12; and five vertebrae of the lumbar spine in the lower back, L1-L5 (see Figure 23).

5.9.1 Experimental Test Data

Damage to the vertebral column, particularly the upper lumbar and lower thoracic regions, occurs frequently in $+G_z$ impact, where the force is directed parallel to the spine. A summary of research on $+G_z$ impact exposure limits before 1975 is contained in Reference 68. Age has a negative effect on the strength of the vertebral column and is discussed in Reference 69.

In a study of clinical and operational data, Kazarian found that, in ejection or light aircraft/helicopter crashes, the thoracolumbar spine is the region most susceptible to injury (Reference 70). The cervico-thoracic junction (C5 to C7) was the second most susceptible region.

Anterior wedge fracture represented the most common, nonfatal injury. The anterior portion of the vertebral body of one vertebra tends to collapse under the load exerted by the next vertebra. It is considered a relatively benign injury and recovery is often complete. Pain and discomfort may result in temporary disability for several weeks.

55

Fracture dislocations are the most serious injuries. Any region of the spinal column can be involved, but in the majority of aircraft crashes the lesion occurs in the thoracic-lumbar and cervico-thoracic regions. Spinal cord lesions with paralysis below the fracture level are not uncommon. The fracture pattern usually consists of a crushed vertebral centrum of one or more vertebral bodies with partial or incomplete forward or sideward dislocation of the upper vertebra on the lower one.

The threshold of spinal injuries for seated humans subjected to $+G_z$ loading was investigated by Coltman, et al. (Reference 71). Fifteen tests were conducted with unembalmed cadavers. It was found that the threshold for spinal injury in the cadavers aged 44 to 63 years was significantly below that for younger, healthier U.S. Army aviators. Thus, bone compression strength tests were conducted to provide a baseline for relating the population of the cadavers used to the U.S. Army aviator population. The parameter used to assess the potential for spinal injury was the spinal load/strength ratio (SLSR). The SLSR was defined as:

$$SLSR = \frac{Applied\ Axial\ Spinal\ Load}{Ultimate\ Compressive\ Strength} \tag{7}$$

The data from the cadaver tests are shown in Figure 24, which plots the SLSR versus the spinal injury rate. This figure indicates that to maintain a 10-percent injury rate the SLSR should be kept at or below 0.26.
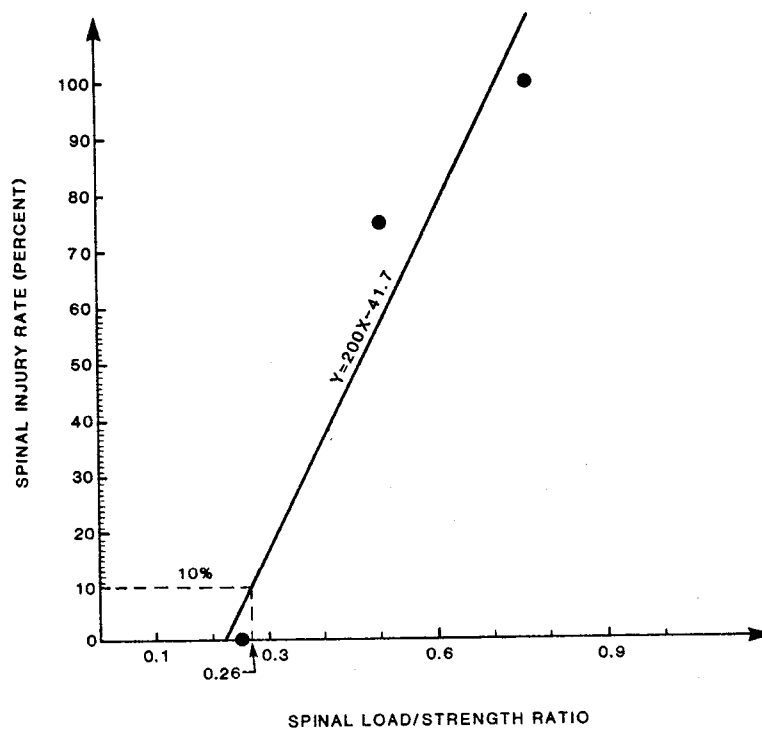
FIGURE 24. SPINAL INJURY RATE AS A FUNCTION OF SPINAL LOAD/STRENGTH RATIO (SLSR).

56

Correlation of the data for the compressive strengths, the spinal injury rates, and the correlation between peak spinal load and energy-absorber limit load factor (obtained from tests with a UH-60 energy-absorbing crewseat), yielded the estimated spinal injury rate as a function of the energy absorber limit load factor (Figure 25).
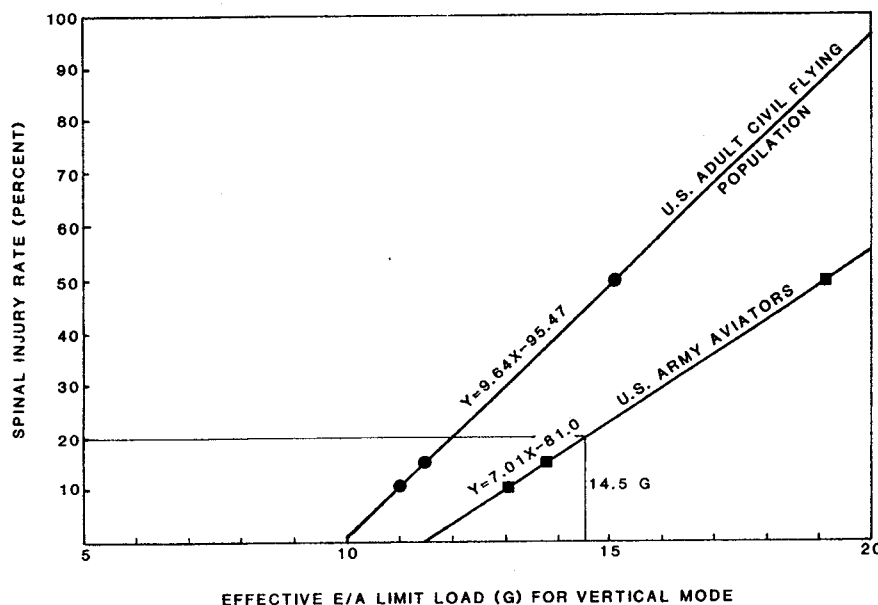
FIGURE 25.   CORRELATION BETWEEN THE ENERGY ABSORBER LIMIT-LOAD
             FACTOR AND SPINAL INJURY RATE.

The spine can also be injured by impact to the head. Hodgson and Thomas also measured loads and strains in the cervical spine of embalmed cadavers which were restrained in a vertical seated position under a hydraulic cylinder. The head was mounted in a loading fixture and strain was measured in C2, C4, and C6 (Reference 72).

5.9.2   Mathematical Model Predictions

Various mathematical models have been developed for prediction of spinal response to $+G_z$ loading. An obvious injury mechanism is the inertial loading sustained by the vertebrae, resulting in compression fractures. Therefore, the earliest models have been one-dimensional spring-mass systems that assume all the load to be borne by the vertebral body. One such model that has been used extensively in ejection seat evaluation is discussed in Section 5.9.2.1.

However, this simplified approach cannot predict all types of spinal injury and cannot assess the significance of spinal curvature. More comprehensive approaches have included the flexural beam model of Soechting (Reference 73) and the discrete parameter model of Orne and Liu (Reference 74) that accounts for the effects of eccentric loading as well as spinal curvature. Sections 5.9.2.2, 5.9.2.3, and 5.9.2.4 describe other models that appear promising for use in assessment of spinal injury potential in aircraft crashes.

57

5.9.2.1 Dynamic Response Index. The human response to short-duration accelerations applied in the upward vertical direction parallel to the spine $(+G_z)$ has been modeled by a single lumped-mass, damped-spring system as shown in Figure 26 (Reference 75). In this model, it has been assumed that the total body mass that acts upon the vertebrae to cause deformation can be represented by the single mass. In use, the relationship

$$\frac{d^2\delta}{dt^2} + 2\zeta\omega_n \frac{d\delta}{dt} + \omega_n^2\delta = z \qquad (8)$$

is solved through the use of a computer. The third term, which includes the deformation of the spine, δ, divided by the gravitational acceleration, g, is referred to as the Dynamic Response Index (DRI). The model is used to predict the maximum deformation of the spine and associated force within the vertebral column for various short-duration acceleration inputs. The spring stiffness for the model was determined from tests of human cadaver vertebral segments; damping ratios were determined from measurements of mechanical impedance of human subjects during vibration and impact.
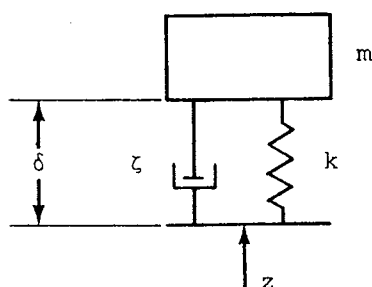
m = mass (lb-sec^2/in.)

δ = deflection (in.)

ζ = damping ratio

k = stiffness (lb/in.)

z = acceleration input (in./sec^2)

$$*DRI = \frac{\omega_n^2 \, \delta_{max}}{g}$$

ω_n = natural frequency of the analog = $\sqrt{k/m}$ (rad/sec)

g = 386 in./sec^2

*Dynamic Response Index

FIGURE 26. SPINAL INJURY MODEL. (FROM REFERENCE 75)

An analytical effort was conducted to determine the degree of correlation between the spinal injury (DRI) model and injuries experienced in operational aircraft ejection seats (Reference 76). Figure 27 shows the relationship between operational acceleration environments and actual spinal injury rates. The response of the model is expressed in DRI values. It can be seen that the injury probability does vary with the DRI but that the cadaver data show a higher probability of injury than do the operational data. It would be expected that the intact, living vertebral column imbedded in the torso would be stronger than cadaver segments; consequently, this result might be predicted.

58
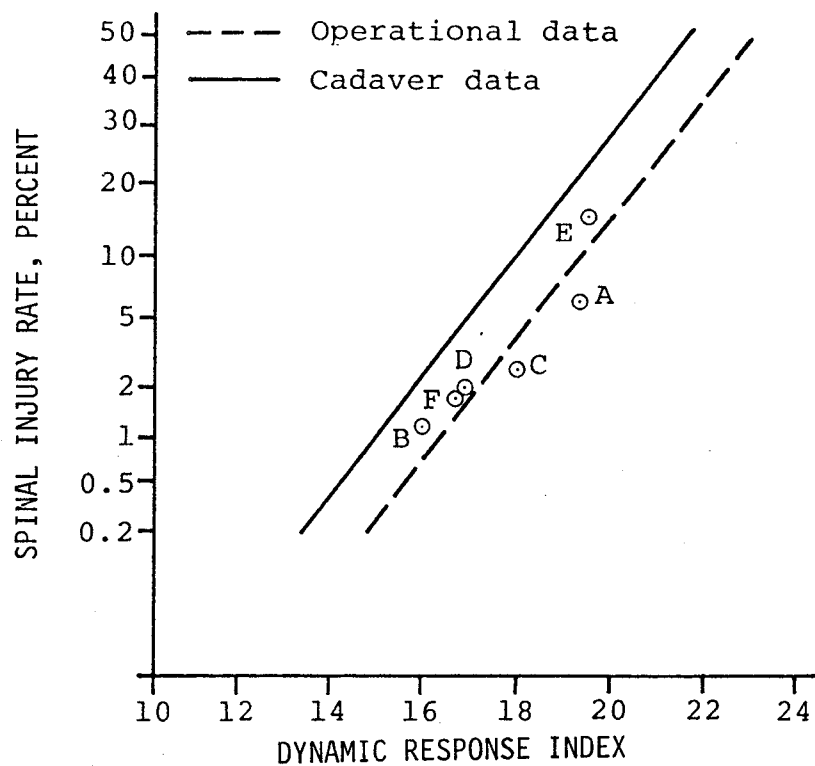
Aircraft type	Nonfatal ejections
A*	64
B*	62
C	65
D*	89
E	33
F	48

*Denotes rocket catapult

FIGURE 27. PROBABILITY OF SPINAL INJURY ESTIMATED FROM LABORATORY DATA COMPARED TO OPERATIONAL EXPERIENCE. (FROM REFERENCE 76)

To establish acceptable ejection seat acceleration environments, the Air Force has adopted a system using a combination of acceleration components and the DRI.

In Specification MIL-S-9479 (Reference 77), the acceleration levels to be imposed on the seat occupant are controlled by acceleration, time, and DRI as shown in the following relationship:

$$\left(\frac{DRI}{DRI_L}\right)^2 + \left(\frac{G_x}{G_{xL}}\right)^2 + \left(\frac{G_y}{G_{yL}}\right)^2 \leq 1.0 \qquad (9)$$

Here G_x and G_y are measured acceleration magnitudes in the x and y directions, and G_{xL} and G_{yL} are the limit acceleration parameters as read from acceleration versus time curves included in the specification. DRI is the DRI value computed from Equation (9) for the positive z direction. DRI_L is the limit value of the DRI. The value of DRI_L is 18 unless the resultant acceleration vector is more than 5 conical degrees off the z axis and aft of the plane of the seat back, in which case, the value of DRI_L is sixteen. The computed value for the left-hand term of Equation (10) may not exceed one.

The DRI is calculated from Equation (9) with model coefficients for the positive spinal case (eyeballs down) defined for the mean age of the Air Force flying population (age 27.9 years). The model coefficients are as follows:

$$\omega_n = 52.9 \text{ rad/sec}$$

$$\zeta = 0.224$$

The DRI has been shown to be effective in predicting spinal injury potential for $+G_z$ acceleration environments in ejection seats. However, it should be remembered that it is a simple model of a complex dynamic system and that the correlations made are for ejection seat acceleration-time pulses that can vary widely from crash pulses. In particular, the crash rate of onset can be an order of magnitude greater than for ejection seat pulses. Also, the position of the spine at the time of impact can have a significant influence on the susceptibility to vertebral damage. Therefore, a helicopter pilot leaning forward in his seat might be expected to respond differently from an upright, well-restrained ejection seat occupant, and thus have lower tolerance to impact.

5.9.2.2 Wayne State University Two-Dimensional Model. A two-dimensional spinal model that considers the details of load transmission among individual vertebrae has been developed by King and Prasad (Reference 78). The model considers the natural spinal curvatures and the effects of flexion and eccentric inertial loading on the spine. Head and neck motions are simulated, and their effects on the forces and moments in the thoracic and lumbar spine can be studied for off-axis impacts in the midsagittal plane. The input acceleration pulse can be an arbitrary function of time. The restraint and support systems have been included to properly simulate a seated vehicle occupant. The experimental data for validation of the model were obtained from cadaveric runs with the spine in the erect and hyperextended mode so that the model incorporates the ability to simulate both spinal configurations.

The following assumptions were made in the mathematical development:

- The 24 vertebral bodies, the head, and the pelvis are rigid bodies constrained to move in the midsagittal plane.

- Each rigid body has three degrees of freedom in the midsagittal plane--two translational and one rotational.

- The intervertebral discs are massless, and deformation of the spine takes place at the discs.

- The discs are replaced by a system of springs and dampers--one spring and damper for axial forces and another spring and damper arrangement for restoring torques due to relative angular motion between adjacent vertebral bodies.

- The facets and laminae are springs connected to the vertebral body by a massless rigid rod.

- Each rigid body is assumed to carry a portion of the torso weight that is eccentric with respect to the center line of the spine.

- The rigid bodies are arranged to simulate the spinal curvatures as closely as possible.

Equations of motion are derived for each vertebra, resulting in a set of 78 second-order differential equations that are solved numerically on a digital computer.

Experiments involving the use of human cadavers were carried out for model validation. An acceleration input was applied at the pelvis while the top of the head was allowed to remain stress free. The parameter used for validation was the force between two adjacent vertebrae, and an intervertebral load cell was developed to provide the magnitude and line of action of the force. Comparisons of model predictions and experimental data are shown in Figure 28 for two 10 G runs with the spine in different positions, where the loads were measured between the second and third lumbar vertebrae. Shown are both the loads between vertebral bodies (IVL) and those in the facets, which limit relative rotation of the vertebrae. The significance of the initial curvature of the spine is evidenced by the difference in response between the erect and hyperextended (backward rotation of the torso) modes.

This model appears to be potentially useful in spinal injury prediction, provided that dynamic fracture loads for vertebrae are known, as discussed in Reference 79.

5.9.2.3 **Air Force Head-Spine Model**. Under the sponsorship of the U.S. Air Force Aeromedical Research Laboratory, a three-dimensional, discrete model of the human spine, torso, and head was developed for the purpose of evaluating mechanical response in pilot ejection. It was developed in sufficient generality to be applicable to other body response problems, such as occupant response in aircraft crash and head-spinal system response to arbitrary loads. There are no restrictions on the distribution of direction of applied loads; therefore, a wide variety of situations can be treated. The model has been described in Reference 80.

TIME, MSEC

50   100   150   200   .250

IVL (model)

IVL (experimental)

IVL = Intervertebral load

Facet load (model)

Facet load (experimental)

(a) ERECT

TIME, MSEC

50   100   150   200   250

IVL (model)

IVL (experimental)

IVL = Intervertebral load

Facet load (experimental)

Facet load (model)

(b) HYPEREXTENDED

LOAD, LB
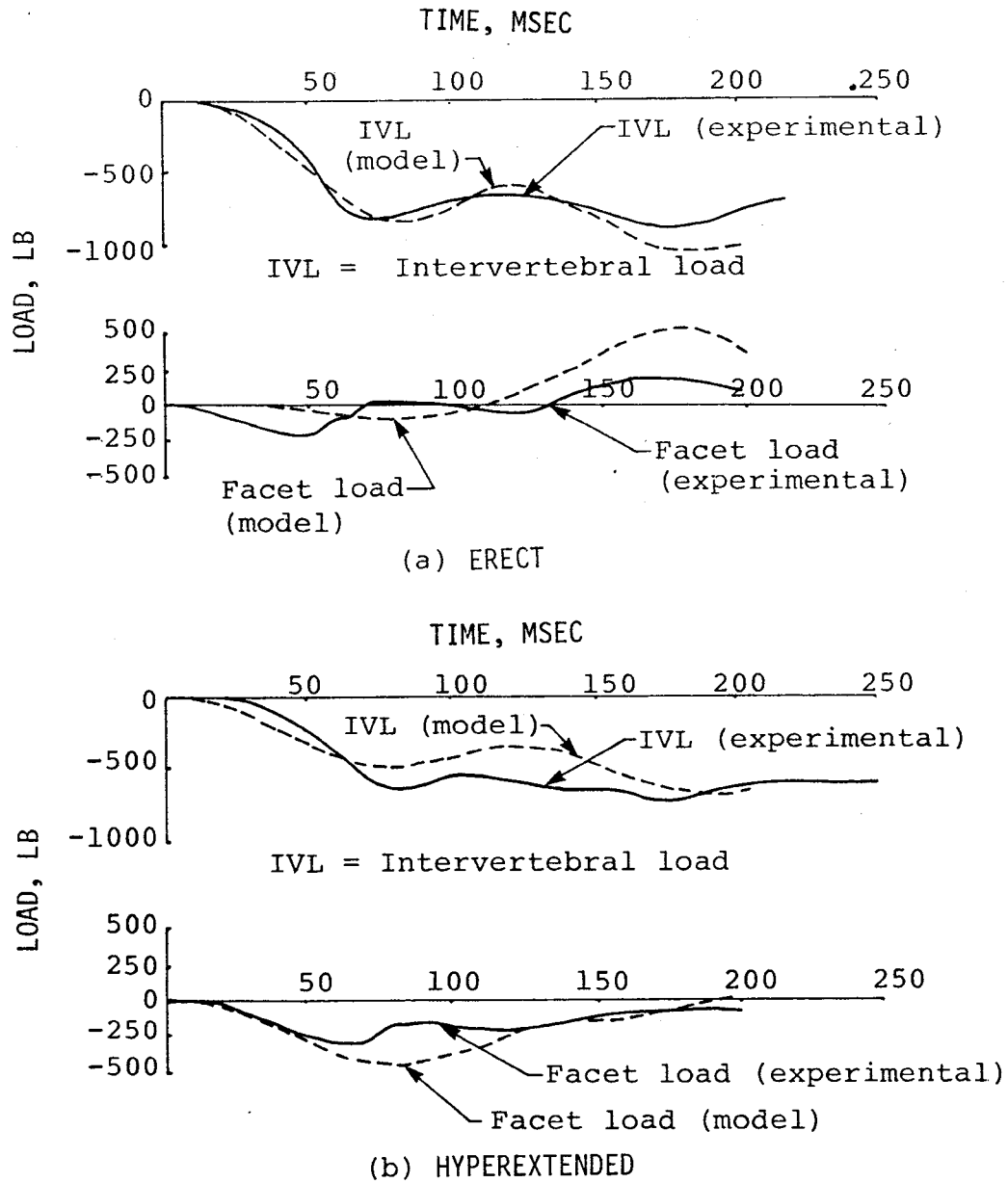
FIGURE 28.   COMPARISON OF MODEL OUTPUT AND EXPERIMENTAL DATA FOR 10-G RUNS WITH THE SPINE IN THE (a) ERECT AND (b) HYPEREXTENDED MODES.   (FROM REFERENCE 78)

The anatomy is modeled by a collection of rigid bodies that represent skeletal segments, such as the vertebrae, pelvis, head, and ribs, interconnected by deformable elements that represent ligaments, cartilaginous joints, viscera, and connective tissues. Techniques for representing other aspects of the ejection environment, such as harnesses and the seat geometry, are included also. The model is valid for large displacements of the spine and treats material nonlinearities. The elements of the model are illustrated in Figure 29.
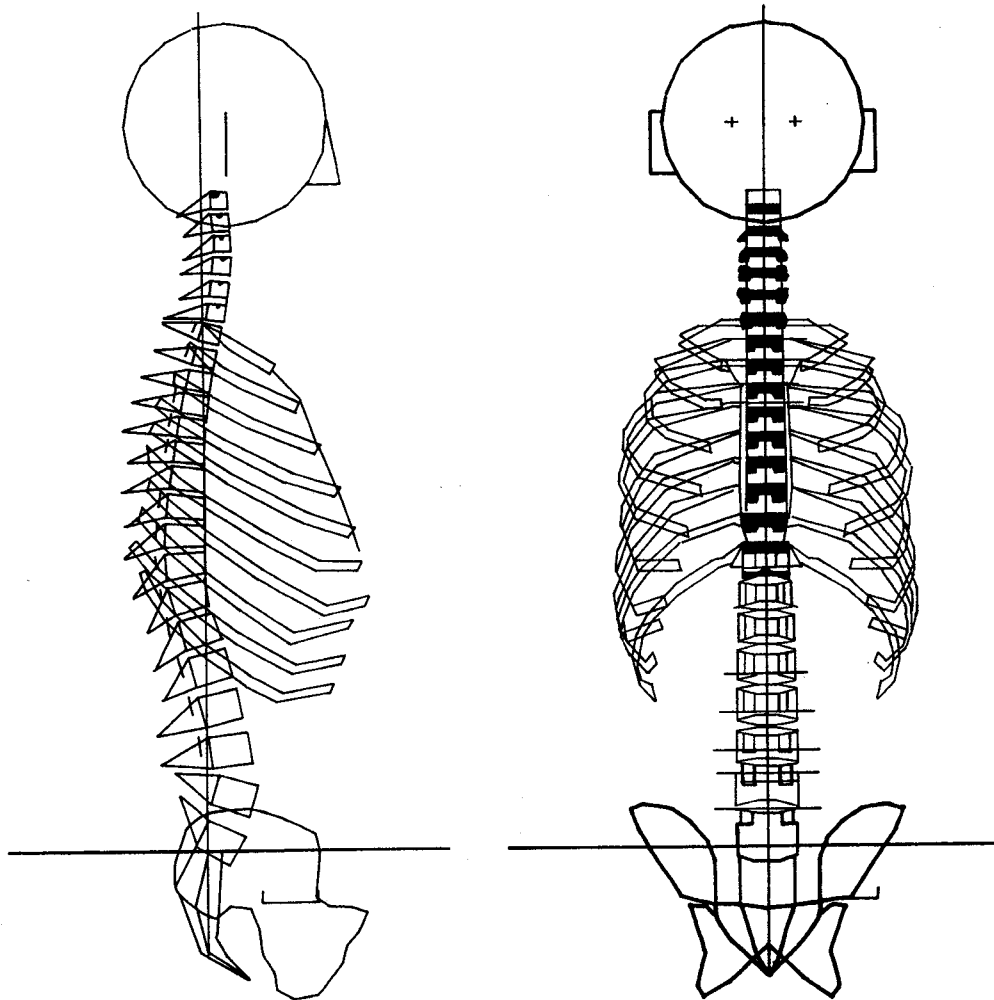
FIGURE 29. THREE-DIMENSIONAL HEAD-SPINE MODEL. (FROM REFERENCE 80)

The basic model is modular in format so that various components can be omitted or replaced by simplified representations. Thus, while the complete model is rather complex and involves substantial computational effort, various simplified models, which are quite effective in duplicating the response of the complete model within a range of conditions, are available. Three methods of solution are available for the analysis: direct integration in time either by an explicit, central difference method or by an implicit, trapezoidal method, and a frequency analysis method.

A variety of conditions have been simulated, including different rates of on-set, ejection at angles, effects of lumbar curvature, and eccentric head load-ings. It has been shown that large initial curvatures and perfectly vertical acceleration loadings, which cause large bending moments, result in substantial flexural response of the spine. It has been further shown that the combination of the spine's low flexural stiffness, initial curvature, and mass eccentricity are such that stability cannot be maintained in a 10 G ejection without restraints or spine-torso-musculature interaction.

The complete models were used mainly to study the effects of the rib cage and viscera on spinal response. The flexural stiffness of the torso is increased substantially by a visceral model, even though it has no inherent flexural stiffness. In addition, the viscera provide significant reductions in the axial loads.

5.9.2.4 Head/Neck Joint Analog. Studies conducted by several groups of researchers have shown that the results of the Naval Biodynamics Laboratory's extensive research program to determine the head/neck response of volunteer subjects to impact acceleration could be described by means of a relatively simple two-pivot analog system (References 51, 52, and 53). The analog, shown in Figure 30, defines the two ends of the neck. The base (T1) and the occipi-tal condyles are defined as the two joints. T1 is the neck/torso joint and the occipital condyles form the head/neck joint. The location and angle of the head anatomical origin (located at the midpoint of a line drawn between the centers of the external ears) can be used to determine the location of the occipital condyles at the top of the neck, The two joints are connected by a straight line. Although the line may not represent the actual length and angle of the neck, it can be used to represent the relative motion of the neck.
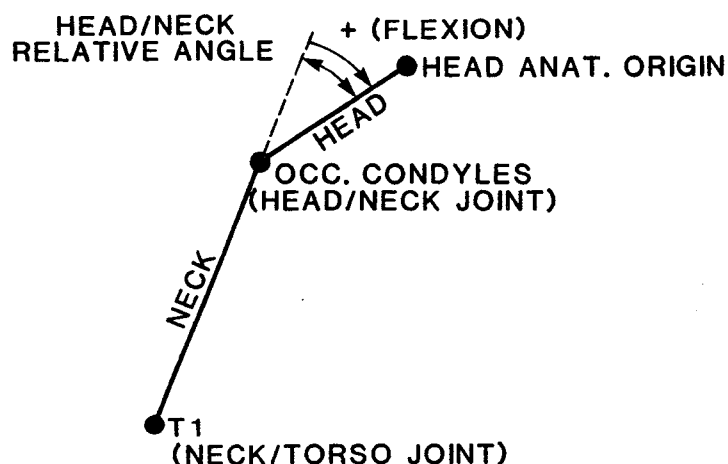
FIGURE 30.   IDENTIFICATION OF JOINTS, LINKS, AND HEAD/NECK
RELATIVE ANGLE IN HEAD/NECK TRAJECTORY PLOTS.

Wismans, et al., proposed a separate analog system for each impact direction (Reference 53). Geometrical parameters of the analog would be identical for each impact direction as far as the neck link length and the upper pivot location are concerned. The location of the lower pivot in the torso appears to be slightly different for each impact direction. Also, the initial position of this linkage system varies per impact direction. The initial neck link rotation is almost 18 degrees in frontal impacts, 11 degrees in oblique impacts, and close to zero in lateral ones.

Seeman, et al. (Reference 51), used the linkage model to simulate the response of the beam-like Hybrid III dummy neck to $-G_x$ sled acceleration. They found that it was possible to obtain quite human-like simulations by either relocating the neck/torso joint rearward and below the T1 anatomical origin or by moving the head/neck joint up to the head anatomical origin and the neck/torso joint rearward of the T1 anatomical origin.

It should be pointed out that the majority of the work on this model has been in the $-G_x$ impact direction. Also, currently the proposed analog system can only be considered valid for low severity impacts, i.e., the NBDL human volunteer test conditions. Additional information must still be obtained for higher exposure levels from human cadaver tests. If such data become available, adjustment of the proposed analog system might be necessary.

5.9.3 Vertebral Properties

Accurate strength and deflection properties of the seated human torso when exposed to inertial loads are urgently needed. Reference 81 includes a consolidation of the data from King, Kazarian, and Hodgson (References 78, 82, and 83) for the head and spinal column exposed to $+G_z$ loading.

The vertebral ultimate compression strengths for Army aviators and the U.S. adult civil flying population are shown in Figure 31 (from Reference 71). The U.S. Army aviator data is based on cadavers with a mean age of 31 years and the U.S. adult civil flying population is based on cadavers with a mean age of 56 years.

5.10 LEG INJURY TOLERANCE

Femoral fracture due to longitudinal impact on the knee has been studied extensively, probably because of the frequency of this type of injury in automobile accidents.

Based on cadaver data obtained by Patrick, et al. (Reference 84), King, et al., recommended a peak fracture load of 1700 lb as a realistic criterion (Reference 85). Experiments reported by Powell, et al., point to this value as being conservative for impacts of less than 20 m/sec (Reference 86). Federal Motor Vehicle Safety Standard 208 specified a maximum axial load of 2250 lb.

65
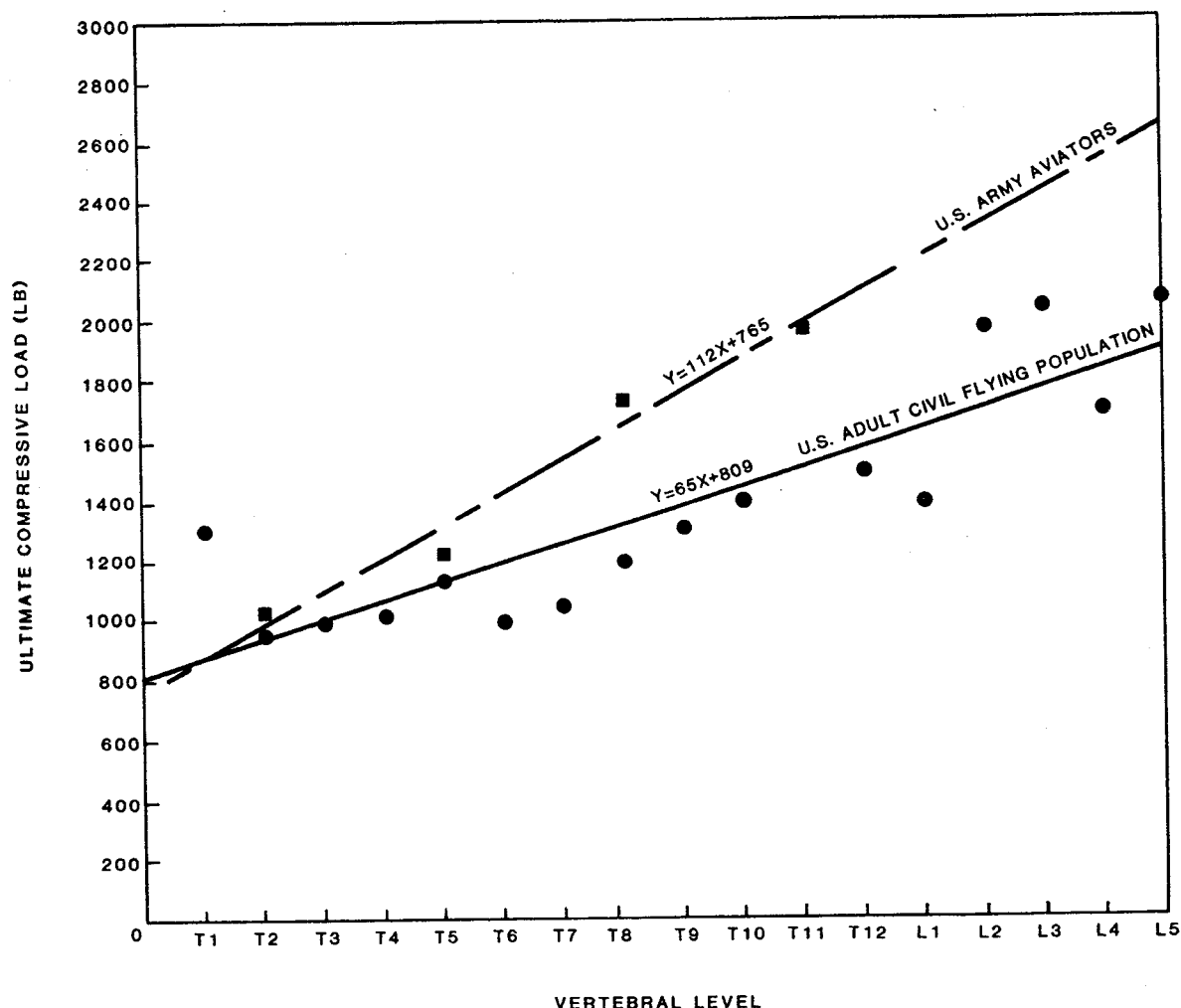
FIGURE 31. VERTEBRAL ULTIMATE COMPRESSIVE STRENGTH FOR
VARIOUS POPULATIONS.

Viano has presented a criterion that assesses the dependence of the permissible human knee load on the duration of the primary force exposure (Reference 87). Based on the knee impact data from previous experiments with both fresh and embalmed cadavers, Viano suggests the following femur injury criterion (FIC) to define a permissible peak knee load:

$$F(kN) = 23.14 - 0.71 \ T(msec), \ T < 20 \ m/sec$$

$$F(kN) = 8.90, \ T \geq 20 \ m/sec \tag{10}$$

or, in English units,

$$F(lb) = 5200 - 160 \ T(msec), \ T < 20 \ m/sec$$

$$F(lb) = 2000, \ T \geq 20 \ msec \tag{10a}$$

66

The relationship of Equation (10) is illustrated in Figure 32.
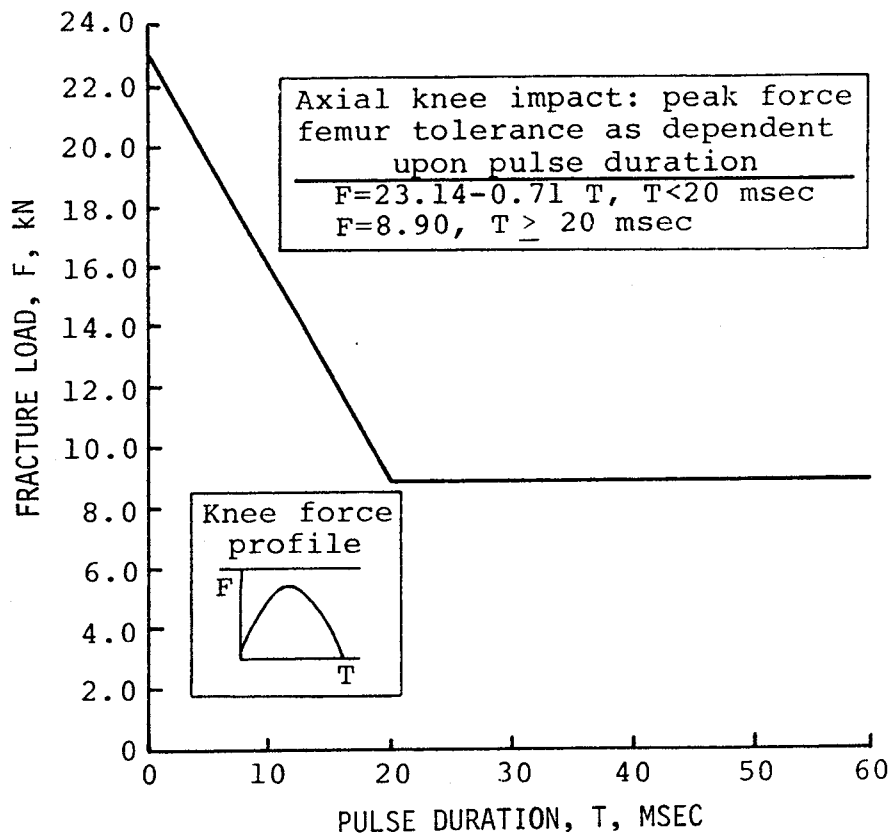
FIGURE 32. FEMUR INJURY CRITERION. (FROM REFERENCE 87)

5.11 ABBREVIATED INJURY SCALE

The Abbreviated Injury Scale (AIS), first published in 1971, was developed as a comprehensive system for rating injuries by types and severity that would be acceptable to physicians, engineers, and researchers working in automotive crash investigation. (Its development is summarized in Reference 88). Over the last decade, the AIS has evolved as the universal system of choice for assessing impact injury severity. It has been revised several times since its initial publication as the sophistication of injury assessment, particularly among emergency room traumatologists, has increased. The latest revision was published in 1985 (Reference 89). The AIS rates seven regions of the human body in terms of seven Severity Codes, shown in Table 13.

67

TABLE 13. ABBREVIATED INJURY SCALE SEVERITY CODES

AIS No.	Severity Code
1	Minor
2	Moderate
3	Serious
4	Severe
5	Critical
6	Maximum Injury, Virtually Unsurvivable
9	Unknown

The Injury Severity Score (ISS) is being used by many researchers. It is a mathematically derived code number determined from the highest AIS codes in each of the three most severely injured body regions. An engineer concerned with interpretation or use of the AIS or the ISS is referred to Reference 89, which contains a complete description of the Injury Scale and how to use it.

6. OCCUPANT MOTION ENVELOPES

6.1 INTRODUCTION

The purpose of this chapter is to present the extent of an aircraft occupant's motion in a crash. This knowledge is vital in designing for occupant protection from injury due to impact with the aircraft interior, a topic discussed in Volume IV.

The body kinematics associated with an aircraft crash are quite violent, even in accidents of moderate severity. The flailing of body parts is very pronounced when the occupant is restrained with a lap belt only. However, even with a lap belt and a shoulder harness that are drawn up tightly, multidirectional flailing of the head, arms, and legs, and to a lesser extent, the lateral displacement of the upper torso within its restraint harnessing, is extensive. If it were possible to provide adequate space around the occupant, this flailing action would not be a particular problem. Since space for occupants is usually at a premium in aircraft, especially in cockpit areas, it is not feasible to locate structural parts of the aircraft sufficiently remote to keep the occupant from striking them. The only alternative is to design the occupant's immediate environment so that, when the body parts do flail and contact rigid and semirigid structures, injury potential is minimized.

An occupant who is even momentarily debilitated by having his head strike a sharp, unyielding structural object or by a leg injury can easily be prevented from rapidly evacuating the aircraft and may not survive a postcrash fire or a water landing.

Several approaches are available to alleviate secondary impact problems. The most direct approach, which should be taken if practical, is to relocate the hazardous structure or object out of the occupant's reach. Such action is normally subject to trade-offs between safety and operation or human engineering considerations. If relocation is not a viable alternative, the hazard might be reduced by mounting the offending structure on frangible or energy-absorbing supports and applying a padding material to distribute the contact force over a larger area. Application of protection padding for both energy absorption and load distribution is discussed in Volume IV.

The following sections describe head and body excursions during forward impact sled tests with various restraint system configurations. It should be noted that these strike envelopes represent the effectiveness of various restraint systems under $-G_x$ loads. They cannot be used to identify the extent of the head and body excursions under vertical impact. In this case, the head travels until it hits an object such as the cyclic stick or knee, even with a restraint system that includes a shoulder harness.

6.2 FULL RESTRAINT

Body extremity strike envelopes are represented in Figures 33 through 35 for a 95th-percentile Army aviator wearing a restraint system that meets the requirements of MIL-S-58095 (Reference 12). The restraint system consists of a lap belt, lap belt tiedown strap, and two shoulder straps. The forward motion shown in Figures 33 through 35 was obtained from a test utilizing a 95th-percentile anthropomorphic dummy subjected to a spineward ($-G_x$) acceleration of 30 G. The lateral motion is based on expected restraint system deflections in a 30-G lateral crash impact.

HEEL REST LINE FOR COCKPIT

AIRCRAFT FLOOR LINE FOR TROOP COMPARTMENT
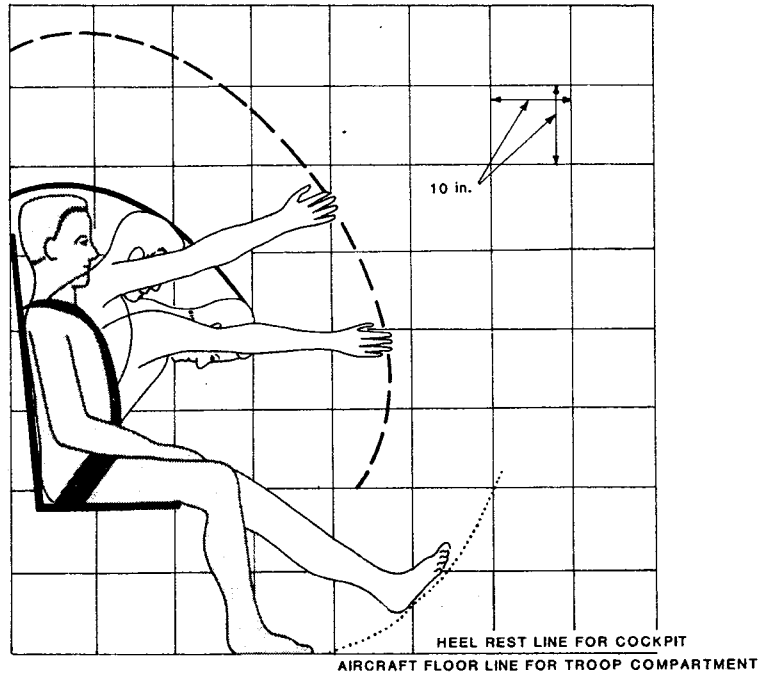
FIGURE 33. FULL-RESTRAINT EXTREMITY STRIKE ENVELOPE - SIDE VIEW.
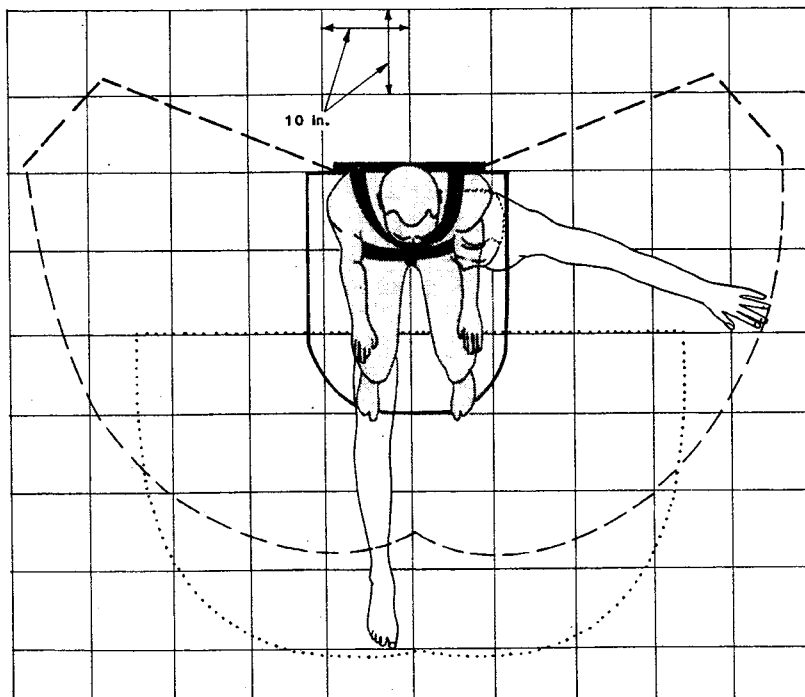
FIGURE 34. FULL-RESTRAINT EXTREMITY STRIKE ENVELOPE - TOP VIEW.

70
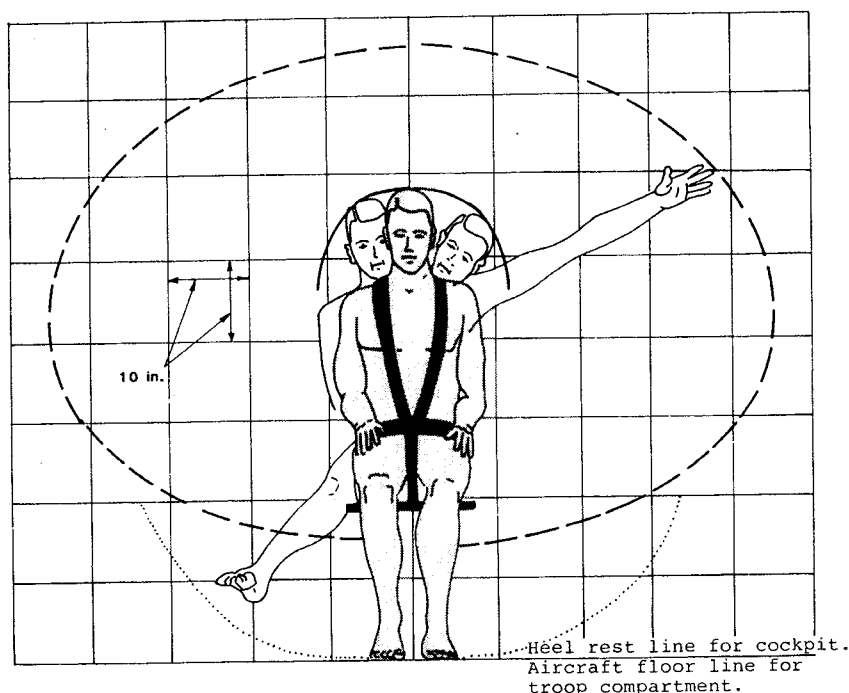
FIGURE 35. FULL RESTRAINT EXTREMITY STRIKE
ENVELOPE - FRONT VIEW.

6.3 LAP-BELT-ONLY RESTRAINT

Although upper torso restraint is required in new Army aircraft, strike
envelopes for a 95th-percentile aviator wearing lap-belt-only restraint are
presented for possible use in Figures 36 through 38. They are based on 4-G
accelerations and 4 in. of torso movement away from the seat laterally and
forward.

6.4 INFLATABLE BODY AND HEAD RESTRAINT SYSTEM

An experimental prototype inflatable body and head restraint system (IBAHRS)
reduces occupant upper torso, head, and neck motion in comparison to a full
restraint (MIL-S-58095) and a lap-belt-only restraint (Reference 90). A major
advantage of the IBAHRS is that it is crash sensor activated. However, since
the airbags deflate immediately after inflation, they are effective for
a single crash pulse only, although the system provides the added benefit of
protection with the basic restraint system to which the airbags are attached.
It was also found that incorporating the IBAHRS enhanced the existing MIL-S-
58095 restraint system and did not reduce the function of the basic restraint.
A comparison of head displacements using the IBAHRS and the host MIL-S-58095
restraint is shown in Figure 39 (from Reference 91). This comparison demon-
strates how the inflated airbags pick up the slack between the restraint
webbing and the compressed body under impact.

71

Heel rest line for cockpit.
Aircraft floor line for
troop compartment.

10 in.
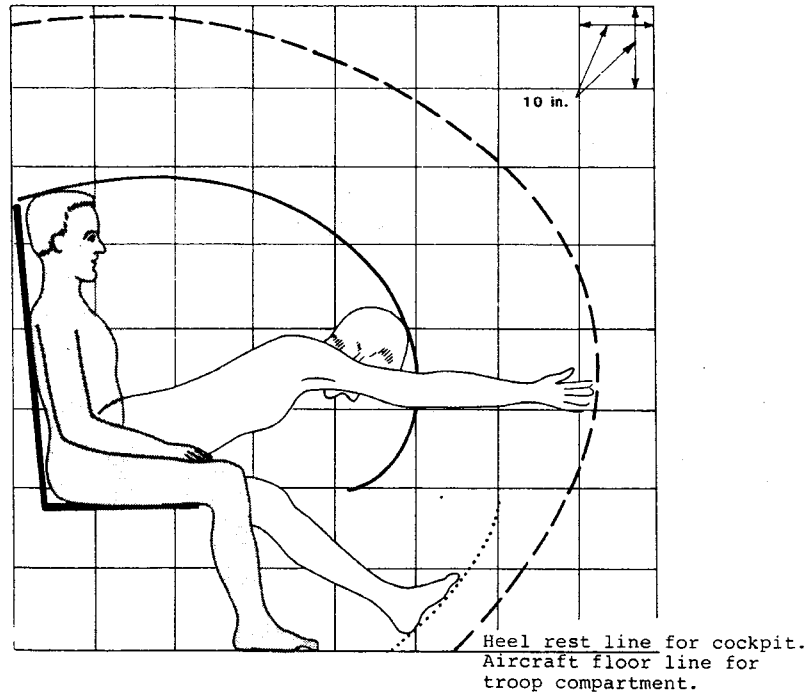
**FIGURE 36. LAP-BELT-ONLY EXTREMITY STRIKE
ENVELOPE - SIDE VIEW.**

10 in.
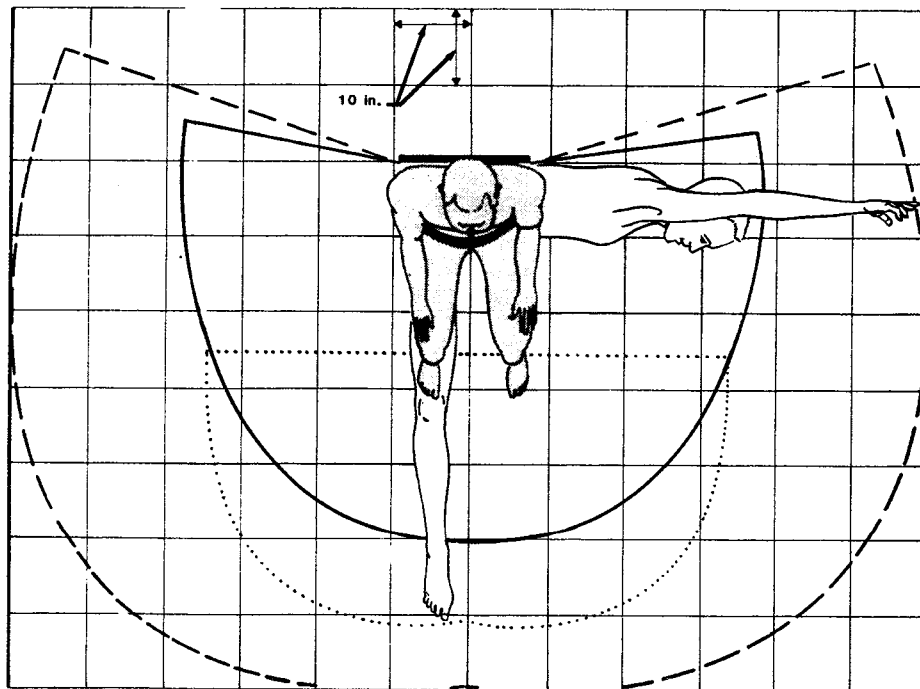
**FIGURE 37. LAP-BELT-ONLY EXTREMITY STRIKE
ENVELOPE - TOP VIEW.**

72
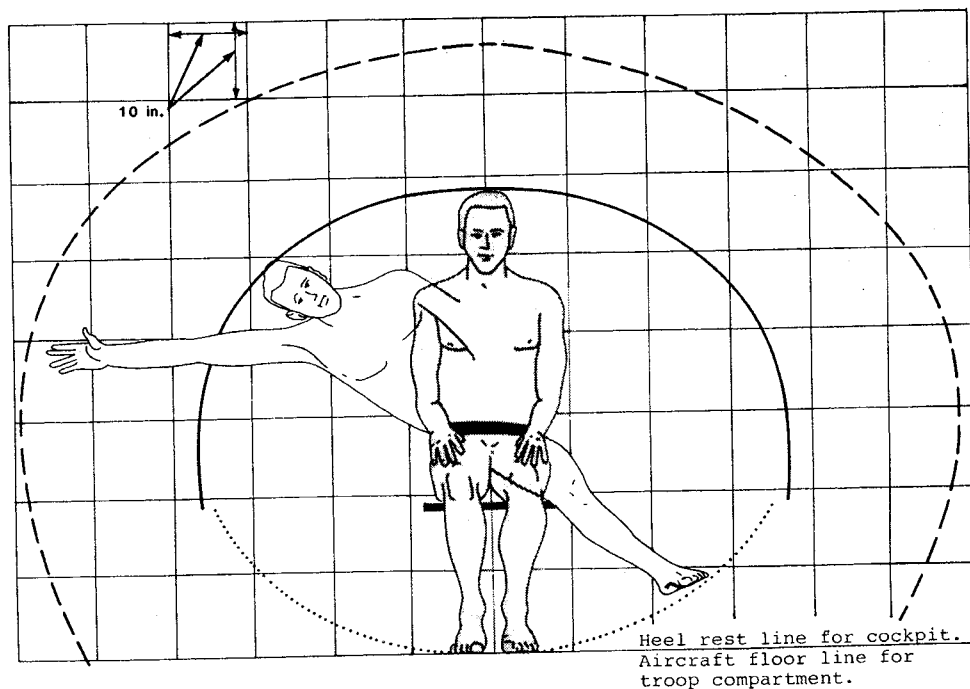
FIGURE 38. LAP-BELT-ONLY EXTREMITY STRIKE ENVELOPE - FRONT VIEW.

In an extensive series of sled tests sponsored by the U.S. Army, several types of restraint systems were compared by dynamic impact crash testing to determine the strike envelopes associated with each restraint system (Reference 90). The restraints included the IBAHRS, the standard MIL-S-58095 system, the MIL-S-58095 system with a power haul-back reel instead of an inertia reel, and a reflected strap shoulder harness restraint with and without a power haul-back reel. The results of this study demonstrated that the IBAHRS reduced occupant upper torso, head, and neck motion compared to the other restraint systems.

HEAD STRIKE ENVELOPE

15 Gx
40 FT/SEC
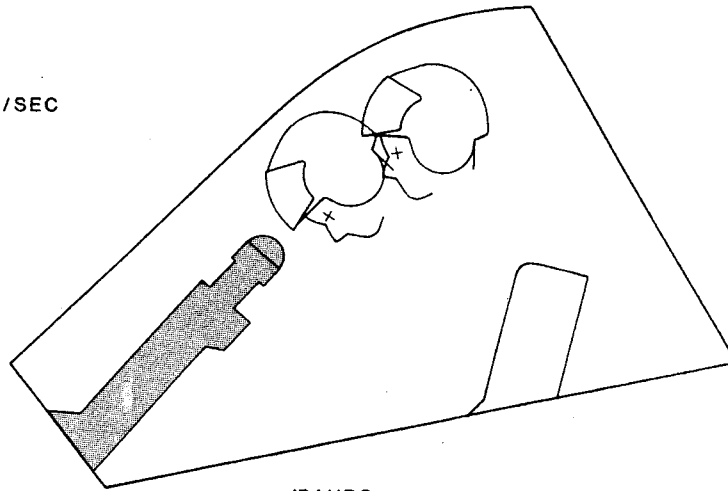
IBAHRS

15 Gx
40 FT/SEC
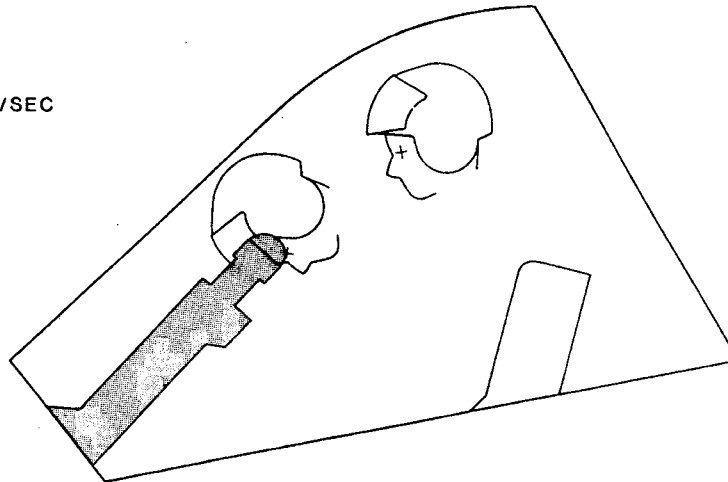
MIL-S-58095

FIGURE 39.   HEAD DISPLACEMENT FOR IBAHRS AND
MIL-S-58095 RESTRAINT TESTS, 15-G
PULSE, 95TH-PERCENTILE DUMMY.

74

7. HUMAN BODY DIMENSIONS AND MASS DISTRIBUTION

7.1 INTRODUCTION

This chapter presents information on the dimensions and properties of the human body. Anthropometric measurements are external dimensions of the human body that can be used to define aircraft requirements such as seat height and width, eye height, or cabin height. A specialized type of anthropometric measurement is the "link length," or distance between joint centers, which can be used in locating control positions and is essential for the design of mathematical or physical simulators of the human body. Finally, the inertial properties of the body and parts of the body also are required in the design of human simulators.

7.1 ANTHROPOMETRY

Anthropometry is a specialized area of physical anthropology that is concerned with the measurement of the human body and its parts. Two types of anthropometric measurements have been recorded, and the use of both types in vehicle design has been summarized in Reference 92. Conventional dimensions of the body obtained with subjects in rigid, standardized positions are easily obtained. Extensive collections of such data are used in clothing design and may determine certain vehicle design parameters including seat height and eye height. A second class of data, which may be referred to as workspace dimensions, is more difficult to obtain and can be applied only to the specific workspace studied. However, these workspace dimensions are essential in designing aircraft interiors for maximum occupant protection.

7.1.1 Conventional Anthropometric Measurements

Conventional anthropometric measurements of greatest interest in aircraft interior design include those dimensions illustrated in Figure 40, as well as standing height and body weight. The most recent anthropometric survey of U.S. Army male aviators is contained in Reference 93, and the dimensions of greatest potential usefulness are presented in Table 14. Corresponding dimensions for male nonaviators, taken from Reference 94, are listed in Table 15. Similarly, corresponding dimensions for U.S. Army women, taken from Reference 95, are listed in Table 16. There are no data for women aviators as yet, so the data in Table 16 must be used by the aircraft designers until more specific data are available. These dimensions are nude measurements; the dimensions of bulky clothing and helmets must be considered for specific applications.

Because anthropometric surveys involve a large population sample, they generally follow a normal (bell-shaped) distribution. A normal distribution, as shown in Figure 41, can be described in terms of its mean or average value and its dispersion about the mean, often expressed as standard deviation.

The percentile value, which corresponds to a rank order, is a useful statistic for designers. If a group of subjects were ordered from least to greatest for any given measurement, such as standing height, the first percentile would be that part exceeded by 99 percent of the group; the 5th-percentile would be that exceeded by 95 percent of the group. The 50th-percentile, or median, would be that half of the group exceeded by the other half. For a normally distributed sample, the median value is the same as the mean, or average.
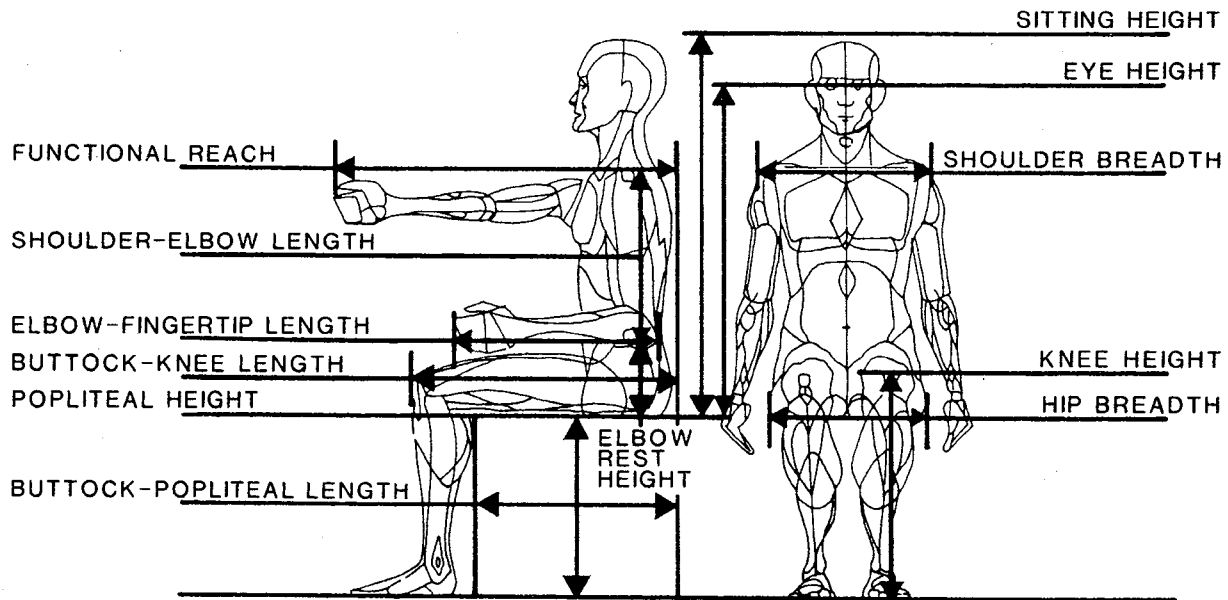
FIGURE 40. CONVENTIONAL SEATED ANTHROPOMETRIC DIMENSIONS.

TABLE 14. SUMMARY OF ANTHROPOMETRIC DATA FOR
U.S. ARMY MALE AVIATORS (REFERENCE 93)

Measurement	Percentiles (in.)		
	5th	50th	95th
Weight (lb)	133.0	171.0	212.0
Stature	64.6	68.7	72.8
Seated height	33.7	35.8	37.9
Shoulder breadth	17.0	18.7	20.3
Functional reach	28.8	31.1	34.2
Hip breadth, sitting	13.2	14.8	16.7
Eye height, sitting	29.0	31.0	33.1
Knee height, sitting	19.3	20.8	22.6
Elbow rest height, sitting	7.4	9.1	10.8
Popliteal height	15.1	16.6	18.3
Shoulder-elbow length	13.3	14.4	15.6
Elbow-fingertip length	17.6	19.0	20.3
Buttock-popliteal length	17.7	19.3	21.0
Buttock-knee length	22.0	23.7	25.4

76

TABLE 15.   SUMMARY OF ANTHROPOMETRIC DATA
FOR MALE SOLDIERS (REFERENCE 94)

Measurement	Percentiles (in.)		
	5th	50th	95th
Weight (lb)	126.0	156.0	202.0
Stature	64.5	68.7	73.1
Seated height	33.3	35.7	38.1
Shoulder breadth	16.3	17.8	19.6
Hip breadth, sitting	11.9	13.0	14.5
Eye height, sitting	28.6	31.0	33.3
Knee height, sitting	19.6	21.3	23.1
Popliteal height	16.0	17.5	19.2
Shoulder-elbow length	13.3	14.5	15.7
Elbow-fingertip length	17.4	18.8	20.4
Buttock-popliteal length	18.0	9.6	21.3
Buttock-knee length	21.6	23.4	25.3

TABLE 16.   SUMMARY OF ANTHROPOMETRIC DATA FOR
U.S. ARMY WOMEN (REFERENCE 95)

Measurement	Percentiles (in.)		
	5th	50th	95th
Weight (lb)	102.8	131.4	164.3
Stature	60.1	64.1	68.5
Seated height	31.1	33.5	35.8
Shoulder breadth	15.1	16.5	18.0
Functional reach	25.2	28.0	31.1
Hip breadth, sitting	12.4	13.9	15.6
Eye height, sitting	26.7	29.1	31.2
Knee height, sitting	18.5	20.0	21.8
Elbow rest height, sitting	6.4	8.2	9.9
Popliteal height	15.0	16.4	18.0
Shoulder-elbow length	12.1	13.2	14.4
Elbow-fingertip length	15.7	17.1	18.7
Buttock-popliteal length	-	-	-
Buttock-knee length	20.9	22.7	24.9
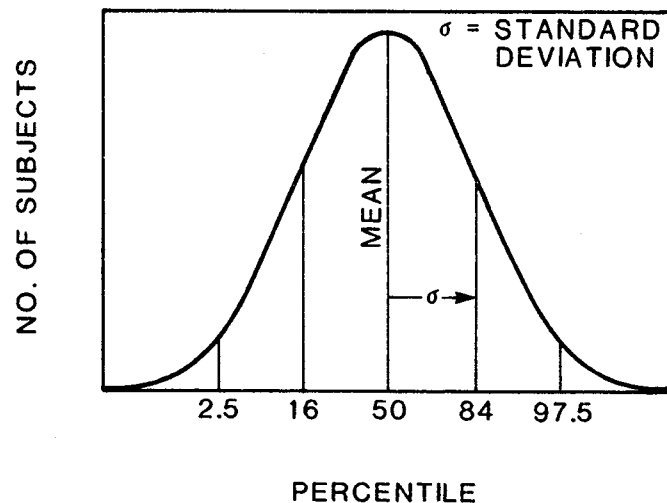
FIGURE 41. NORMAL DISTRIBUTION CURVE.

For a normal distribution, 68 percent of the sample is included within plus or minus one standard deviation of the mean, and 95 percent within plus or minus two standard deviations.

An example of the use of the statistics of anthropometric data in setting design limits for a vehicle dimension (seat height adjustment range) is presented in Reference 92.

7.2.2 Equipment Weights

Personnel equipment weights to be considered in the design of aircraft systems are shown in Table 17. The effective weight of a seated occupant in the vertical direction is the sum of the following quantities: 80 percent of the occupant's body weight, 80 percent of the weight of the occupant's clothing less boots, and 100 percent of the weight of any equipment carried totally on the occupant's body above knee level.

7.2.3 Body Joints and Ranges of Motion

Few body joints involve rotation about fixed axes or pivot points. Rather, the instantaneous center of rotation may depend on position, as illustrated in Figure 42 for the shoulder joint. Dempster reported on an extensive study of workspace requirements for seated operators, in which he determined "link lengths" between effective joint centers for major body parts (References 96 and 97), rather than standard anthropometric dimensions based on external measurements. These link lengths have a number of crash-resistance-related applications: (1) in developing or expanding the strike envelopes shown in Chapter 5, (2) in designing crash test dummies, and (3) in providing numbers for mathematical simulators. From the data of several investigations, Singley and Haley developed the skeletal joint locations for a 50th-percentile male Army aviator that are illustrated in Figure 43 (Reference 81).

78

TABLE 17. PERSONNEL EQUIPMENT WEIGHTS (LB)

	Percentiles		
Item	5th-Female	50th-Male	95th-Male
SPH-4, Flying Helmet	3.38	3.38	3.44
Nomex Flight Clothing	3.10	3.10	3.10
Combat Boots, Leather Uppers	4.12	4.12	4.12
Leather Flying Gloves	.28	.28	.28
Pen Light	.10	.10	.10
Survival Vest w/Gear	7.50	7.50	7.50
Armor Plate	-	12.20	14.50
Flotation Gear	2.70	2.70	2.70
Weapon w/Belt, Holster, and Ammo	3.90	3.90	3.90
Winter Jacket and Trousers	5.25	5.25	5.25
MOPP* Gear for Pilot	9.0	9.0	9.0
MOPP* Gear for Troop	11.5	11.5	11.5

*Mission orientation protective posture
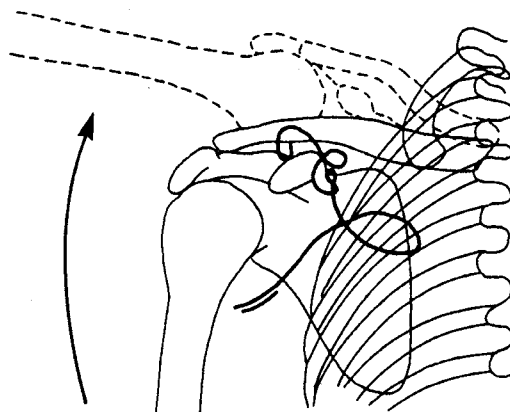
MOPP = MISSION ORIENTATION
PROTECTIVE POSTURE

FIGURE 42. PATH OF INSTANTANEOUS CENTER OF ROTATION DURING SHOULDER ABDUCTION. (FROM REFERENCE 96)

Joint ranges of motion are required in the same areas of application listed above the link lengths. These movements, illustrated in Figure 44, are measured from a standard anatomical position defined as an erect standing posture with the palm surfaces of the hands positioned anteriorly. Various studies have determined the ranges of motion that may be attained voluntarily and under external force; Table 18 lists angles obtained by Glanville and Kreezer (Reference 98) for the movements defined in Figure 44.

Top of head
(crown) ————————————— RL 174.6*

Skull base and
Cl intersection ————————— RL 160.3
C2-C3 hinge ————————————— RL 157.1

C7-Tl hinge RL ——————————— RL 148.7

RL 141.6 ——————————— RL 142.4

RL 135.1

RL 127.5

RL 118.7

RL 112.8 ——————— RL 111.8

RL 104.4
RL 101.6
RL 100.9

RL 96.5

RL 91.2

RL 83.6

RL 50.2

RL 42.5*

*-Horizontal reference line
  in centimeters

SITTING HEIGHT, CM

HORIZONTAL SCALE, CM
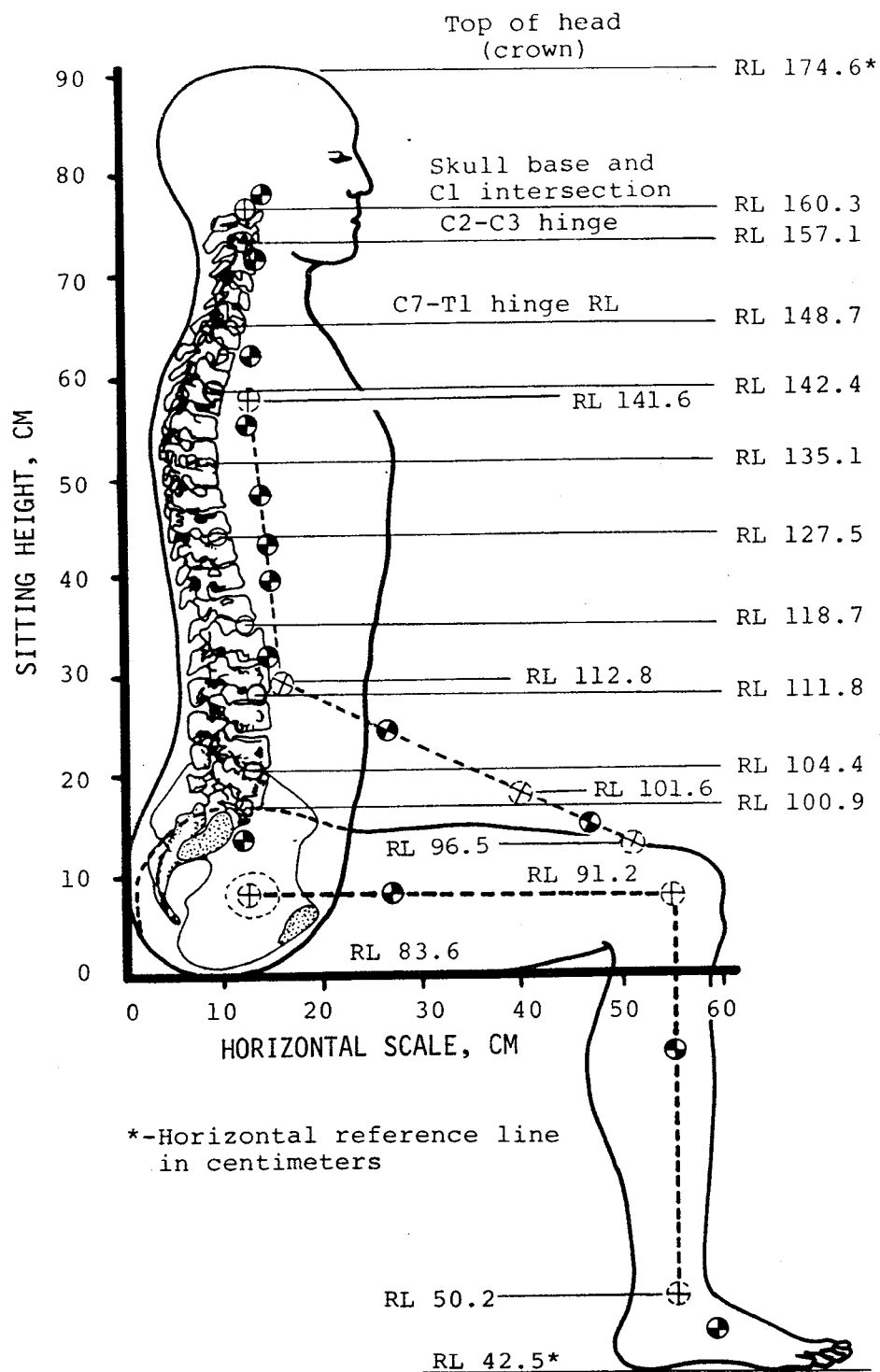
**FIGURE 43.   SITTING SKELETAL JOINT LOCATIONS BASED ON A 50TH-
PERCENTILE MALE ARMY AVIATOR.   (FROM REFERENCE 81)**
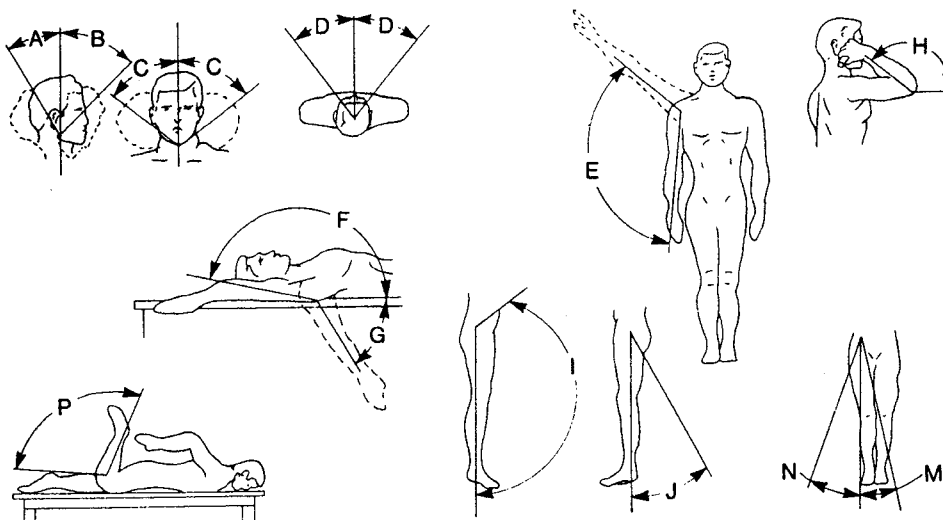
FIGURE 44. JOINT RANGES OF MOTION.

TABLE 18. RANGE OF JOINT ROTATION (REFERENCE 98)

Body Component Motion	Symbol	Motion Description	Measured Rotation (degree) Voluntary	Forced
Head - with respect to torso	A	Dorsiflexion	61	77
	B	Ventriflexion	60	76
	C	Lateral flexion	41	63
	D	Rotation	78	83
Upper arm - at shoulder	E	Abduction (coronal plane)	130	137
	F	Flexion	180	185
	G	Hyperextension	58	69
Forearm - at elbow	H	Flexion	141	146
Thigh - at hip	I	Flexion	102	112
	J	Hyperextension	45	54
	K	Medial rotation	-	-
	L	Lateral rotation	-	-
	M	Adduction	-	-
	N	Abduction	71	79
Lower leg - at knee	P	Flexion	125	138

7.3 INERTIAL PROPERTIES

Inertial properties of the human body have been used in design of escape systems, and moments of inertia of live subjects in a seated position were determined by Santschi, Debois, and Omoto (Reference 99). However, anthropomorphic dummies and mathematical simulations require inertial properties of body segments, specifically moments of inertia, mass, and center-of-mass locations and moments of inertia with respect to transverse (y) axes were measured on segmented cadavers (References 96 and 97).

Clauser, McConville, and Young determined center-of-mass locations and developed regression equations for cadaver segments (Reference 100). From data of various sources, Singley and Haley (Reference 81) determined the segment masses and center-of-mass locations presented in Table 19 and Figure 45 for a 50th-percentile male Army aviator. Chandler, et al., measured moments of inertia with respect to six axes for fourteen segments of six cadavers and, from them, calculated the principal moments of inertia for the segments (Reference 101). Their results are presented in Table 20.

TABLE 19. CENTER-OF-MASS DISTRIBUTION OF SEATED TORSO –
50TH-PERCENTILE MALE ARMY AVIATOR (REFERENCE 81)

Body Segment Identify	Segment Mass (kg)	Z-Axis Location (cm)*	X-Axis Location (cm)**
Head	4.74	77.6	10.1
Neck (C1-C7)	1.63	71.3	9.7
Upper thoracic (T1-T3)	4.07	62.4	10.0
Upper mid thoracic (T4-T6)	4.07	55.6	9.7
Lower mid thoracic (T7-T9)	4.66	48.1	11.2
Upper arm	4.44	43.5	12.2
Lower thoracic (T10-T12)	5.29	40.2	13.0
Lumbar (L1 and L2)	4.48	31.8	13.2
Lumbar (L3 and L4)	4.87	24.5	13.1
Forearm	2.62	24.6	23.7
Lumbar (L5)	2.52	19.0	12.2
Hand	0.92	15.3	45.1
Pelvis	8.89	13.0	11.2
Thigh (hip)	15.83	7.6	27.2
Lower leg	6.38	-8.6	55.0
Foot	1.99	-37.1	59.0
TOTAL	77.40		

*Location is based on floor level of zero with 50th-percentile male head crown equal to reference line of 174.6 cm.

**Location is based on seat back with reference line equal to zero. Seat back is perpendicular to seat bottom, and torso touches seat back at head, shoulders, and buttocks.
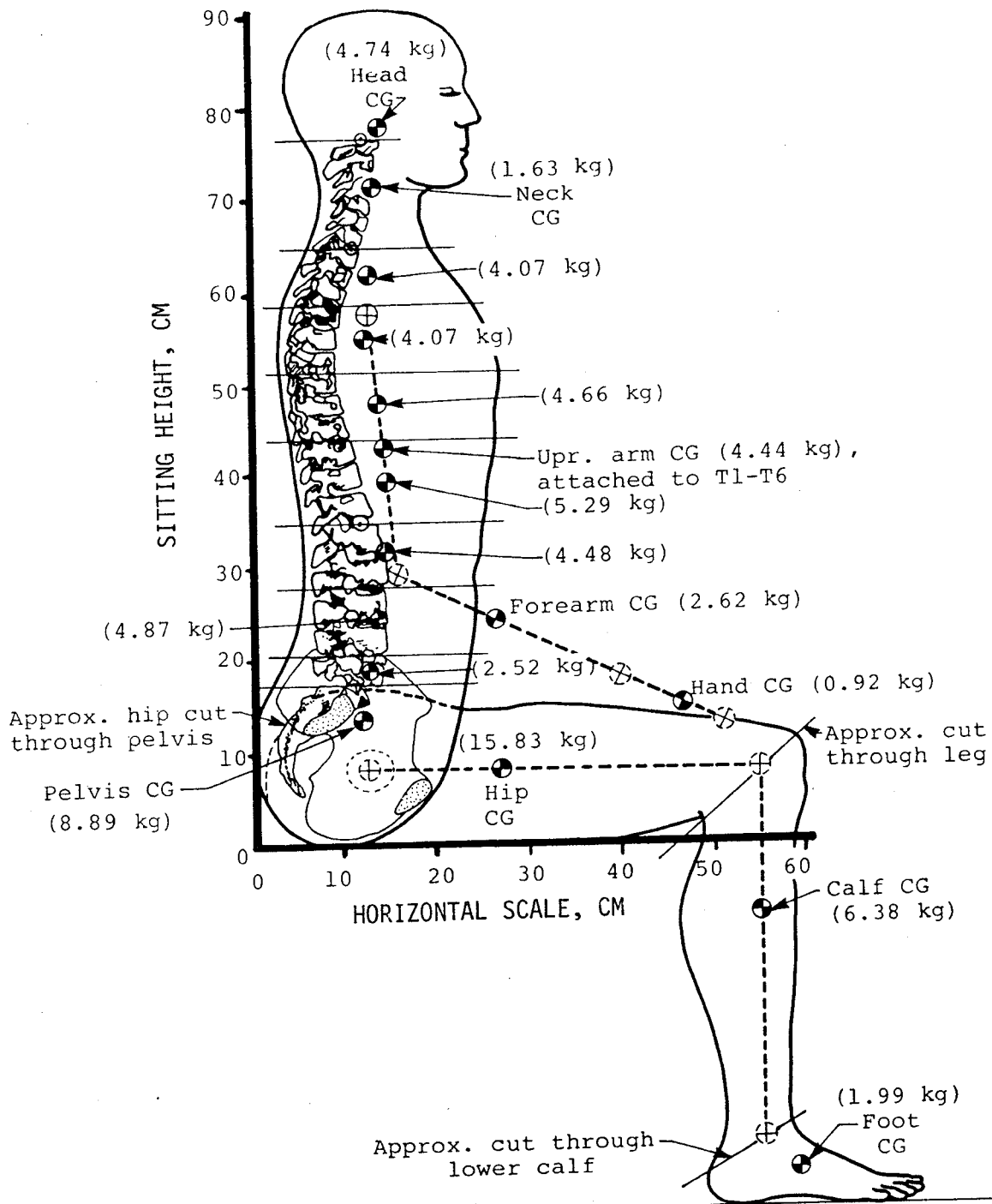
FIGURE 45. MASS DISTRIBUTION OF SEATED TORSO REFERENCED TO THE SKELETAL STRUCTURE FOR A 50TH-PERCENTILE MALE ARMY AVIATOR. (FROM REFERENCE 81)

TABLE 20. SEGMENT MOMENTS OF INERTIA ABOUT THE
CENTER OF MASS (REFERENCE 101)

Body Segment	Moment of Inertia (10^3 gm-cm^2)*		
	I_{xx}	I_{yy}	I_{zz}
Head	174.00	164.40	202.90
Torso	16,194.00	10,876.00	3,785.00
Upper arm	143.60	135.20	22.00
Forearm	65.80	63.80	8.70
Hand	7.19	5.86	1.97
Thigh	1,144.00	1,190.00	218.70
Calf	393.10	391.20	28.90
Foot	32.62	30.76	7.29

*Mean values of stature and weight reported to be
172.2 cm and 69.6 kg, respectively, for sample of
six cadavers.

7.4 SCALING OF MEASUREMENTS

References 93 and 94 contain a significant volume of anthropometric data,
whose statistics have been completely analyzed. In other words, the mean,
standard deviation, and percentiles are listed for all measurements. How-
ever, the link lengths presented in Section 7.2.3 and the inertial properties
presented in Section 7.3 are based on rather small samples. If the user of
this guide wishes to scale the dimensions of Figures 43 or 45 to an occupant
size other than the 50th-percentile male Army aviator, it is recommended that
the scaling be based on the most similar anthropometric dimension. For
example, the lower leg length shown in Figure 43 is 41.0 cm. In order to con-
vert this dimension to a 95th-percentile value, it would be multiplied by the
ratio of popliteal heights from Table 14. The 95th-percentile lower leg
length is then calculated as

$$L_{95} = \left(L_{50} \right) \left(\frac{PH_{95}}{PH_{50}} \right)$$

$$= \left(41.0 \right) \left(\frac{18.3}{16.6} \right)$$

$$= 45.2 \text{ cm}$$

(11)

84

The center-of-mass location then can be determined for the new length using the same percentage of total segment length as shown in Figure 43. For example, according to Figure 43, the center of mass of the lower leg is approximately 38.8 percent of the distance down from the knee joint to the ankle joint. Retaining this percentage for the 95th-percentile occupant, the distance down from the knee joint to the lower leg center of mass is 0.388 (45.2) = 17.5 cm. Scaling segment masses presents a greater problem as there is no complete set of segment data for all size occupants. The simplest scaling approach would be to multiply the masses of Figure 45 by the ratio of total body masses (or weights) from Reference 93 or 94. For a more rigorous approach, the regression equations of Reference 100 might be used.

7.5 ANTHROPOMETRIC DATA FOR USE IN SIMULATIONS

The basic dimensions of occupant segments that are required in writing the equations of motion are illustrated in Figure 46 (Reference 102). Table 21 presents these segment lengths for the standard 50th-percentile male occupants and the Part 572 dummy. Body segment weights, center of mass locations, and moments of inertia also may be found in Reference 102.

A tri-service data base of anthropometric and mass distribution data has been developed for use in the construction of three-dimensional human analogues. Reference 103 provides body dimensions, joint locations, and mass distribution properties for small, mid, and large-sized male aviators appropriate for the 1980 to 1990 time period. The data are meant to serve as a basis for three-dimensional mathematical models and test dummies. The dimensions reported were generated from multiple regressions of stature and overall body weight. This method provides internally consistent body dimensions for each model but does not necessarily provide appropriate descriptive statistics for a population of any single dimension. The authors of the report strongly recommend that the data in the document not be used for purposes of fit analysis, sizing of personal protective equipment and clothing, or for work space design or evaluation.
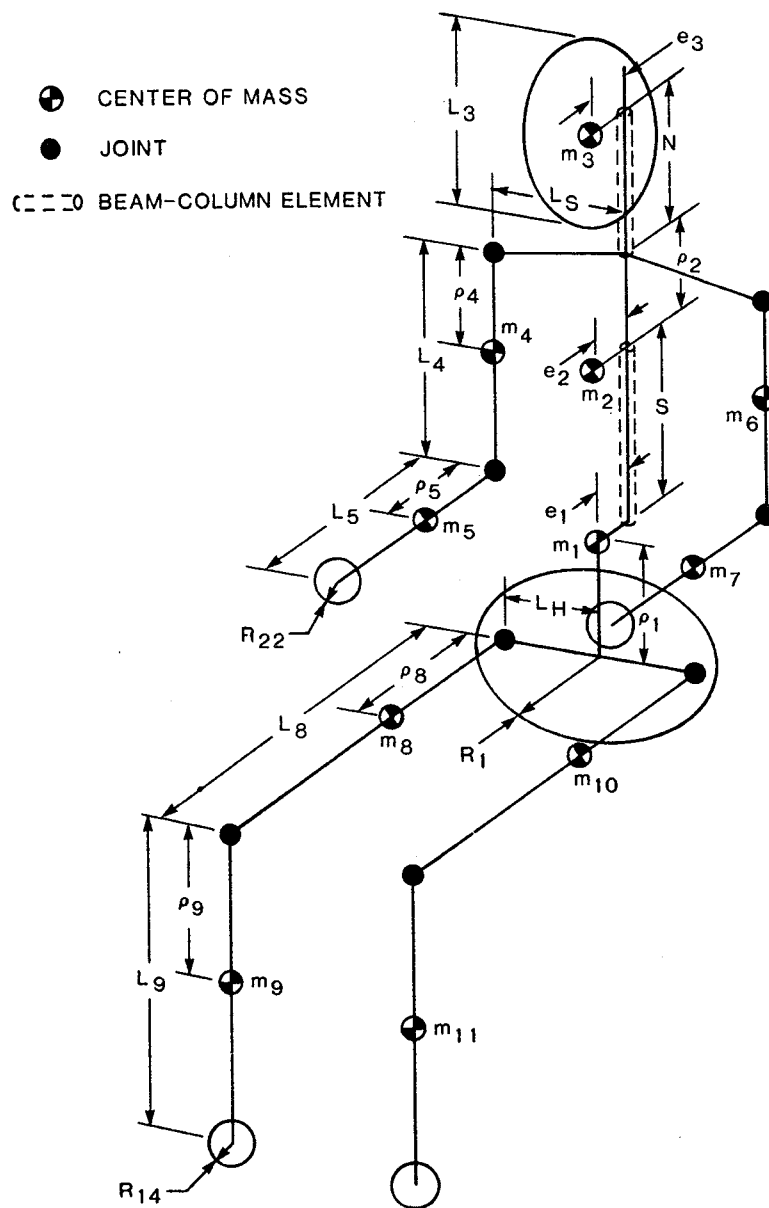
FIGURE 46. PROGRAM SOM-LA BODY SEGMENT DIMENSIONS.

TABLE 21. BODY SEGMENT LENGTHS (IN.)

Segment	50th-Percentile Male Aircrewmember	Part 572 Dummy
Lower Torso, L_1	9.44	10.5
Upper Torso, L_2	13.1	11.5
Neck, N	5.10	$4.88^{(2)}$
Head, L_3	$8.50^{(1)}$	$8.35^{(2)}$
Upper Arm, L_4	11.6	11.3
Lower Arm, L_5	$14.8^{(3)}$	$13.3^{(3)}$
Upper Leg, L_8	17.1	16.5
Lower Leg, L_9	$18.4^{(3)}$	$18.0^{(3)}$
Spine, S	$12.4^{(3)}$	$10.85^{(3)}$
Seated Height	$37.0^{(3)}$	$36.0^{(3)}$

(1) Scaled from manikin drawing.
(2) Scaled from Part 572 drawing.
(3) Calculated.

87

8. CRASH TEST DUMMIES

8.1 INTRODUCTION

The technology of crash test dummies has advanced significantly since 1968, when the first standard dummy was defined. Several designs currently are available, and many one-of-a-kind systems have been developed by various laboratories for their own use. However, for use in aircraft system evaluation, special consideration must be given to the effects of the vertical component of impact force, which make the aircraft crash environment quite different from that of an automobile, for which most dummies have been developed.

This chapter briefly outlines the evolution of current dummy technology, indicates the design features that are desirable for aircraft system testing, and summarizes research and comparative performance of dummies and humans.

8.2 DUMMY TECHNOLOGY

8.2.1 History of Dummy Development

One of the earliest dummy designs was a rugged ejection seat dummy built by Sierra Engineering Company for the Air Force in 1949. According to Reference 104 this dummy had limited articulation and poor biomechanical fidelity, but it filled an important need, not only for aircraft system manufacturers but for the automobile industry as well.

A significant step toward the present anthropomorphic dummies was made by Swearingen, who, in 1949, needed a dummy better than the rigid test articles then available in order to evaluate explosive decompression for an aircraft cabin as a result of window failure. He designed a 120-lb dummy with articulated principal joints, realistic distribution of body weight, and centers of gravity approximating the human body. More than 500 blast tests were made with this dummy to determine the hazard of explosive decompression.

In 1951, Swearingen completed an improved dummy, capable of withstanding 35 to 50 G, which was used in evaluating a new safety harness for general aviation (Reference 105).

In 1954, Alderson Research Laboratories, Inc., created the first mass production dummy, unique for its modular design. The design permitted new parts to be added as needs changed and as knowledge grew over the subsequent decade. In 1967, both of the major dummy manufacturers marketed new devices that featured increased articulation in the vertebral column and shoulders, as well as increased chest compliance. These changes effected some improvement in biomechanical response but still fell far short of what is available today.

In 1968, SAE Recommended Practice J963 was published as a partial definition of a standard 50th-percentile male anthropomorphic test device (Reference 106). J963 recommended weights, center-of-gravity locations, dimensions for body segments, and the ranges of motion for body joints. Although moments of inertia and many design details were left unspecified, this was a first step toward a standard test device. Alderson upgraded its design to meet J963 in 1968 and 1971, while the Sierra counterpart appeared in 1970.

8.2.2 Part 572 Dummy

The role of the anthropomorphic dummy in automobile safety testing was formally changed in 1971 by the National Highway Traffic Safety Administration. Prior to that time, dummies had been used for determining relative performance of similar safety systems. The new law carried the implications that dummies must determine the absolute potential for injury to human occupants in an automobile crash and that different testing organizations should obtain the same results. The transition from relative to absolute measuring instrument forced the requirement for the dummy to be a standardized test instrument, as well as a reasonable simulation of a human being, since the legal performance limits are based on human tolerance data.

In 1972, General Motors Corporation produced the Hybrid II dummy, a 50th-percentile male anthropomorphic test device. This dummy utilizes torso and limbs from the Alderson VIP-50A dummy with modifications made to the chest to allow increased deflection and damping. The head assembly was adapted from the Sierra 292-1050 design with several anatomical modifications. Both the neck and lumbar spine consist of a butyl rubber cylinder, the latter being reinforced by an internal steel cable.

Along with a number of other modifications, the design of the Hybrid II formed the basis for the Code of Federal Regulations, Title 49 (49CFR) Part 572 specification for dummies (Reference 107). Its specified dimensions and inertial properties are displayed in Figure 47 and Tables 22 through 24. Segment moments of inertia reported in Reference 108 for a Hybrid II dummy are listed in Table 25.
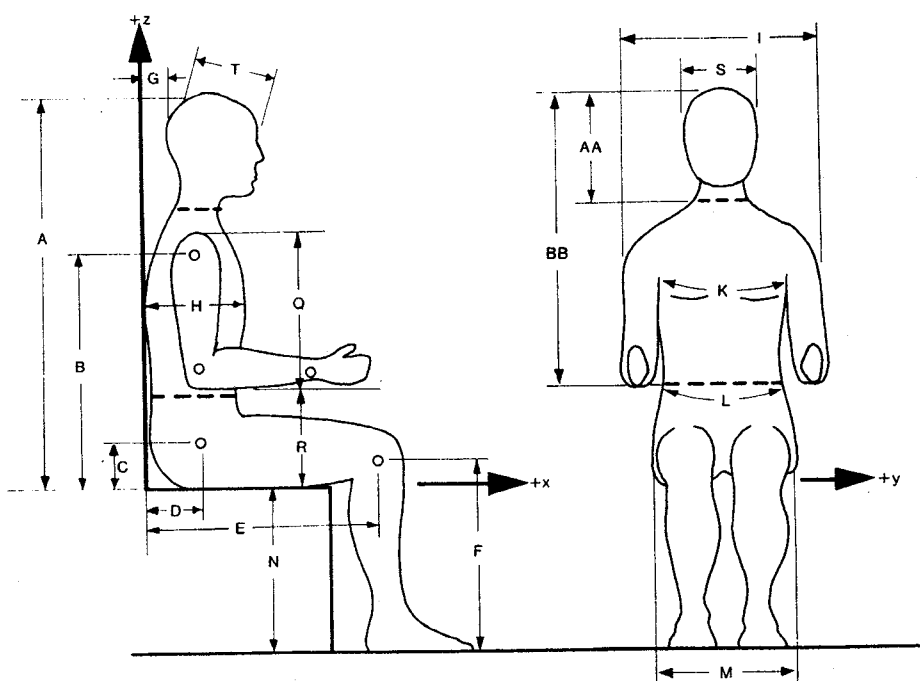
FIGURE 47. DUMMY EXTERNAL DIMENSIONS.

TABLE 22. DUMMY EXTERNAL DIMENSIONS (PART 572)

Designation	Figure 37 Code	Part 572 Specification (in.)
Seated height	A	35.7 ± 0.1
Shoulder pivot height	B	22.1 ± 0.3
Hip pivot height	C	3.9
Hip pivot from back line	D	4.8
Knee pivot from back line	E	20.4 ± 0.3
Knee pivot from floor	F	19.6 ± 0.3
Head back from back line	G	1.7
Chest depth	H	9.3 ± 0.2
Shoulder width	I	18.1 ± 0.3
Chest circumference over nipples	K	37.4 ± 0.6
Waist circumference at minimum girth	L	32.0 ± 0.6
Hip width	M	14.7 ± 0.7
Popliteal height	N*	(17.3 ± 0.2)
Shoulder-elbow length	Q*	(14.1 ± 0.3)
Elbow rest height	R*	(9.5 ± 0.5)
Head width	S*	(6.1 ± 0.2)
Head length	T*	(7.7 ± 0.2)
Head segment line	AA	9.3
Shoulder-thorax segment line	BB	25.1

*Added to Part 572 data, SAE specification value in parentheses.

TABLE 23. DUMMY COMPONENT WEIGHTS (PART 572)

Segment	Part 572 Specification (lb)
Head	11.2 ± 0.1
Upper torso (including lumbar spine)	41.5 ± 1.6
Lower torso (including visceral sac and upper thighs)	37.5 ± 1.5
Upper arm	4.8 ± 0.2
Lower arm	3.4 ± 0.1
Hand	1.4 ± 0.1
Upper leg	17.6 ± 0.7
Lower leg	6.9 ± 0.3
Foot	2.8 + 0.1
Total dummy (including instrumentation in head, torso, and femurs)	164.0 ± 3.0

TABLE 24. CENTER-OF-GRAVITY LOCATIONS (PART 572)

Segment	x and z Reference Origin	Part 572 Specification x (in.)	z (in.)
Head	Back and top of head	+4.0 + 0.2	-4.7 ± 0.1
Upper torso	Backline and top of head	+4.1 + 0.3	-17.2 ± 0.3
Lower torso and upper thigh	Backline and top of head	+4.9 + 0.5	-31.0 ± 0.5
Upper arm	Shoulder pivot	0.0 + 0.3	-5.0 ± 0.3
Lower arm	Elbow pivot	+4.2 + 0.3	0.0 ± 0.3
Hand	Wrist pivot	+2.2 + 0.3	0.0 ± 0.3
Upper leg	Knee pivot to upper leg rotation center	-6.7 + 0.3	0.0 ± 0.3
Lower leg	Knee pivot to ankle pivot	0.0 + 0.3	-8.0 ± 0.3
Foot	Ankle pivot	+2.2 + 0.3	-1.7 ± 0.3

NOTE: Axis system is shown in Figure 37 (drawing of external dummy dimensions), using +x forward and +z up.

TABLE 25. HYBRID II MASS MOMENTS OF INERTIA
(REFERENCE 108)

Body Segment	Moment of Inertia (in.-lb-sec^2) I_x	I_y	I_z
Head	0.226	0.275	-
Head/neck	0.310	0.367	0.233
Upper torso (includes lumbar spine)	2.18	1.79	-
Lower abdomen, pelvis, and visceral sac	2.32*	1.73*	-
Right upper arm	0.134	0.132	0.022
Right forearm (no hand)	0.012	0.068	0.071
Right upper leg	0.127	0.873	0.890
Right lower leg (no foot)	0.599	0.575	0.359

*Included lumbar section.
NOTES:
1. Instrumentation was installed in the head, chest, and femurs during the measurements.
2. Estimated accuracy of measurements: ± 3 percent.

91

8.2.3 Hybrid III Dummy

General Motors continued development of anthropomorphic dummies and in 1975 produced the Hybrid III dummy (Reference 109). This dummy has markedly improved component biofidelity, particularly in the head and neck system, thorax, and redistributed lower torso weight. In addition, the Hybrid III includes transducers for measurement of neck loads and chest deflections.

The Hybrid III head consists of an aluminum skull covered by constant-thickness vinyl skin. The neck, shown in Figure 48, consists of three rigid aluminum vertebral elements molded in a butyl elastomer which provides the high damping characteristics. Aluminum end plates attach the neck segment to the head and thorax, with a steel cable running through the center of the neck.
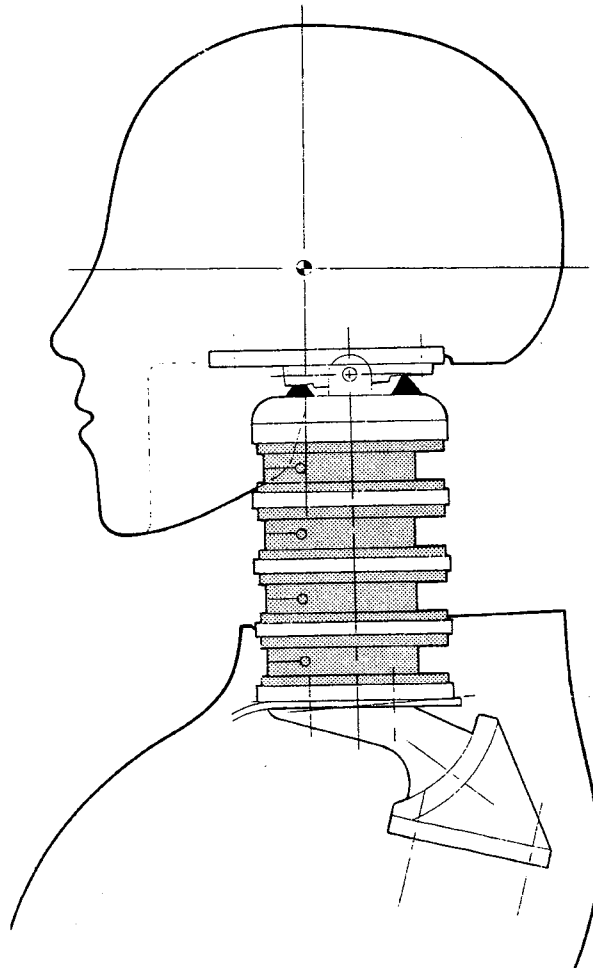
FIGURE 48. HYBRID III NECK.

The thorax of the Hybrid III consists of six metal ribs connected to a welded steel spine. The whole assembly is ballasted for correct weight and center of gravity location. This spine provides attachment points for the neck, clavicles, ribs, and lumbar spine.

The lumbar spine of the Hybrid III is made of curved polyacrylate elastomer with molded end plates for attachment to the thorax and pelvis. Two steel cables run through the central section. The lower body has correct weight distribution and is ordinarily cast in a seated position. The Hybrid III may also be obtained with freely articulating hips and a straight rubber spine element as opposed to the curved spinal element in the seated Hybrid III. This dummy, denoted as the standing Hybrid III, is most commonly used in pedestrian impact and aircraft ejection testing where full leg extension is important.

The Hybrid III test dummy was incorporated into the Department of Transportation's specifications for crash test dummies in 1986 (Reference 110). Since October 23, 1986, manufacturers have had the option of using either the Part 572 dummy or the Hybrid III for compliance testing until August 31, 1991. As of September 1, 1991, the Hybrid III will replace the original Part 572 test dummy and will be used as the exclusive means of determining a vehicle's conformance with the performance requirements of Federal Motor Vehicle Safety Standard No. 208.

The drawings and specifications for the Hybrid III dummy are available from the National Highway Traffic Safety Administration (NHTSA) (Reference 110). The Hybrid III's geometrical and inertial properties have been determined for both the standard and the standing Hybrid III dummies. These data may be found in Reference 111.

8.2.4 Side Impact Dummies

NHTSA has proposed adoption of a new side impact test dummy (SID) for use in their upgraded side impact standard (Reference 112). The proposed SID is identical to the Part 572 dummy described in Section 8.2.2 with several exceptions. The thorax and knees have been redesigned to produce more human-like acceleration responses in the lateral directions. Modifications include accelerometers for ribs, spine and pelvis, a shock absorber between the rib cage and spine, and a rubber hinge where the ribs attach to the spine. In addition, to keep the design of the SID as simple as possible, the dummy does not have articulating arms or shoulders. Instead, the mass of the arms has been incorporated into the mass of the thorax, and urethane foam stump arms have been added for appropriate biofidelity characteristics.

Impact test results of the SID dummy have been compared with those of cadavers in actual vehicle-to-vehicle crash tests (Reference 62), and the responses of the SID corresponded well with the response of the cadavers. However, in rigid-wall impacts, the SID experiences higher accelerations than a cadaver. Thus, the SID responses will have adequate biofidelity with padded structures typical of the interior of a vehicle, but not with rigid structures. It should be noted that the SID has been developed specifically for impulsive, intrusive loading and not for longer-term lateral accelerations typical of aircraft crashes.

At the same time that the SID was being developed in this country, efforts also were under way in Europe to develop a side impact dummy. As in the USA, the Part 572 dummy was modified with the intention of using it for both lateral and frontal impacts (Reference 113). Since the response of the Part 572 dummy's thorax and shoulder was much too stiff compared to cadaver tests, the arm was modified by reducing the size of the structural members and increasing the padding. The mobility of the shoulder was increased in both forward and upward directions and the rib cage was redesigned to give more realistic lateral chest deflection.

Since that time, a unified European side impact dummy (EUROSID) has been designed and developed by a group of European research laboratories working together under the auspices of the European Experimental Vehicles Committee (Reference 114). The head is a standard Hybrid III head, but the neck, chest, shoulder, abdomen, pelvis, and legs have been modified to allow evaluation of injuries seen in cadavers. The EUROSID was designed to measure thoracic injury on the basis of chest deflection, but NHTSA found that the chest deflection measurement was not able to distinguish differences in impact intensities such as between rigid and padded surfaces. However, the EUROSID thorax peak acceleration responses compared reasonably well with the SID. Again, as with the SID, the EUROSID has been developed specifically for evaluating automobile side impacts involving intrusive and impulsive loads on the occupant.

8.3 COMPARISON OF DUMMY AND HUMAN RESPONSE

There are two basic questions regarding the use of a mechanical system such as a dummy to evaluate the degree of protection a vehicle system would afford its human occupants. First, how closely does the dummy response simulate human response? Second, how does performance vary from one dummy to another and from one test laboratory to another?

The first question presents a problem. The response of live human subjects can, of course, be determined only at safe acceleration levels, substantially below crash-resistance design conditions. The response of human cadavers at higher acceleration levels has been used in dummy design, but questions do exist as to the quality of simulation provided by cadavers. Walsh and Romeo reported on a series of sled tests and full-scale car crash tests wherein fresh, unembalmed cadavers and dummies were exposed to identical crash conditions (Reference 115). Both belt restraints and airbags were used. Although the overall kinematic response between cadaver and dummy agreed fairly well, some injuries that could not have been detected with the dummy were observed in the cadaver.

Although the Part 572 and Hybrid III dummies are vast improvements over earlier dummies, there are still some significant differences in the response of the dummies and humans. For instance, current dummy heads (vinyl flesh over aluminum skull) will not provide proper acceleration data in facial impact environments because the face is too stiff. Since crushing of the facial bones can provide shock absorption and attenuate the accelerations experienced by the brain, severe blows to the face of a dummy will result in unrealistically high head accelerations (Reference 43).

94

Problems also arise in the comparison of human and Hybrid III head and neck dynamic responses. Data from human volunteer head and neck dynamic responses and those of a Hybrid III head and neck were compared and analyzed in detail by Seemann, et al. (Reference 51). The authors found that there were significant differences in the human volunteer and dummy responses for -x and +z acceleration tests. For instance, when the body is subjected to a +z acceleration profile, human heads often initially go into significant extension followed by flexion. The Hybrid III head/neck system does not. Instead, it first goes into flexion in response to a +z acceleration profile, indicating that the Hybrid III neck is much too stiff to respond in a human-like manner in the sagittal plane. In the -x acceleration profile, the downward travel of the human head far exceeded that of the dummy head. The timing of the response was also considerably different, with the dummy head rebounding while the human head continued its downward travel.

Several test programs have been conducted to compare the dynamic response of different dummy designs. Chandler and Christian demonstrated that, as dummies become more complex, the number of test variables may exceed those that the experimenter can control (Reference 116). The requirement for standard test practices also was noted. Massing, Naab, and Yates compared several dummies in tests with either belt restraints, airbags, or energy-absorbing steering columns (Reference 108). Some of the sled tests were repeated at two different laboratories. As an example of the results, mean head resultant accelerations for ten repeated tests on each of five dummies with belt restraints are shown in Figure 49. Figure 50 shows the mean head accelerations for ten repeated tests with the same dummy conducted at two different facilities, the FAA Civil Aeromedical Institute (CAMI) and Calspan Corporation. Because only one dummy was tested at the two different facilities, data are insufficient to permit generalization with respect to comparative performance. However, Figure 50 indicates that differences in performance did exist. Detailed analyses of the data are presented in Reference 74.

A series of front barrier crash tests utilizing various vehicles and unrestrained dummies compared the responses of the Part 572 and Hybrid III dummies (Reference 117). The results of the testing and analysis indicate that the two dummies' measurements were generally comparable and reasonable. Response differences which did occur were found to be the result of either dummy anthropomorphic differences or vehicle response differences. For instance, the Hybrid III driver HIC values were higher than the Part 572 because the Part 572 dummy's higher seated height more frequently caused the Part 572 to graze the sun visor, whereas the Hybrid III more often struck its face on the steering wheel rim.

Computer simulations conducted by Kaleps and Whitestone (Reference 111) showed that Hybrid III crash responses were quite similar to those of the Part 572 dummy, with primary differences being phase shifts, slightly smoother response curves for the Hybrid III, and also somewhat faster responses for the Hybrid III. These effects were interpreted to be due to slightly different initial positions, a numerically more stable data set for the Hybrid III, and a generally stiffer structure for the Hybrid III. They also found that there was very little difference in the response between the seated and the standing Hybrid III. The only readily observable difference was that the seated dummy penetrated deeper into the seat pan than the standing dummy during the crash simulation.
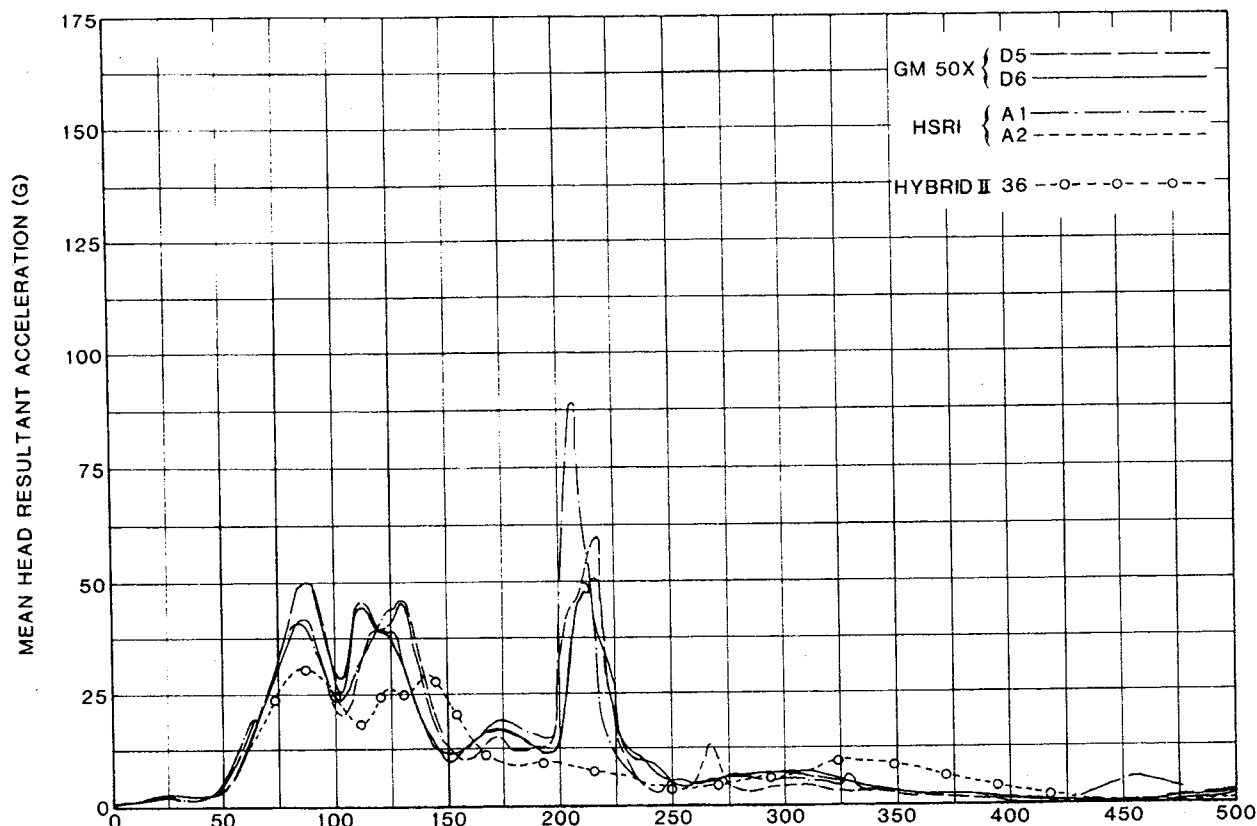
FIGURE 49. COMPARISON OF MEAN HEAD RESULTANT ACCELERATION RESPONSES FOR THREE DIFFERENT DUMMY DESIGNS. (FROM REFERENCE 108)

Backaitis and St-Laurent studied the chest deflection characteristics of volunteers and Hybrid III dummies under various loading conditions (Reference 118). The test results revealed that the thorax of the Hybrid III dummy, when dynamically loaded by a diagonal shoulder belt, was somewhat stiffer than that of volunteers for both tensed and relaxed conditions. They also found that dummy thorax deflection readings are highly affected by the surface area of a loading probe and the location and direction of the applied load. The Hybrid III dummy's thorax deflection gauge underestimated compressions administered externally to the thorax by small-area loading probes but overestimated externally produced rib cage compressions when loading occurred by large-area probes. The tests also showed that the deflection pattern of the Hybrid III dummy's thorax had a parabolic shape, with the least amount of deflection occurring at mid-sternum. In humans, however, surface deflection shows a linear increase toward the bottom of the rib cage.
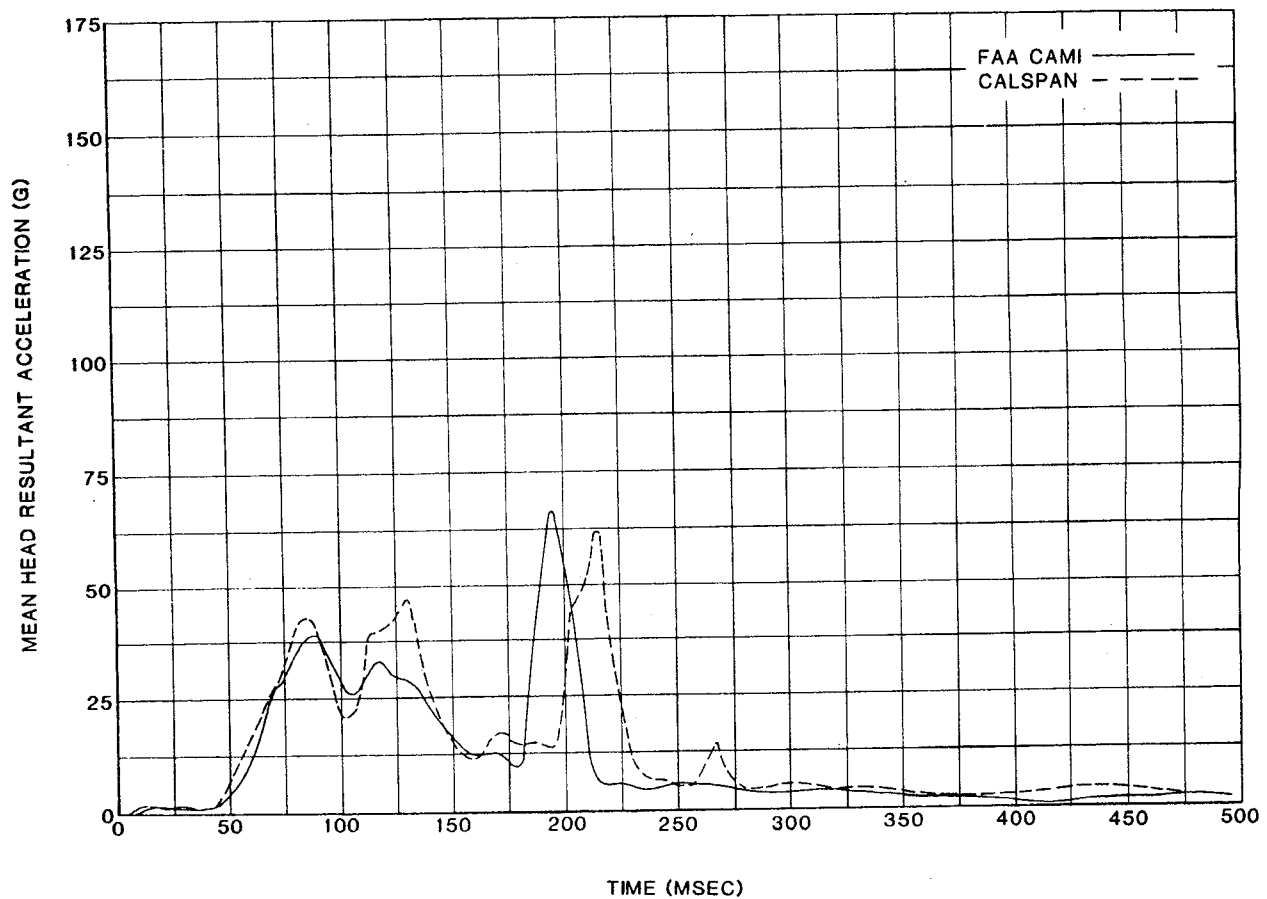
FIGURE 50. COMPARISON OF MEAN HEAD RESULTANT ACCELERATION RESPONSES FOR HSRI DUMMY CONDUCTED AT TWO LABORATORIES. (FROM REFERENCE 108)

Leung, et al., conducted a series of analytical studies and sled tests to determine the submarining tendencies of the Part 572 dummy. They found that the Part 572 dummy submarines more easily than human cadavers because of its different pelvic shape (Reference 119). When they changed the dummy by modifying the abdominal tissue and pelvis shape, the submarining tendency more nearly simulated that of the human cadaver than the standard Part 572 dummy.

The Hybrid III dummy has a pelvis similar to the standard Part 572 dummy, but it can be augmented with a submarining-indicating pelvis. This submarining indicator has load gages attached at the iliac crests, under the flesh, to measure the lap belt loads on the pelvis. This device is incorporated to optimize lap belt placement. One way that the Hybrid III differs from the Part 572 is in the way that it simulates a driver's slouched seating position. This simulation is possible with a smaller abdomen than the Part 572 and with a 45-degree segment in the lumbar spine.

97

8.4 SUITABILITY OF DUMMIES FOR AIRCRAFT SYSTEM EVALUATION

All of the recently developed dummies described in Section 8.2 were designed for automotive testing. In dynamic testing of an energy-absorbing seat, design for aircraft occupant weight can play a critical role. It would be desirable, although generally not practical, to evaluate a seat for a range of occupant sizes. A 95th-percentile dummy would verify the strength of the seat structure and restraint system as well as the adequacy of the energy-absorbing stroke. Testing with a 50th-percentile dummy would demonstrate the performance of the system for an occupant of average height and weight. A 5th-percentile dummy would probably experience accelerations of higher magnitude and would establish the severity of a given set of impact conditions for the smaller occupant. However, both the expense of dummy purchase and the cost of conducting dynamic tests may make such a test program impractical. An alternative procedure might be to establish the occupant protection capability of a seat design by analysis and to conduct a dynamic test with a 95th-percentile dummy to verify system strength.

The design of different anthropomorphic dummies for military testing must be based on the military aviator population. Body dimensions, joint locations, and mass distribution properties for small-, mid-, and large-size male aviators has been generated as a tri-service database for three-dimensional, mathematical models and test dummies (Reference 103). These dimensions are available for the dummy designer's guidance.

Another factor that must be considered in dummy selection for aircraft seat testing is that none of the dummies described for automotive testing has been designed for accurate response to vertical impact. The spinal column, which is a critical region of human tolerance to aircraft crash loading, has been designed to simulate response to $-G_x$ loading rather than the more critical $+G_z$ direction.

At present, it seems that use of the Hybrid III dummy, sized to 5th-, 50th-, and 95th-percentile versions of the U.S. Army aviator, provides the best approach.

8.5 EJECTION SYSTEM MANIKINS

There are ongoing activities within both the Air Force and the Navy to develop advanced anthropomorphic manikins for ejection system testing. Tieber presents a summary of the ongoing Air Force efforts as well as an evaluation of the requirements for an ejection system manikin in Reference 120. These ejection manikin design requirements are summarized in Table 26.

8.5.1 GARD and LRE Manikins

The grandfather of ejection manikins is the GARD manikin, jointly developed by Grumman Aircraft and Alderson Research Laboratories in the 1950's. While the GARD manikin duplicated the location of the human center of gravity in the ejection seat, the body articulations were very limited. Therefore, a new attempt was taken in the 1970's to develop a more complete replica of the human for ejection seat testing. The Limb Restraint Evaluator (LRE) was constructed to test the effectiveness of limb restraint systems being incorporated into current operation ejection seats. However, the need for increased biofidelity in

TABLE 26. MANIKIN DESIGN REQUIREMENTS

Requirement Categories	Requirement Areas	Requirement Drivers
Anthropmetry	Dimensions, mass and inertia properties, shape	Population to be modeled
Data Acquisition	Channels, sample rate, acquisition and storage, size, heat and power requirements	System to be tested
Usability	Durability, setup, calibration and pretest checkout, maintenance, data extraction	Test conditions
Structural	Strength and load bearing capability, packaging, placement and mounting of components	Anticipated loads and test conditions
Biofidelity	Response to impact and inertia loads, articulation, realism of tissue	Test objectives
Aerodynamics	Realistic motion in flight	Test conditions

the duplication of the dynamic characteristics of the human dictated the development of an Advanced Dynamic Anthropomorphic Manikin (ADAM).

8.5.2 Advanced Dynamic Anthropomorphic Manikin (ADAM)

The current Crew Escape Technologies (CREST) program, sponsored by the Air Force at Wright Patterson Air Force Base, includes the development of the ADAM. The design goals and concepts of the ADAM are to closely represent the static and dynamic characteristics of the human body to test the capabilities of the CREST ejection seat during emergency egress from an aircraft. The major goals in the design of ADAM were the following:

- High degree of biofidelic representation of the human regarding:

  - Anthropometric dimensions
  - Mass characteristics
  - Dynamic response

- Measurement of the dynamic response characteristics during ejection such as:

  - Head loads
  - Pelvic loads
  - Accelerations within the manikin
  - Joint rotations

- Development of an onboard computer controlled instrumentation system for 128 data channels that would:

  - Provide signal conditioning and storage for 4+ seconds
  - Telemeter the data to a ground station

- Survive the environmental conditions associated with ejection testing (i.e., windblast, high G loading, temperature, etc.).

Some of the basic features of the ADAM that set it apart from the Hybrid III, GARD, and LRE are discussed in References 121 and 122. A comparison of manikin mechanical characteristics and instrumentation system characteristics are shown in Tables 27 and 28.

TABLE 27. COMPARISON OF MANIKIN MECHANICAL CHARACTERISTICS

	GARD			LRE	ADAM			HYBRID III		
Characteristics (percentile)	5	50	95	95	Small	Med.	Large	5	50	95
Height (in.)	65.2	69.1	73.1	72.2	66.2	70.2	74.3	64.8	66.2	73.6
Weight Total (lb)	132.5	161.9	200.8	214.0	139.5	179.5	215.4	147.	155.5	207.9
Number of Articulations		18		39		43			26	
Number of Instrumented Articulations		0		33		39			0	
Range of Motions		Limited		Near Human Limits		Human Limits			Limited	
Elastomer Stops		No		No		Yes, In All Joints			Yes, In Some Joints	
Flexible Neck		No		Yes		Yes			Yes	
Flexible Spine		No		No		Yes			Yes	
Articulated Lumbar Spine		No		Yes		Yes			No	
Torque Adj. Joints		Yes		No		Yes			Yes	
Pelvis Design		Seated/Standing		Seated		Seated/Standing			Seated	

TABLE 28. CHARACTERISTICS OF INSTRUMENTATION SYSTEMS

Manikin	Type	Telemetry	Onboard Recording	Umbilical	Number of Data Channels
GARD	Passive Digital	Yes	No	No	22
LRE	Computer Controlled (Partial)	Yes	Yes	Yes	96
ADAM	Computer Controlled (Complete)	Yes	Yes'	Yes	128
HYBRID III	Passive Analog	No	No*	Yes	Variable (<30)

*The Naval Research and Development Center (NADC) developed an onboard data acquisition system for the Hybrid III.

The anthropometry and mass characteristics to which the small- and large-size ADAM were designed are based on the tri-services data base (Reference 103). While the majority of the ADAM components were specially designed to meet the design specifications, the existing Hybrid III head and neck were utilized. Nevertheless, a manikin neck that can correctly respond under $+G_z$ dynamic load is currently being developed and is discussed in Section 8.7. The manikin limbs are designed to undergo significant dynamic motions if limb flail occurs at speeds up to 700 KEAS. In order to duplicate as closely as possible the degrees of freedom in the human body, there are 43 degrees of freedom designed into ADAM. A partial listing of the joint degrees of freedom and rotation limits are shown in Table 29. "Soft stops" were designed to duplicate the increasing resistance to joint rotation as the limits of rotation are being approached. Figure 51 shows a representative joint rotative force of the human elbow. The data presented in Figure 51 indicate that as the lower arm reaches its limits of motion with respect to the upper arm (flexion/extension), the F_x force resisting the motion increases significantly. The lower arm is extended when the angle at the elbow is approximately 180 degrees, and flexed when the lower arm to upper arm angle is close to 10 degrees. At the time of publication the ADAM was currently undergoing verification testing for use in the CREST development program (Reference 103).

TABLE 29. JOINT DEGREES OF FREEDOM AND ROTATION LIMITS OF ADAM MANIKIN

Joint	Description of Motion	Angular Motion (Degrees)
Wrist	Flexion	85
	Extension	85
	Abduction	45
	Adduction	25
Elbow	Flexion	140
Forearm	Supination	95
	Pronation	75
Shoulder	Flexion	178
	Extension	57
	Traverse Abduction	134
	Traverse Adduction	48
	Coronal Abduction	170
Sternoclavicular Joint	Pronation	10
	Retraction	10
	Elevation	10
	Depression	10
Upper Arm Rotations		115
		15
Ankle	Flexion	45
	Extension	25
	Inversion	34
	Eversion	18
Knee	Standing Flexion	125
	Tibial Rotation at 90° Flexion	
	Internal	35
	External	45
	Tibial Rotation at 0° Flexion	
	Internal	0
	External	0
Hip	Flexion	115
	Extension	0
	Supine Abduction	60
	Supine Adduction	30
	90° Flexion Abduction	50
	90° Flexion Adduction	30
	Rotation 90° Hip Flexion	40
		40
	Rotation Full Extension	40
		40
	Rotation Prone 90° Knee	40
		40

FORCED SWEEP OF THE LOWER ARM FOR
ELBOW EXTENSION/FLEXION
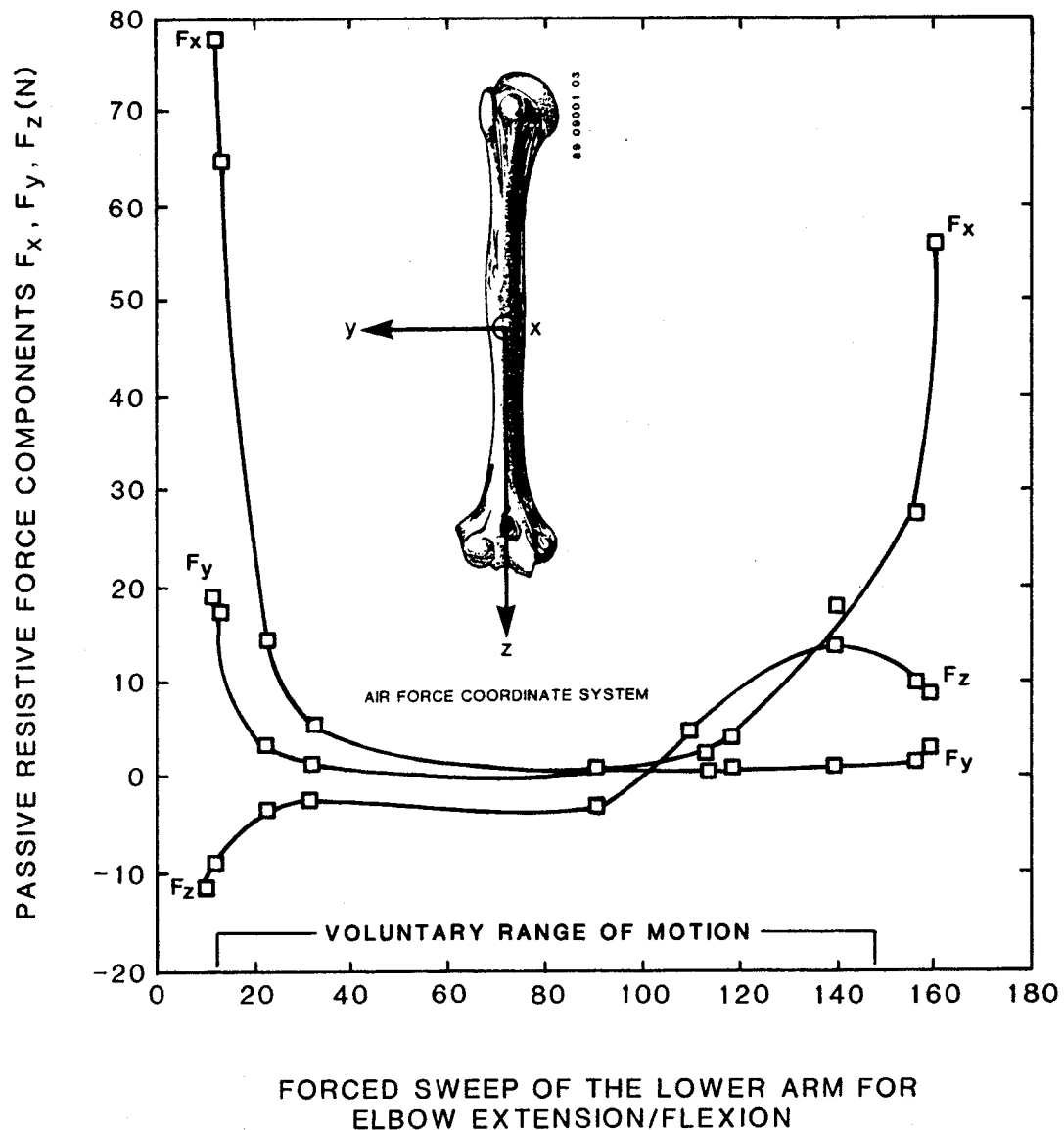
FIGURE 51. ELBOW RESISTIVE FORCE VERSUS ROTATION ANGLE.

8.6 INSTRUMENTATION IN MANIKINS

A major current development effort sponsored by the U.S. Navy involves a new instrumentation system for incorporation into the Hybrid III dummy (References 123 and 124). The objectives of the program are: (1) to make an existing dummy more suitable for ejection system testing, (2) to develop an instrumentation package that will allow the three-dimensional tracking of dummy-based coordinate systems within the seat, (3) to incorporate a microprocessor controlled data acquisition and storage system into the manikin,

and (4) to establish the degree of biofidelity exhibited by the manikin. The instrumentation package consists of miniature accelerometers, both linear and angular, and rate gyros which will be used to monitor the responses of the manikin's head center of gravity, the base of the neck segment, and the base of the lumbar spine. The data acquisition, recording, and storage system consists of on-board signal conditioning, A/D conversion, and RAM storage which can support 50 channels of data sampled at 2000 Hz for 6.6 seconds. The configuration is volume compatible with the space available in the Hybrid III dummy and could be adopted for mounting without miniaturization.

The Data Acquisition and Storage System (DASS) has been tested independently and in a Hybrid III dummy on the ejection tower, horizontal accelerator, and dunker of the Navy. The Navy dunker subjected the instrumented dummy in a simulated aircraft cockpit section to a shock pulse caused by water impact and subsequent contact with springs at the end of the submerged dunker track. The tests demonstrated the advantages of having a self-contained portable data acquisition system. Miniaturization of the data acquisition and storage system has been initiated to minimize weight and power consumption and, consequently, minimize further manikin modifications to accommodate changes in weight and center of gravity locations.

The authors point out that the instrumentation system is an integral part of the dummy design and that it cannot be tacked on later as requirements change. The dummy instrumentation must be consistent with that used in developing the human response data in order to maximize ease of performance validation. Standardization is essential in order to have repeatable data between test series and test facilities. This is illustrated in Figure 52 which shows the seat acceleration profile filtered at 500 Hz (top) and 15 Hz (bottom). The higher frequency filter maintains the exhibited acceleration profile. However, the higher frequency filter presents a problem in quantifying peak G's since it is not obvious how best to fit the data with a smooth function. Excessive filtering, as shown in the bottom of Figure 52, may give an insight into the waveform of the underlying driving function, but it will also tend to underestimate the peak G attained and impart a phase shift to the time scale. The basic question is whether or not an occupant can respond to an acceleration profile as demonstrated in Figure 52 at the top or whether the individual spikes are of such short duration and contain so little energy as to be absorbed by the deformable body tissue, rib cage, and intervertebral discs. If the latter is the case, then some signal averaging is in order.

Gragg analyzed anthropomorphic dummy and ejection seat data from two sled test programs to determine the value of the dummy data for predicting the probability of spinal and/or disabling injury (Reference 125). He compared G_x, G_y, and Dynamic Response Index (DRI) data. The DRI was computed from G_z. Gragg concluded that the anthropomorphic dummy data should never be used if the seat bucket data are available. In some instances, it would be possible to substitute dummy DRI data for seat DRI data, but G_x and G_y dummy data should never be substituted for G_x and G_y seat data.

Laananen and Coltman measured the forces transmitted through the lumbar spine of anthropomorphic dummies to determine repeatability and biofidelity during seat testing. Two Alderson anthropomorphic dummies, one a 50th-percentile and one a 95th-percentile and both having the pelvic structure and lumbar

104
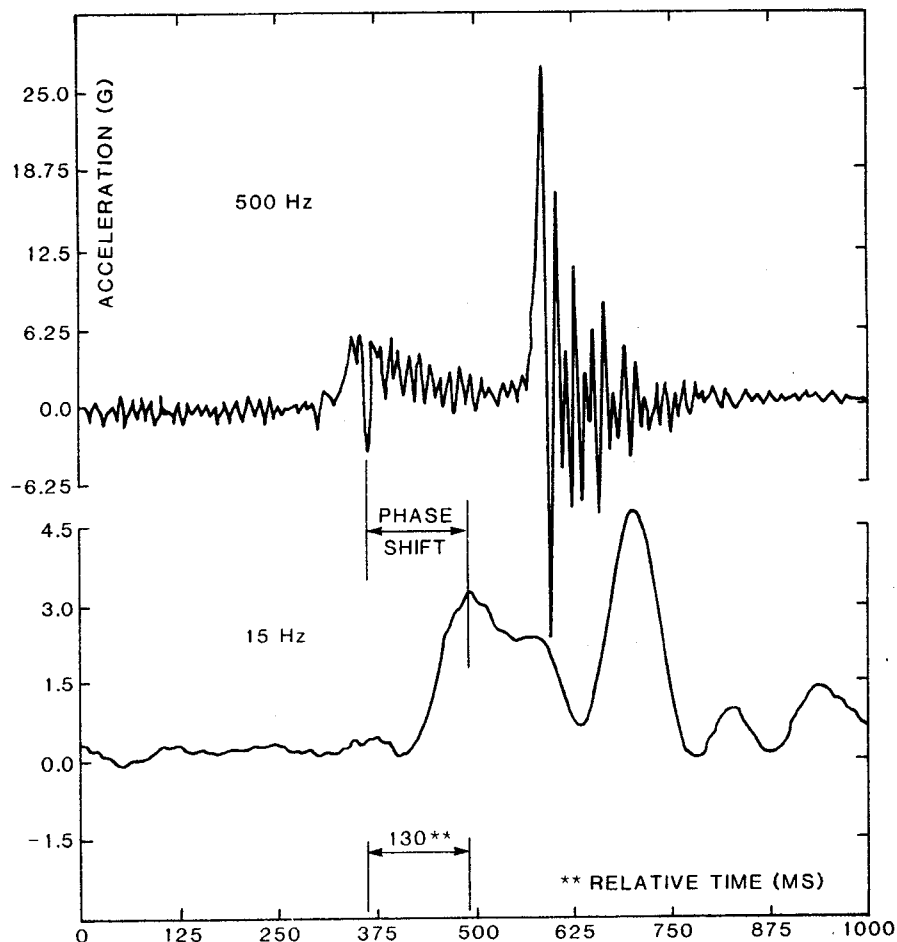
FIGURE 52.   ACCELERATION DATA FILTERED AT 500 Hz AND 15 Hz.

region of the Part 572 configuration, were modified to accept a load cell at the base of the lumbar spine. The dummies were then subjected to $+G_z$ accelerations in rigid and energy-absorbing helicopter seats. Detailed data are presented in Reference 126. The results of the program indicated that forces and moments in the spine of a Part 572 or similarly designed anthropomorphic dummy could be measured with a rather simple modification. However, the modifications made to the dummies appeared to have altered the x direction dynamic response of the upper torso. The change in response was observed only in the energy-absorbing seat test where the peak chest acceleration reached 20 G and higher and probably resulted from an altered natural frequency for torso bending due to installation of the load cell and adapters. Any future design of a standardized transducer installation must consider the dynamic response characteristics of the torso.

The test data showed that the interaction between the Part 572 dummy and seat pan is very similar to the response measured with human cadavers, but there is not a good correlation between dummy and cadaver body accelerations. Thus,

105

seat performance criteria based on seat pan acceleration may not be as sensitive to occupant type as criteria based on body segment acceleration.

However, the authors also point out that the data might indicate that injury mechanism within the body, e.g., spinal deformation, cannot be reliably predicted from seat pan acceleration since internal body response can vary significantly for various occupant types with similar inputs from the seats.

8.7 IMPROVED MANIKIN NECK

Efforts are being made to upgrade the biofidelity of the neck of anthropomorphic dummies. Wismans conducted a detailed analysis of a large number of human volunteer tests conducted by the Naval Biodynamics Laboratory (NBDL). These human subjects were exposed to frontal, lateral, and oblique accelerations with a severity of up to 15 G and 17 m/sec. This analysis resulted in a simple analog system for each direction that completely specifies the observed dynamic behavior. The most important finding was that the observed human head/ neck response can be represented adequately by a linkage system with two pivots. This simulation is discussed in some detail in Section 5.9.2.4. The detailed analysis done by Wismans is found in Reference 38.

Richards and Van Ingen developed performance guidelines for an improved manikin neck based on investigation and analysis of human neck dynamic responses. The optimum biofidelic manikin neck system should be designed so that a direct relationship exists between the moment exerted on the head at the occipital condyles and the relative change in head/torso angle. This moment-angle relationship consists of the head rotating forward due to inertial forces and a reacting moment at the occipital condyles that occurs in the opposite direction and tends to rotate the head backward. Also, a high forward moment should be exerted by the neck on the head when a critical head/neck angle is exceeded (head rotating backward with respect to the neck). The neck structure should exhibit ordinary elastic properties, with the moment generated at the base of the neck a direct relation of the change in neck/torso angle (moment backward as neck rotates forward). They found that the Hybrid III neck system is designed so that the moment applied to the head is a function of head/neck angle, not head/torso angle. Therefore, it is not possible to faithfully model the motion of the human head using such a design.

Work on the design of a more biofidelic neck was in progress at the time of publication.

REFERENCES

1. Military Standard, MIL-STD-1290A(AV), LIGHT FIXED- AND ROTARY-WING AIR-CRAFT CRASH RESISTANCE, Department of Defense, Washington, DC, 20301, 26 September 1988.

2. Gell, C. F., TABLE OF EQUIVALENTS FOR ACCELERATION TERMINOLOGY, Aerospace Medicine, Vol. 32, No. 12, December 1961, pp. 1109-1111.

3. Gupta, B. P., HELICOPTER OBSTACLE STRIKE TOLERANCE CONCEPTS ANALYSIS, Bell Helicopter Textron; Technical Report 78-46. Applied Technology Laboratory, U.S. Army Research and Technology Laboratories (AVRADCOM), Fort Eustis, VA, April 1979; AD A069877.

4. Haley, J., "Analysis of U.S. Army Helicopter Accidents to Define Impact Injury Problems," Paper 9-1, Linear Acceleration of Impact Type Symposium, AGARD-CP-88-71.

5. Shanahan, D. F., and Shanahan, M. O., INJURY IN U.S. ARMY HELICOPTER CRASHES, September 1979 through October 1985, Journal of Trauma, April 1989.

6. Department of the Army Regulation: Accident Reporting and Records, Washington, DC, Headquarters Department of the Army, 1980; AR 385-40.

7. Department of the Army Pamphlet, AIRCRAFT ACCIDENT INVESTIGATION AND REPORTING, Headquarters, Department of the Army, Washington D.C., 1983; DA PAM 385-95.

8. Shanahan, D. F., and Shanahan, M. O., KINEMATICS OF U.S. ARMY HELICOPTER CRASHES, 1979-1985, Aviation, Space, and Environmental Medicine, Vol 60, Pages 12-21, February 1989.

9. Snyder, R. G., HUMAN IMPACT TOLERANCE, Paper 700398, International Automobile Safety Compendium, Society of Automotive Engineers, New York, 1970, pp. 712-782.

10. Rothe, V. E., et al., CREW SEAT DESIGN CRITERIA FOR ARMY AIRCRAFT, TRECOM Technical Report 63-4, U.S. Army Transportation Research Command, Fort Eustis, Virginia, February 1963.

11. Laananen, D. H., WHOLE-BODY HUMAN TOLERANCE TO IMPACT WITH LAP BELT-ONLY RESTRAINT, TI-83405, Simula Inc., Phoenix, Arizona, Department of Transportation, FAATC, July 28, 1983.

12. Military Specification, MIL-S-58095A(AV), SEAT SYSTEM: CRASH-RESISTANT, NON-EJECTION, AIRCREW, GENERAL SPECIFICATION FOR, Deparment of Defense, Washington, D.C., 31 January 1986.

13. Eiband, A. M., HUMAN TOLERANCE TO RAPIDLY APPLIED ACCELERATIONS: A SUMMARY OF THE LITERATURE, NASA Memorandum 5-19-59E, National Aeronautics and Space Administration, Washington, D. C., June 1959.

REFERENCES (CONTD)

14. Snyder, R. G., HUMAN TOLERANCE TO EXTREME IMPACTS IN FREE FALL, Aerospace Medicine, Vol. 34, No. 8, August 1963, pp. 695-709.

15. Stapp, J. P., JOLT EFFECTS OF IMPACT ON MAN, Brooks Air Force Base, San Antonio, Texas, November 1961.

16. Beeding, E. L., Jr., and Mosely, J. D., HUMAN DECELERATION TESTS, Air Force Missile Development Center; AFMDC Technical Note 60-2, Holloman Air Force Base, New Mexico, January 1960, AD 23148.

17. Zaborowski, A. V., HUMAN TOLERANCE TO LATERAL IMPACT WITH LAP BELT ONLY, Proceedings, Eighth Stapp Car Crash and Field Demonstration Conference, Society of Automotive Engineers, New York, 1964.

18. Zaborowski, A. V., LATERAL IMPACT STUDIES - LAP BELT SHOULDER HARNESS INVESTIGATIONS, Proceedings, Ninth Stapp Car Crash Conference, Society of Automotive Engineers, New York, 1965.

19. Ewing, C. L., et al., DYNAMIC RESPONSE OF THE HUMAN HEAD AND NECK TO +G_y IMPACT ACCELERATION, Proceedings, Twenty-first Stapp Car Crash Conference, Society of Automotive Engineers, New York, 1977, pp. 547-586.

20. Hollister, N. R., et al., BIOPHYSICS OF CONCUSSION, Wright Air Development Center; WADC Technical Report 58-193, Wright-Patterson Air Force Base, Ohio, 1958.

21. Ommaya, A. K., and Hirsch, A. E., TOLERANCES FOR CEREBRAL CONCUSSION FROM HEAD IMPACT AND WHIPLASH IN PRIMATES, Journal of Biomechanics, Vol. 4, 1971, pp. 13-21.

22. Slobodnik, B. A., SPH-4 Helmet Damage and Head Injury Correlation, Aviation, Space, and Environmental Medicine, February 1979, pp 139-146.

23. Goldsmith, W., BIOMECHANICS OF HEAD INJURY, In Biomechanics-Its Foundation and Objectives, ed. by Fung, Y. C., Perrone, N., and Anliker, M., Prentice-Hall, Inc., Englewood Cliffs, New Jersey, 1972, pp. 585-634.

24. Gurdjian, E. S., Roberts, V. L., and Thomas, L. M., TOLERANCE CURVES OF ACCELERATION AND INTRACRANIAL PRESSURE AND PROTECTIVE INDEX IN EXPERIMENTAL HEAD INJURY, Journal of Trauma, Vol. 6, 1966, pp. 600-604.

25. Holburn, A. H. S., MECHANICS OF BRAIN INJURIES, British Medical Bulletin, Vol. 3(6) 1945, pp. 147-149.

26. Kornhauser, M., PREDICTION AND EVALUATION OF SENSITIVITY TO TRANSIENT ACCELERATION, Journal of Applied Mechanics, Vol. 21, 1945, p. 371.

REFERENCES (CONTD)

27. Ommaya, A. K., et al., SCALING OF EXPERIMENTAL DATA ON CEREBRAL CONCUS-SION IN SUB-HUMAN PRIMATES TO CONCUSSION THRESHOLD FOR MAN, Proceedings, Eleventh Stapp Car Crash Conference, Society of Automotive Engineers, New York, October 10-11, 1967.

28. Ommaya, A. K., et al., COMPARATIVE TOLERANCE FOR CEREBRAL CONCUSSION BY HEAD IMPACT AND WHIPLASH INJURY IN PRIMATES, 1970 International Auto-mobile Safety Conference Compendium, Society of Automotive Engineers, New York, 1970.

29. Patrick, L. M., Lissner, H. R., and Gurdjian, E. S., SURVIVAL BY DESIGN - HEAD PROTECTION, Proceedings, Seventh Stapp Car Crash Conference, Society of Automotive Engineers, New York, 1963.

30. Gadd, C. W., USE OF A WEIGHTED-IMPULSE CRITERION FOR ESTIMATING INJURY HAZARD, Proceedings, Tenth Stapp Car Crash Conference, Society of Auto-motive Engineers, New York, 1966.

31. SAE Information Report, HUMAN TOLERANCE TO IMPACT CONDITIONS AS RELATED TO MOTOR VEHICLE DESIGN--SAE J885a, SAE Handbook, Part 2, Society of Automotive Engineers, Warrendale, Pennsylvania, 1979, pp. 34.114 - 34.117.

32. HUMAN TOLERANCE TO IMPACT CONDITIONS AS RELATED TO MOTOR VEHICLE DESIGN - SAEJ885 APR 80, SAEJ885, Society of Automotive Engineers, Inc., Warrendale, Pennsylvania, April 1980.

33. FEDERAL MOTOR VEHICLE SAFETY STANDARD NO. 208, OCCUPANT CRASH PROTEC-TION, Code of Federal Regulations, Title 49, Part 571.208, U.S. Govern-ment Printing Office, Washington, D.C., 1987.

34. Nusholtz, G. S., et al., CRITICAL LIMITATIONS ON SIGNIFICANT FACTORS IN HEAD INJURY RESEARCH, Thirtieth Stapp Car Crash Conference Proceedings, Society of Automotive Engineers, Inc., Warrendale, Pennsylvania, October 1986.

35. Lockett, F. J., BIOMECHANICS OF HEAD TOLERANCE CRITERIA, N83-29990, National Physical Laboratory, Teddington, Middlesex, TW11 OLW, Great Britain.

36. Smith, R. W., THE RESPONSE OF THE UNEMBALMED CADAVERIC AND LIVING CEREBRAL VESSELS TO GRADED INJURY - A PILOT STUDY, University of California, San Diego, SAE 791021, Society of Automotive Engineers, Inc., Warrendale, Pennsylvania, 1979.

37. Rodden, B. E., et al., AN ALGORITHM FOR DETERMINING THE HEAD INJURY CRITERION (HIC) FROM RECORDS OF HEAD ACCELERATION, Defence and Civil Institute of Environmental Medicine, SAE 830469, Society of Automotive Engineers, Inc., Warrendale, Pennsylvania, March 1983.

REFERENCES (CONTD)

38. Slattenschek, A., and Tauffkirchen, W., CRITICAL EVALUATION OF ASSESS-
MENT METHODS FOR HEAD IMPACT APPLIED IN APPRAISAL OF BRAIN INJURY
HAZARD, IN PARTICULAR IN HEAD IMPACT ON WINDSHIELDS, Paper 700426, 1970
International Automobile Safety Conference Compendium, Society of Auto-
motive Engineers, New York, 1970, pp. 1084, 1112.

39. Brinn, J., and Staffeld, S. E., THE EFFECTIVE DISPLACEMENT INDEX - AN
ANALYSIS TECHNIQUE FOR CRASH IMPACTS OF ANTHROPOMETRIC DUMMIES, Pro-
ceedings, Fifteenth Stapp Car Conference, Society of Automotive
Engineers, New York, 1971, pp. 817-824.

40. Melvin, J. W., and Evans, F. G., A STRAIN ENERGY APPROACH TO THE MECHAN-
ICS OF SKULL FRACTURE, Proceedings, Fifteenth Stapp Car Crash Confer-
ence, Society of Automotive Engineers, New York, 1971, pp. 666-685.

41. Enouen, S. W., THE DEVELOPMENT OF EXPERIMENTAL HEAD IMPACT PROCEDURES
FOR SIMULATING PEDESTRIAN HEAD INJURY, Thirtieth Stapp Car Crash
Conference Proceedings, Society of Automotive Engineers, Inc.,
Warrendale, Pennsylvania, October 1986.

42. Hodgson, V. R., and Thomas, L. M., COMPARISON OF HEAD ACCELERATION IN-
JURY INDICES IN CADAVER SKULL FRACTURE, Proceedings, Fifteenth Stapp
Car Crash Conference, Society of Automotive Engineers, New York, 1971,
pp. 190-206.

43. Fan, W. R. S., INTERNAL HEAD INJURY ASSESSMENT, Proceedings, Fifteenth
Stapp Car Crash Conference, Society of Automotive Engineers, New York,
1971, pp. 645-665.

44. Nyquist, G. W., FACIAL IMPACT TOLERANCE AND RESPONSE, Thirtieth Stapp
Car Crash Conference Proceedings, Society of Automotive Engineers, Inc.,
Warrendale, Pennsylvania, October 1986.

45. Swearingen, J. J., EVALUATION OF HEAD AND FACE INJURY POTENTIAL OF CUR-
RENT AIRLINE SEATS DURING CRASH DECELERATIONS, AM 66-18, Office of
Aviation Medicine, Federal Aviation Agency, Washington, D.C., June 1966.

46. Mertz, H. J., and Patrick, L. M., STRENGTH AND RESPONSE OF THE HUMAN
NECK, Proceedings, Fifteenth Stapp Car Crash Conference, Society of Auto-
motive Engineers, New York, 1971, pp. 207-255.

47. King, A. I., TOLERANCE OF THE NECK TO DIRECT IMPACT, Wayne State Univer-
sity, N00014-75-C-1015, Office of Naval Research, Department of the
Navy, Arlington, Virginia, March 1979, AD A066797.

48. Gadd, C. W., Culver, C. C., and Nahum, A. M., A STUDY OF RESPONSES AND
TOLERANCES OF THE NECK, Proceedings, Fifteenth Stapp Car Crash Confer-
ence, Society of Automotive Engineers, New York, 1971, pp. 256-268.

REFERENCES (CONTD)

49. Hodgson, V. R., TOLERANCE OF THE HEAD AND NECK TO -Gx INERTIAL LOADING OF THE HEAD, Wayne State University, N00014-75-C-1015, Office of Naval Research, Department of the Navy, Arlington, Virginia, March 1981, AD A097632.

50. Muzzy, W. H. III, et al., THE EFFECT OF MASS DISTRIBUTION PARAMETERS ON HEAD/NECK DYNAMIC RESPONSE, Thirtieth Stapp Car Crash Conference Proceedings, Society of Automotive Engineers, Inc., Warrendale, Pennsylvania, October 1986.

51. Seeman, M. R., et al., COMPARISON OF HUMAN AND HYBRID III HEAD AND NECK DYNAMIC RESPONSE, Thirtieth Stapp Car Crash Conference Proceedings, Society of Automotive Engineers, Inc., Warrendale, Pennsylvania, October 1986.

52. Basio, A. C. and Bowman, B. M., SIMULATIONS OF HEAD-NECK DYNAMIC RESPONSE IN -Gx AND +Gy, Thirtieth Stapp Car Crash Conference Proceedings, Society of Automotive Engineers, Warrendale, Pennsylvania, October 1986.

53. Wismans, J., et al., OMNI-DIRECTIONAL HUMAN HEAD-NECK RESPONSE, Thirtieth Stapp Car Crash Conference Proceedings, Society of Automotive Engineers, Inc., Warrendale, Pennsylvania, Octover 1986.

54. Guill, F. C., FACTORS INFLUENCING THE INCIDENCE AND SEVERITY OF "EJECTION ASSOCIATED" NECK INJURIES SUSTAINED BY U.S. NAVY EJECTEES - 1 JANUARY 1969 THROUGH 31 DECEMBER 1979 - A PRELIMINARY REPORT, Proceedings of the Twenty-first Annual SAFE Symposium, SAFE Association, Van Nuys, California, November 1983.

55. Melvin, J. W., HUMAN NECK INJURY TOLERANCE, SAE 790135, in The Human Neck Anatomy, Injury Mechanisms and Biomechanics, Society of Automotive Engineers, Inc., Warrendale, Pennsylvania, 1979.

56. Kroell, C. K., Schneider, D. C., and Nahum, A. M., IMPACT TOLERANCE AND RESPONSE OF THE HUMAN THORAX II, Proceedings, Eighteenth Stapp Car Crash Conference, Society of Automotive Engineers, New York, 1974, pp. 383-457.

57. THE ABBREVIATED INJURY SCALE (AIS), Joint Committee of the American Medical Association, American Association for Automotive Medicine, and the Society of Automotive Engineers; American Association for Automotive Medicine, Morton Grove, Illinois, 1976 Revision.

58. Neathery, R. F., ANALYSIS OF CHEST IMPACT RESPONSE DATA AND SCALED PERFORMANCE RECOMMENDATIONS, Proceedings, Eighteenth Stapp Car Crash Conference, Society of Automotive Engineers, New York, 1974, pp. 459-493.

59. Mertz, H. J., and Gadd, C. W., THORACIC TOLERANCE TO WHOLEBODY DECELERATION, Proceedings, Fifteenth Stapp Car Crash Conference, Society of Automotive Engineers, New York, 1971, pp. 135-157.

REFERENCES (CONTD)

60. Kroell, C. K., et al., INTERRELATIONSHIP OF VELOCITY AND CHEST COMPRES-SION IN BLUNT THORACIC IMPACT TO SWINE II, Thirtieth Stapp Car Crash Conference Proceedings, Society of Automotive Engineers, Inc., Warrendale, Pennsylvania, October 1986.

61. Lau, I. V., and Viano, D. C., THE VISCOUS CRITERION - BASES AND APPLI-CATIONS OF AN INJURY SEVERITY INDEX FOR SOFT TISSUES, Thirtieth Stapp Car Crash Conference Proceedings, Society of Automotive Engineers, Inc., Warrendale, Pennsylvania, October 1986.

62. Morgan, R. M., et al., SIDE IMPACT - THE BIOFIDELITY OF NHTSA'S PROPOSED ATD AND EFFICACY OF TTI, Thirtieth Stapp Car Crash Conference Proceedings, Society of Automotive Engineers, Inc., Warrendale, Pennsylvania, October 1986.

63. Huelke, D. F. and Melvin, J. W., ANATOMY, INJURY FREQUENCY, BIO-MECHANICS, AND HUMAN TOLERANCES, University of Michigan Medical School, SAE 800098, Society of Automotive Engineers, Inc., Warrendale, Pennsylvania, 1980.

64. Gogler, E., et al., BIOMECHANICAL EXPERIMENTS WITH ANIMALS ON ABDOMINAL TOLERANCE LEVELS, Proceedings, Twenty-First Stapp Car Crash Conference, Society of Automotive Engineers, New York, 1977, pp. 713-751.

65. Nahum, A. M. and Melvin, J., The Biomechanics of Trauma, Appleton-Century-Crofts, Norwalk, Connecticut, 1985, pg. 175.

66. Cavanaugh, J. M., et al., LOWER ABDOMINAL TOLERANCE AND RESPONSE, Thirtieth Stapp Car Crash Conference Proceedings, Society of Automotive Engineers, Inc., Warrendale, Pennsylvania, October 1986.

67. Rouhana, S. W., et al., THE EFFECT OF LIMITING IMPACT FORCE ON ABDOMINAL INJURY: A PRELIMINARY STUDY, Thirtieth Stapp Car Crash Conference Proceedings, Society of Automotive Engineers, Inc., Warrendale, Pennsylvania, October 1986.

68. Von Gierke, H. E., and Brinkley, J. W., IMPACT ACCELERATIONS, In Foundation of Space Biology and Medicine, Volume II, Book One, Scientific and Technical Information Office, National Aeronautics and Space Administration, Washington, D. C., 1975, pp. 214-246.

69. Stech, E. I., Payne, P. R., DYNAMIC MODELS OF THE HUMAN BODY, AMRL-TR-66-157, Aerospace Medical Research Laboratory, Wright-Patterson Air Force Base, Ohio, 1969.

70. Kazarian, L. E., STANDARDIZATION AND INTERPRETATION OF SPINAL INJURY CRITERIA, AMRL-TR-75-85, Aerospace Medical Research Laboratory, Air Force Systems Command, Wright-Patterson Air Force Base, Ohio, April 1978, AD A054959.

REFERENCES (CONTD)

71. Coltman, J. W., et al., CRASH-RESISTANT CREWSEAT LIMIT-LOAD OPTIMIZATION THROUGH DYNAMIC TESTING WITH CADAVERS, Simula Inc., USAAVSCOM TR-85-D-11, Aviation Applied Technology Directorate, U.S. Army Aviation Research and Technology Activity, Fort Eustis, Virginia, January 1986.

72. Hodgson, V. R. and Thomas, L. M., A MODEL TO STUDY CERVICAL SPINE INJURY MECHANISMS DUE TO HEAD IMPACT, Engineering Aspects of the Spine, I Mech E Conference Publications 1980-2, Mechanical Engineering Publications Limited, London, May 1980, pp 89-91.

73. Soechting, J. F., RESPONSE OF THE HUMAN SPINAL COLUMN TO LATERAL DECELERATION, Journal of Applied Mechanics, Vol. 40, 1973, pp. 643-649.

74. Orne, D., and Liu, Y. K., A MATHEMATICAL MODEL OF SPINAL RESPONSE TO IMPACT, Journal of Biomechanics, Vol. 4, 1971, pp. 49-71.

75. Stech, E. L., and Payne, P. R., DYNAMIC MODELS OF THE HUMAN BODY, Frost Engineering Development Corp.; AMRL Technical Report 66-157, Aerospace Medical Research Lab, Wright-Patterson Air Force Base, Ohio, November 1969, AD 701383.

76. Brinkley, J. W., and Shaffer, J. T., DYNAMIC SIMULATION TECHNIQUES FOR THE DESIGN OF ESCAPE SYSTEMS: CURRENT APPLICATIONS AND FUTURE AIR FORCE REQUIREMENTS, Aerospace Medical Research Lab; AMRL Technical Report 71-292, Wright-Patterson Air Force Base, Ohio, December 1971, AD 740439.

77. Military Specification, MIL-S-9479, SEAT SYSTEM, UPWARD EJECTION, AIRCRAFT, GENERAL SPECIFICATION FOR, Department of Defense, Washington, D. C., March 1971.

78. King, A. I., and Prasad, P., AN EXPERIMENTALLY VALIDATED MODEL OF THE SPINE, Journal of Applied Mechanics, Vol. 41, No. 3, September 1974, pp. 546-550.

79. Hakim, N. S., and King, A. I., STATIC AND DYNAMIC ARTICULAR FACET LOADS, Proceedings, Twentieth Stapp Car Crash Conference, Society of Automotive Engineers, New York, 1976, pp. 607-639.

80. Belytschko, T., Schwer, L., and Schultz, A., A MODEL FOR ANALYTICAL INVESTIGATION OF THREE-DIMENSIONAL HEAD-SPINE DYNAMICS - FINAL REPORT, University of Illinois at Chicago Circle; AMRL Technical Report 76-10, Aerospace Medical Research Laboratory, Wright-Patterson Air Force Base, Ohio, April 1976, AD A025911.

81. MODELS AND ANALOGUES FOR THE EVALUATION OF HUMAN BIODYNAMIC RESPONSE, PERFORMANCE, AND PROTECTION, AGARD Conference Proceedings No. 253, NATO Advisory Group for Aerospace Research and Development, Neuilly sur Seine, France, 1968.

REFERENCES (CONTD)

82. Kazarian, L., and Graves, G. A., COMPRESSIVE STRENGTH CHARACTERISTICS OF THE HUMAN VERTEBRAL CENTRUM, AMRL Technical Report 77-14, Aerospace Medical Research Laboratory, Wright-Patterson Air Force Base, Ohio, 1977.

83. Hodgson, V. R., and Thomas, L. M., HEAD IMPACT RESPONSE -PROPOSAL NUMBER VRI 7.2, Society of Automotive Engineers, Inc., New York, 1975.

84. Patrick, L. M., Kroell, C. K., and Mertz, H. G., FORCES ON THE HUMAN BODY IN SIMULATED CRASHES, Proceedings, Ninth Stapp Car Crash Conference, Society of Automotive Engineers, New York, 1965, pp. 237-259.

85. King, J. J., Fan, W. R. S., and Vargovick, R. J., FEMUR LOAD INJURY CRITERIA - A REALISTIC APPROACH, Proceedings, Seventeenth Stapp Car Crash Conference, Society of Automotive Engineers, New York, 1973, pp. 509-524.

86. Powell, W. R., et al., INVESTIGATION OF FEMUR RESPONSE TO LONGITUDINAL IMPACT, Proceedings, Eighteenth Stapp Car Crash Conference, Society of Automotive Engineers, New York, 1974, pp. 539-556.

87. Viano, C. C., CONSIDERATIONS FOR A FEMUR INJURY CRITERION, Proceedings, Twenty-First Stapp Car Crash Conference, Society of Automotive Engineers, New York, 1977, pp. 445-473.

88. States, M. M., et al., FIELD APPLICATION AND DEVELOPMENT OF THE ABBREVIATED INJURY SCALE, Proceedings, Fifteenth Stapp Car Crash Conference, Society of Automotive Engineers, New York, 1971, pp. 710-738.

89. THE ABBREVIATED INJURY SCALE, 1985 REVISION, American Association for Automotive Medicine, Des Plaines, Illinois, 1985.

90. Singley, G. T., III, TEST AND EVALUATION OF IMPROVED AIRCREW RESTRAINT SYSTEMS, USAAVRADCOM-TR-81-D-27, Applied Technology Laboratory, U.S. Army Research and Technology Laboratories, Fort Eustis, Virginia, September 1981, AD A107576.

91. Domzalski, L., INFLATABLE BODY AND HEAD RESTRAINT SYSTEM (IBAHRS): DYNAMIC Gx CRASH SIMULATION TEST PROGRAM, Naval Air Development Center, NADC-84140-60, Naval Air Systems Command, Washington, D.C., June 1984.

92. Roe, R. W., and Kyropoulos, P., THE APPLICATION OF ANTHROPOMETRY TO AUTOMOTIVE DESIGN, Paper 700553, Society of Automotive Engineers, New York, 1970.

93. Churchill, E., et al., ANTHROPOMETRY OF U.S. ARMY AVIATORS - 1970, Anthropology Research Project, Yellow Springs, Ohio; Technical Report 72-52-CE, U.S. Army Natick Laboratories, Natick, Massachusetts, December 1971, AD 743528.

REFERENCES (CONTD)

94. THE BODY SIZE OF SOLDIERS - U.S. ARMY ANTHROPOMETRY-1966, USANL Technical Report 72-51-CE, U.S. Army Natick Laboratories, Natick, Massachusetts December 1971, AD743465.

95. Churchill, E., et al., ANTHROPOMETRY OF WOMAN OF THE U.S. ARMY - 1977, Webb Associates, Inc., Yellow Springs, Ohio, Tech. Rep. 77/024, U.S. Army Natick Research and Development Command, Natick, Massachusetts, June 1977.

96. Dempster, W. T., SPACE REQUIREMENTS FOR THE SEATED OPERATOR, Wright Air Development Center; WADC Technical Report 55-159, Wright-Patterson Air Force Base, Ohio, 1955, AD 087892.

97. Dempster, W. T., and Gaughran, G. R. L., PROPERTIES OF BODY SEGMENTS BASED ON SIZE AND WEIGHT, American Journal of Anatomy, Vol. 120, 1967, pp. 33-54.

98. Glanville, A. D., and Kreezer, G., THE MAXIMUM AMPLITUDE AND VELOCITY OF JOINT MOVEMENTS IN NORMAL MALE HUMAN ADULTS, Human Biology, Vol. 9, 1937, pp. 197-211.

99. Santischi, W. R., DuBois, J., and Omoto, C., MOMENTS OF INERTIA AND CENTERS OF GRAVITY OF THE LIVING HUMAN BODY, AMRL Technical Data Report 63-36, Aerospace Medical Research Lab, Wright-Patterson Air Force Base, Ohio, 1963.

100. Clauser, C. E., McConville, J. T., and Young, J. W., WEIGHT, VOLUME, AND CENTER OF MASS OF SEGMENTS OF THE HUMAN BODY, Antioch College; AMRL Technical Report 69-70, Aerospace Medical Research Lab, Wright- Patterson Air Force Base, Ohio, August 1969, AD 710622.

101. Chandler, R. F., et al., INVESTIGATION OF INERTIAL PROPERTIES OF THE HUMAN BODY, Report No. DOT-HS-801-430, U.S. Department of Transportation, Washington, D.C., March 1975.

102. Laananen, D. H., et al., COMPUTER SIMULATION OF AN AIRCRAFT SEAT AND OCCUPANT IN A CRASH ENVIRONMENT, VOLUME I - TECHNICAL REPORT, TR-82401, Simula Inc., Tempe, Arizona, DOT/FAA/CT-82/33-I, March 1983.

103. ANTHROPOMETRY AND MASS DISTRIBUTION HUMAN ANALOGUES, VOLUME I: MILITARY MALE AVIATORS, Aerospace Division, Air Force Systems Command, Wright-Patterson Air Force Base, Dayton, Ohio, June 1987.

104. LeFevre, R. L., and Silver, J. N., DUMMIES - THEIR FEATURES AND USE, Proceedings, Automotive Safety Engineering Seminar, Society of Automotive Engineers, New York, June 20-21, 1973.

105. Swearingen, J. J., DESIGN AND CONSTRUCTION OF A CRASH TEST DUMMY FOR TESTING SHOULDER HARNESS AND SAFETY BELTS, Civil Aeronautics Administration, Civil Aeronautics Medical Research Laboratory (now FAA Civil Aeromedical Institute), Oklahoma City, Oklahoma, April 1951.

REFERENCES (CONTD)

106. SAE Recommended Practice, ANTHROPOMORPHIC TEST DEVICE FOR USE IN DYNAMIC TESTING OF MOTOR VEHICLES, SAE J963, SAE Handbook, Society of Automotive Engineers, Warrendale, Pennsylvania, 1978, pp. 34.107 - 34.110.

107. Code of Federal Regulations, ANTHROPOMORPHIC TEST DUMMY, Title 49, Chapter 5, Part 572, Federal Register, Vol. 38, No. 62, April 2, 1973, pp. 8455-8458.

108. Massing, D. E., Naab, K. N., and Yates, P. E., PERFORMANCE EVALUATION OF NEW GENERATION OF 50TH-PERCENTILE ANTHROPOMORPHIC TEST DEVICES: VOLUME I - TECHNICAL REPORT, Calspan Corporation; DOT-HS Technical Report 801-431, Department of Transportation, National Highway Traffic Safety Administration, Washington, D. C., March 1975, PB 240-920.

109. Foster, J. K., Kortge, J. O., and Wallanin, M. J., HYBRID III-A BIO-MECHANICALLY-BASED CRASH TEST DUMMY, Proceedings, Twenty-First Stapp Car Crash Conference, Society of Automotive Engineers, New York, 1977, pp. 973-1014.

110. Part 572 - ANTHROPOMORPHIC TEST DUMMIES, SUBPART E - HYBRID III TEST DUMMY, Code of Federal Regulations, Title 49, Part 572, U.S. Government Printing Office, Washington, D.C., 1987.

111. Kaleps, I., and Whitestone, J., HYBRID III GEOMETRICAL AND INERTIAL PROPERTIES, SAE Paper 880638, Society of Automotive Engineers, Inc., Warrendale, Pennsylvania, 1988.

112. FEDERAL MOTOR VEHICLE SAFETY STANDARDS; SIDE IMPACT PROTECTION, Docket 88-09,; Notice 1, Federal Register, Volume 53, No. 17, January 27, 1988, pp. 2239-2260.

113. Stalnaker, R. L., et al., MODIFICATION OF PART 572 DUMMY FOR LATERAL IMPACT ACCORDING TO BIOMECHANICAL DATA, SAE Paper 791031, Society of Automotive Engineers, Inc., Warrendale, Pennsylvania, 1979.

114. Neilson, L., et al., THE EUROSID SIDE IMPACT DUMMY, Tenth International Technical Conference on Experimental Safety Vehicles, National Highway Traffic Safety Administration, Washington, D.C., July 1985, pp. 153 - 164.

115. Walsh, M. M., and Romeo, D. M., RESULTS OF CADAVER AND ANTHROPOMORPHIC DUMMY TESTS IN IDENTICAL CRASH SITUATIONS, Proceedings, Twentieth Stapp Car Crash Conference, Society of Automotive Engineers, Warrendale, Pennsylvania, 1976, pp. 108-131.

116. Chandler, R. F., and Christian, R. A., COMPARATIVE EVALUATION OF DUMMY PERFORMANCE UNDER $-G_x$ IMPACT, Proceedings, Thirteenth Stapp Car Crash Conference, Society of Automotive Engineers, New York, 1969, pp. 61 - 75.

REFERENCES (CONTD)

117. Saul, R. A., FRONTAL CRASH RESPONSES: PART 572 VERSUS HYBRID III DUMMY RESPONSE EVALUATION, DOT HS 807 048, National Highway Traffic Safety Administration, Washington, D.C., July 1986, PB 87-15110 6.

118. Backaitis, S. H., and St. Laurent, A., CHEST DEFLECTION CHARACTERISTICS OF VOLUNTEERS AND HYBRID III DUMMIES, Thirtieth Stapp Car Crash Conference Proceedings, Society of Automotive Engineers, Inc., Warrendale, Pennsylvania, October 1986.

119. Leung, Y.C., et al., AN ANTI-SUBMARINING SCALE DETERMINED FROM THEORETICAL AND EXPERIMENTAL STUDIES USING THREE-DIMENSIONAL GEOMETRICAL DEFINITION OF THE LAP-BELT, SAE Paper 811020, Society of Automotive Engineers, Inc., Warrendale, Pennsylvania, 1981.

120. Tieber, J. A., THE STATE OF THE ART OF ANTHROPOMORPHIC MANIKINS AND REQUIREMENTS FOR THE EVALUATION OF ADVANCED AIRCRAFT EJECTION SYSTEMS, Proceedings of the Twenty-second Annual SAFE Symposium, SAFE Association, Van Nuys, California, December 1984.

121. White, R. P., Jr., ADAM: THE NEXT STEP IN DEVELOPMENT OF THE TRUE HUMAN ANALOG, Procedings of the Twenty-fourth Annual Symposium SAFE Association, SAFE Association, Van Nuys, California, December 1986.

122. White, R. P., Jr., ADAM: THE PHYSICAL BEING, Proceedings of the Twenty-fifth Annual SAFE symposium, SAFE Association, Van Nuys, California, November 1987.

123. Frisch, G. D., and Frisch, P. H., THE DEVELOPMENT OF A DYNAMIC RESPONSE SENSING AND RECORDING SYSTEM FOR INCORPORATION INTO A STATE-OF-THE-ART-MANIKIN, Proceedings of the Twenty-first Annual SAFE Symposium, SAFE Association, Van Nuys, California, November 1983.

124. Frisch, G. D., et al., STRUCTURAL INTEGRITY TESTS OF A MODIFIED HYBRID III MANIKIN AND SUPPORTING INSTRUMENTATION SYSTEM, Proceedings of the Twenty-second Annual SAFE Symposium, SAFE Association, Van Nuys, California, December 1984.

125. Gragg, C. D., COULD ANTHROPOMETRIC DUMMY DATA BE USED TO PREDICT INJURY TO HUMANS?, Proceedings of the Twenty-second Annual SAFE Symposium, SAFE Association, Van Nuys, California, December 1984.

126. Laananen, D. H., and Coltman, J. W., MEASUREMENT OF SPINAL LOADS IN TWO MODIFIED ANTHROPOMORPHIC DUMMIES, Simula Inc., TR-82405, U.S. Army Aeromedical Research Laboratory, Fort Rucker, Alabama, May 1982.

BIBLIOGRAPHY

Daniel, R. P., A BIO-ENGINEERING APPROACH TO CRASH PADDING, Paper 680001, Society of Automotive Engineers, New York, 1968.

DeHaven, H., MEAN DECELERATIONS SUSTAINED BY NINE (9) SURVIVORS OF FREE FALL---55 TO 185 FEET, Human Factors Design Sheet, Aviation Crash Injury Research, Phoenix,
rizona, 1958.

Ewing, C. L., and Thomas, D. J., HUMAN HEAD AND NECK RESPONSE TO IMPACT ACCELERATION, Joint Report issued by Naval Aerospace Medical Research Laboratory (NAMRL Monograph 21) and U.S. Army Aeromedical Research Laboratory (USAARL 73-1), August, 1972.

Ewing, C. L., and Unterharnscheidt, F., NEUROPATHOLOGY AND CAUSE OF DEATH IN U.S. NAVAL AIRCRAFT ACCIDENTS, Recent Experience/Advances in Aviation Pathology, Conference Proceedings No. 190, North Atlantic Treaty Organization Advisory Group for Aerospace Research and Development, Neuilly sur Seine, France, June 1977, AD AO 40356.

Gadd, C. W., TOLERABLE SEVERITY INDEX IN WHOLE-HEAD, NONMECHANICAL IMPACT, Proceedings, Fifteenth Stapp Car Crash Conference, Society of Automotive Engineers, New York, 1971.

Glancey, J. J., and Desjardins, S. P., A SURVEY OF NAVAL AIRCRAFT CRASH ENVIRONMENTS WITH EMPHASIS ON STRUCTURAL RESPONSE, Dynamic Science; Department of the Navy, Office of Naval Re search, Arlington, Virginia, December 1971, AD 739 37.

Griffin, L. I., III, ANALYSIS OF THE BENEFITS DERIVED FROM CERTAIN PRESENTLY EXISTING MOTOR VEHICLE SAFETY DEVICES: A REVIEW OF THE LITERATURE, University of North Carolina; MVMAHSRC Technical Report 7303, Motor Vehicle Manufacturers Association of the United States, Inc., Detroit, Michigan, December 1973.

Haley, J. L., Jr., et al., HELMET DESIGN CRITERIA FOR IMPROVED CRASH SURVIVAL, Aviation Safety Engineering and Research, A Division of Flight Safety Foundations; USAAVLABS Technical Report 65-44, U.S. Army Aviation Materiel Laboratories, Fort Eustis, Virginia, January 1966, AD 628 678.

Headley, R. N., et al., HUMAN FACTORS RESPONSES DURING GROUND IMPACT, Wright Air Development Center; WADC Technical Report 60-590, Wright-Patterson Air Force Base, Ohio, November 1959.

Horsch, J. D., and Patrick, L. M., CADAVER AND DUMMY KNEE IMPACT RESPONSE, Paper 760799, Automobile Engineering Meeting, at Dearborn, Michigan, Society of Automotive Engineers, Warrendale, Pennsylvania, October, 1976.

King, A. I., HUMAN TOLERANCE LIMITATIONS RELATED TO AIRCRAFT CRASHWORTHINESS, Wayne State University, Detroit, Michigan.